1988

Effects Of Permanent Dipoles And Static Fields On Molecular Spectra

Mary Ann Kmetic

NOTICE

The quality of this microform is heavily dependent upon the quality of the original thesis submitted for microfilming. Every effort has been made to ensure the highest quality of reproduction possible.

If pages are missing, contact the university which granted the degree.

Some pages may have indistinct print especially if the original pages were typed with a poor typewriter ribbon or if the university sent us an inferior photocopy.

Previously copyrighted materials (journal articles, published tests, etc.) are not filmed.

Reproduction in full or in part of this microform is governed by the Canadian Copyright Act, R.S.C. 1970, c. C-30.

AVIS

La qualité de cette microforme dépend grandement de la qualité de la thèse soumise au microfilmage. Nous avons tout fait pour assurer une qualité supérieure de reproduction.

S'il manque des pages, veuillez communiquer avec l'université qui a conféré le grade.

La qualité d'impression de certaines pages peut laisser à désirer, surtout si les pages originales ont été dactylographiées à l'aide d'un ruban usé ou si l'université nous a fait parvenir une photocopie de qualité inférieure.

Les documents qui font déjà l'objet d'un droit d'auteur (articles de revue, tests publiés, etc.) ne sont pas microfilmés.

La reproduction, même partielle, de cette microforme est soumise à la Loi canadienne sur le droit d'auteur, SRC 1970, c. C-30.

EFFECTS OF PERMANENT DIPOLES AND STATIC FIELDS ON MOLECULAR SPECTRA

by

Mary Ann Kmetic

Department of Chemistry

Submitted in partial fulfilment
of the requirements for the degree of
Doctor of Philosophy

Faculty of Graduate Studies
The University of Western Ontario
London, Ontario
August 1988

ISBN 0-315-43302-7

ABSTRACT

A relatively simple analytic expression for the absorption spectra of a two-level molecule or atom is derived, within the rotating wave approximation (RWA), which includes the effects of both permanent dipole moments and static electric fields. The derivation is for the interaction of the system with a plane-polarized sinusoidal electromagnetic field (EMF) in the semi-classical electric dipole approximation. This "molecular" RWA resonance profile, and a series of exactly calculated two-level model spectra, are used to investigate some of the single- and multi-photon spectral effects due to permanent dipoles and static electric fields, relative to the well studied atomic problem (no permanent dipoles) in the absence of a static field. These effects can include the occurrence of even as well as odd photon transitions and interesting temperature dependent orientationally averaged spectra. Permanent dipole moments, alone, can cause appreciable narrowing of the spectral resonances, oscillatory fringes around the main resonances as a function of frequency, and significant decreases in the molecule-EMF coupling, all relative to the atomic results. Comparisons with the exactly calculated two-level model spectra are used to study the validity of the RWA resonance profiles and indicate that several features, such as dynamic backgrounds and shifts of the resonance frequencies from the weak EMF limits of

$\omega_{res}^{N} = \Delta E/N$, N = 1,2,3,....; are missing in the RWA spectra as the molecule-EMF coupling strengths increase.

Perturbative corrections to the RWA absorption spectra, and the associated full widths at half maxima for the resonances, are derived, neglecting static fields, and used to help investigate and explain the effects missing in the RWA; the RWA resonance profile is a zeroth plus first order result obtainable from a time-independent Floquet Hamiltonian secular equation. The usefulness and validity of the perturbative corrections are investigated and it is concluded that the corrections to the RWA are not useful computationally, in general, past second order. However, the perturbative corrections are very useful in understanding some of the deficiencies of the RWA. These include the shifts of the N-photon resonance positions to low frequency, with respect to $\Delta E/N$, that can occur for molecules with non-zero permanent dipoles; it is well known that the shift is always to high frequency for atoms. An additional series of exact model calculations, for "giant dipole" molecules, is also used to help discuss the effects of permanent dipole moments on single- and multi-photon spectra and to establish comparisons with the recent literature on the subject.

ACKNOWLEDGEMENTS

I would like to thank the following people:

Dr. W. J. Meath for his assistance, guidance and encouragement, and his friendship. Most of all, I thank him for his "beer story" which has inspired me to earn many beers and obtain results along the way. (Of course, a beer is just as good, or maybe even better, when you haven't earned it - there were a few of those too!)

Dr. R. A. Thuraisingham for many helpful discussions (including "discussions" that had absolutely nothing to do with permanent dipole moments) and words of encouragement during his stay at [redacted]. G'day mate.

Anne Kondo and Maria Koulis (in no special order) for helping with the proofreading. True friends wouldn't really expect to be flown to Paris on the Concorde just for dinner, would they??

Eleanor Egan for patiently typing this thesis. Most of those equations really were Greek!

Jan Zaborniak for coming to my rescue and finishing the "t" thing.

TABLE OF CONTENTS

LIST OF TABLES

LIST OF FIGURES

CHAPTER 1

INTRODUCTION

The purpose of the research discussed in this thesis is to investigate some of the effects due to non-zero diagonal dipole matrix elements, or "permanent dipole moments", with respect to the single- and multi-photon resonance profiles or absorption spectra of molecules. Until some of the work developed in Chapter 3 was reported in the literature, very few papers had been published that dealt explicitly with this topic since most of the detailed mathematical analysis of single- and multi-photon spectra had been carried out for atoms which have no permanent dipole moments. Most of the earlier papers discussed the effects of permanent dipole moments using perturbation theory [1-4] which is of limited validity as a function of time and of the strength of the applied electromagnetic field inducing the spectral transitions. One of these papers [4] also discussed the problem for the two-level molecule for certain very specific molecule-applied static electric field-electromagnetic field configurations which permitted an exact solution of the time-dependent wave equation to be obtained.

An earlier numerical solution [5] for a two-level model was used to discuss some of the effects of permanent dipoles but lacked much physical interpretation of the results. Of course these effects have been implicitly included in calculations of the absorption spectra of

systems possessing permanent dipoles [6-8] and there are several techniques available for solving the time-dependent wave equation numerically for such problems [6-11]. These numerical methods are not convenient for the efficient investigation of the spectral effects arising from changing the various parameters which characterize the interaction of an electromagnetic field with a molecule. Part of this thesis is involved with the development of relatively simple analytic expressions for absorption spectra of two-level molecules which are used to investigate and interpret the essential features of single- and multi-photon spectra as a function of the parameters of the problem, and particularly those features arising from the presence of permanent dipole moments.

In this thesis the semi-classical electric dipole approximation is used to discuss the interaction of light with atoms and molecules. Chapter 2 contains an outline of some of the techniques available to solve the time-dependent wave equation in this approximation, for the interaction of an atom or molecule with an applied time-dependent sinusoidal plane-polarized electromagnetic field. The Dirac variation of constants method [12,13] for the formal solution of the problem is reviewed in Sec. 2.1. The standard time-dependent Rayleigh-Schrodinger perturbation solution [13-16] for the resulting set of first order (in time) coupled differential equations is discussed in Sec. 2.2 which also contains a review of the

difficulties inherent in this approximate solution to the problem. Some of these difficulties can be circumvented in the two-level system through the use of the rotating wave approximation (RWA) [15,17-20] which is outlined in Sec. 2.3. The discussions of Secs. 2.2 and 2.3 are limited to atoms which illustrates the complementary nature of perturbation theory and the RWA. The perturbation results, which can be used to analyze many-level problems, lead to the concept of multi-photon transitions [21] when carried out to higher order, while the RWA, which can be used for long times and relatively stronger applied fields, can deal only with single-photon atomic transitions. Neither the Rayleigh-Schrodinger perturbation treatment nor the RWA yield the Bloch-Siegert shift [22,23] to high frequency, relative to the zero-field resonance positions, of the absorption maxima in the resonance profiles of atoms. However, this shift can be obtained [22,23] by using perturbation theory, with the RWA as the zeroth order problem, as will be discussed later in the thesis. The analytic RWA expression for the single-photon atomic resonance profile, through its simple dependence on the parameters characterizing the atom-electomagnetic field interaction, has been fundamental in the understanding of atomic spectroscopy [17,19,20]. The molecular RWA, which includes the effects of permanent dipoles, is derived in Sec. 3.2.

The difficulties in using approximate methods for obtaining transition probabilities and resonance profiles can be eliminated by using exact techniques to solve the time-dependent wave equation. The matrix formulation (Sec. 2.4.1) of the Dirac variation of constants solution to the time-dependent wave equation is used, in Sec. 2.4.2, to discuss how the exact (numerical) solution of the wave equation for the interaction of an atom or molecule with both static and time varying applied electric fields, can be obtained by constructing the Riemann product integral representation [11,24,25] of the time-evolution operator for the system. The discussion is continued in Sec. 2.4.3 for the special case of interest in this work, that is, for a sinusoidal plane-polarized time-dependent electromagnetic field. For such a problem the time-dependent Hamiltonian is periodic in time and, using Floquet theory [23,26], the full solution of the time-dependence of the populations of the states of the atom or molecule, and the absorption spectrum, can be obtained from the solution of the time-dependent wave equation over the first period of the Hamiltonian [9,10,23,27-30]. This review contains the expressions for the steady state transition probabilities for the atom or molecule interacting with the applied fields, and a discussion of the computational aspects of the Riemann product integral technique for their evaluation as a function of frequency. The long time-(steady state) and (electromagnetic field) phase-averaged transition

probability as a function of frequency is the absorption spectrum for the atom or molecule. The Riemann product integral approach is used to generate the exact absorption spectra or resonance profiles for the two-level problems discussed in Chapters 3 and 4. These spectra, for example, are used to help discuss the validity of the RWA results for the absorption spectra as a function of the parameters of the problem.

Chapter 3 contains the derivation of the rotating wave approximation for the single- and multi-photon absorption spectra, or the resonance profiles, for a two-level system with non-zero permanent dipoles interacting with both applied static and sinusoidal electric fields. The result for the resonance profiles is an analytic function of the parameters of the problem, which include the strengths of the applied fields, the frequency and phase of the sinusoidal electromagnetic field, and the transition and permanent dipoles of the states involved in the transition. These "molecular" RWA N-photon resonance profiles are used to investigate the effects of permanent dipoles and static electric fields on the absorption spectra, both through the analytic nature of the result and through numerical comparison of RWA spectra with exact numerical spectra. This comparison is also used to help assess the validity of the RWA results as a function of the parameters of the problem.

Chapter 3 begins with a discussion of the Hamiltonian for the two-level molecule interacting with static and sinusoidal electric fields. The Hamiltonian is written in a static diagonalized representation which is convenient for obtaining and discussing the solution for the problem when the static field is non-zero [4]. The derivation of the molecular RWA result for the N-photon resonance profile is given in Sec. 3.2. The analytic expressions for the profiles, which are mathematically simple in the absence of an applied static electric field, are used to investigate, predict, and interpret some of the effects of permanent dipole moments and static electric fields on the absorption spectra of molecules and atoms. The limiting case, in which the permanent dipoles and the static field are zero, is the standard atomic RWA result discussed in Chapter 2 and further discussed in Sec. 3.3.1. The effects of permanent dipoles in the absence of a static field are discussed in Sec. 3.3.2, while the effects, both without and with permanent dipoles, in the presence of a static field are discussed in Sec. 3.3.3A and 3.3.3B, respectively. The contrast between the above results and the atomic results, in the absence of static fields, is emphasized. For example, for the two-level problem, the presence of permanent dipoles or a static electric field can lead to even as well as odd photon spectral transitions, whereas for atoms, in the absence of static fields, only odd photon transitions can occur.

The presence of permanent dipoles, or more precisely, a non-zero difference between the dipoles of the states involved in the transition, can lead to very narrow resonance profiles, with asymmetric oscillatory fringes about the main resonances, as compared to the relatively broader Lorentzian profile of the atomic case. An example of the importance of orientationally averaging molecular spectra, with respect to the orientation of the molecule relative to the direction of the applied electric fields, is given in Sec. 3.3.3B. This effect is molecular since dependence on orientation does not arise for an isotropic atom. In the presence of an applied static electric field, this effect can lead to interesting temperature-dependent absorption spectra which are sensitive to the magnitude and relative orientations of the permanent and transition dipoles involved in the transition.

Throughout Chapter 3, the RWA results for the resonance profiles or absorption spectra for a variety of two-level atoms and molecules are compared with the corresponding exact spectra obtained using the methods discussed in Sec. 2.4. The RWA expressions for the resonance profiles aid in the interpretation of the exact spectra; the exact results aid in the assessment of the validity of the RWA.. For strong electromagnetic fields, for example, the RWA results do not account for the shifts in the resonances in the single- and multi-photon absorption spectra from their weak field limits; this shift can

be either to lower or to higher frequency for molecules with permanent dipoles in contradistinction to the higher frequency [22,23] shift for atoms. In addition, the RWA resonance profiles do not provide the dynamic background and the overlapping single- and multi-photon resonances characteristic of strong electromagnetic field spectra.

The perturbation corrections to the RWA solution for the N-photon absorption spectrum for two-level systems, including the effects of permanent dipoles but not the effects of a static electric field, are derived in Chapter 4. These corrections are used to help investigate and explain the effects missing in the RWA, with particular emphasis on effects arising from permanent dipoles. After some preliminary work, Floquet theory and phase factoring techniques [31] are used in Sec. 4.2 to transform the original time-dependent wave equation into a time-independent Floquet Hamiltonian matrix description of the problem. The time-evolution operator for the system is then constructed in terms of the eigenvalues and eigenvectors of the Floquet Hamiltonian and a result for the absorption spectrum is obtained in terms of these quantities. In Sec. 4.3 almost degenerate perturbation theory [32,33] is applied to the Floquet secular equation, choosing the RWA as the zeroth order problem, and higher order perturbative corrections to the RWA expressions for the N-photon resonance profile, and its full width at half maximum, are obtained. Also derived are perturbative

expressions for the frequency shifts from the weak field resonance positions that apply for non-zero permanent dipoles and for an arbitrary N-photon transition. Expansions of the results for the resonance frequency shifts, and the full widths at half maximum of the N-photon resonance profiles, are obtained in powers of the couplings between the electromagnetic field and both the transition and permanent dipoles involved in the transition. There is agreement between the expansions for the frequency shift and the lead terms in the expansion obtained recently by Hattori and Kobayashi [34]; however, there is disagreement with respect to the results for the full widths at half maxima.

The relationship between the perturbative results and the RWA results, are discussed qualitatively in Sec. 4.3; the atomic results, obtained originally by Shirley [23], are obtained from both cases in the limit that the permanent dipole is zero. The analytical perturbation results obtained in Sec.4.3, together with numerical examples based on some of the models discussed in Chapter 3, are used in Secs. 4.3 and 4.4.1 to help explain some of the effects missing in the molecular RWA and its atomic limit. The numerical examples are also used to help discuss the validity of the perturbative corrections to the RWA for the N-photon molecular resonance profile and related quantities. The various examples studied indicate convergence difficulties with the perturbative corrections

which limit their computational use as a function of the electromagnetic field-transition and permanent dipole couplings. However, these corrections are very useful in understanding some of the important effects missing in the RWA treatment of the problem. A further discussion of the spectra of molecules with large permanent dipoles is given in Sec. 4.4.2 with illustrative examples evaluated using the exact approaches to the solution of the problem, discussed in Sec. 2.4, which avoid the difficulties associated with perturbative methods. This discussion relates that of Sec. 3.3.2 with recent literature material [34,35] on "giant dipole molecules".

A summary of some of the more important results arising from this work is given in Chapter 5.

Atomic units [36] are used throughout this thesis. The relevant units and their conversion factors [37] to S.I. units are listed below:

Atomic Unit	Value in S.I. Units
Charge (e)	1.6022×10^{-19} C
Length (a_0)	5.2918×10^{-11} m
Mass (m_e)	9.1095×10^{-31} kg
Angular momentum ($\hbar$)	1.0546×10^{-34} Js
Time	2.4189×10^{-17} s
Frequency	4.1341×10^{-16} s^{-1}
Energy (hartree)	4.3598×10^{-18} J
Electric dipole moment (ea_0)	8.4784×10^{-30} Cm
Electric field amplitude (ea_0^{-2})	5.1423×10^{11} Vm^{-1}

CHAPTER 2

GENERAL DISCUSSION OF SOLUTIONS TO THE TIME-DEPENDENT WAVE EQUATION

This chapter contains a general review of various approaches for solving the time-dependent wave equation. Both approximate and exact methods are discussed with emphasis being placed on those methods relevant to the remainder of this thesis.

2.1 The Dirac Variation of Constants Method for Solving the Time-Dependent Schrödinger Equation

The interaction of atoms or molecules with an applied external time-dependent perturbation (e.g. electric fields, magnetic fields) is described by the time-dependent Schrodinger equation [13-15]

$$i\frac{d}{dt}\Psi(\underline{r},t) = H(\underline{r},t)\Psi(\underline{r},t) \qquad (2.1.1)$$

where $\Psi(\underline{r},t)$ is the exact time-dependent wave function and $H(\underline{r},t)$ is the total Hamiltonian operator which is comprised of two terms

$$H(\underline{r},t) = H_o(\underline{r}) + V(\underline{r},t) \qquad (2.1.2)$$

Here $\underline{r}$ denotes the spatial dependence of all the particles in the system and t represents time. $V(\underline{r},t)$ represents the interaction of an atom or molecule with an applied time-

dependent field.

$H_o(\underline{r})$ is the unperturbed or stationary state Hamiltonian which is independent of time and corresponds to no perturbation ($V(\underline{r},t) = 0$) in Eq. (2.1.2). Under this condition Eq. (2.1.1) simplifies to

$$i\frac{d}{dt}\Psi(\underline{r},t) = H_o(\underline{r})\Psi(\underline{r},t) = E\,\Psi(\underline{r},t) \qquad (2.1.3)$$

where E is the energy of the unperturbed system. Eq. (2.1.3) is a differential equation, separable in time, which is easily solved to give the time-dependence of the stationary state wave functions [14,15]

$$\Psi_k(\underline{r},t) = \phi_k(\underline{r})\exp(-iE_kt) \qquad (2.1.4)$$

The time-independent wave functions and stationary state energies, $\phi_k(\underline{r})$ and E_k respectively, are obtained by solving the Schrödinger time-independent wave equation

$$H_o(\underline{r})\phi_k(\underline{r}) = E_k\phi_k(\underline{r}) \qquad (2.1.5)$$

subject to the usual boundary conditions of quantum mechanics. Here k is a set of quantum numbers specifying the allowed stationary states of the $H_o(\underline{r})$ system.

In what follows, the stationary state information is often taken as given. The difficult problem of including the time-dependent perturbation, $V(\underline{r},t)$, in Eq. (2.1.1) was

first discussed using the Variation of Constants technique, by Dirac [12-15]. In this method, the wave function is written in the interaction representation as a sum involving the complete basis set of orthonormal wave functions, $\phi_k(\underline{r})$, for the unperturbed stationary state problem. Thus

$$\Psi(\underline{r},t) = \sum_{k=1}^{\infty} b_k(t)\phi_k(\underline{r})\exp(-iE_kt) \qquad (2.1.6)$$

where the $b_k(t)$ are time-dependent coefficients. Using Eqs. (2.1.5) and (2.1.6) in Eq. (2.1.1) yields, after some simplification,

$$i\sum_{k=1}^{\infty}\frac{db_k(t)}{dt}\phi_k(\underline{r})\exp(-iE_kt) = \sum_{k=1}^{\infty} b_k(t)V(\underline{r},t)\phi_k(\underline{r})\exp(iE_kt) \qquad (2.1.7)$$

This equation is then multiplied by $\phi_j^*(\underline{r})$ and integrated over all configuration space giving

$$i\frac{db_j(t)}{dt} = \sum_{k=1}^{\infty} b_k(t)V_{jk}(t)\exp(i[E_k - E_j]t) \quad , \quad j = 1,2,\ldots,\infty \qquad (2.1.8)$$

where

$$V_{jk}(t) = \langle \phi_j(\underline{r}) | V(\underline{r},t) | \phi_k(\underline{r}) \rangle$$

$$= \int \phi_j^*(\underline{r}) V(\underline{r},t) \phi_k(\underline{r}) d\tau \qquad (2.1.9)$$

The coefficients $b_k(t)$ are determined by solving the coupled set of differential equations given by Eq. (2.1.8) subject to the initial conditions. These conditions stipulate which stationary states are populated before the time-dependent perturbation $V(\underline{r},t)$ is switched on at $t = t_0$.

The time-dependent population of each state, given by $|b_k(t)|^2$ and depending on the parameters which define the molecule and on the applied perturbation, will be discussed in more detail later for the interaction of an atom or molecule with a sinusoidal electromagnetic field (continuous wave laser). Further, if Eqs. (2.1.8) are solved exactly for a problem with a self-adjoint Hamiltonian, the time-dependent wave function given by Eq. (2.1.6) is normalized for all time t,

$$\langle \Psi(\underline{r},t) | \Psi(\underline{r},t) \rangle = \sum_{k=1}^{\infty} |b_k(t)|^2 = 1 \qquad (2.1.10)$$

if it is normalized at $t = 0$ [38].

The time-dependent Schrödinger equation and the solution discussed above neglect relaxation or decay effects. These can be treated phenomenologically [1,17,28,39-42] by introducing appropriate radiative widths, γ_k, for the energy levels E_k being considered.

This is done by replacing the stationary state energy eigenvalues E_k by $E_k - \frac{1}{2}i\gamma_k$ where γ_k accounts for spontaneous decay processes or other mechanisms of decay that give excited states a finite lifetime relative to the ground state of the atom or molecule under consideration. The time-dependent wave function for state k is then given by

$$\Psi_k(\underline{r},t) = \phi_k(\underline{r})\exp(-i[E_k-\tfrac{1}{2}i\gamma_k]t) \qquad (2.1.11)$$

where the imaginary part of the "energy", γ_k, is normally much smaller than the real part E_k. The time-dependent wave function is now written as

$$\Psi(\underline{r},t) = \sum_{k=1}^{\infty} b_k(t)\phi_k(\underline{r})\exp(-iE_kt) \qquad (2.1.12)$$

where

$$b_k(t) = \bar{b}_k(t)\exp(-\tfrac{1}{2}\gamma_kt) \qquad (2.1.13)$$

Substitution of this result into the time-dependent wave equation, followed by manipulations similar to those leading to Eq. (2.1.8), yields a set of coupled differential equations for the $\bar{b}_k(t)$ which include decay effects;

$$i\frac{d\tilde{b}_j(t)}{dt} = \sum_{k=1}^{\infty} \tilde{b}_k(t)V_{jk}(\underline{r},t)\exp(-i[(E_k-E_j)-\tfrac{1}{2}(\gamma_k-\gamma_j)]t)$$

(2.1.14)

Neglecting $V(\underline{r},t)$ yields $\tilde{b}_j(t)$ = constant and a state amplitude which decays exponentially with time in the absence of an external field

$$b_k(t) = (\text{constant})\exp(-\tfrac{1}{2}\gamma_k t) \ , \ V(\underline{r},t) = 0$$

(2.1.15)

and

$$|b_k(t)|^2 = (\text{constant})\exp(-\gamma_k t) \ , \ V(\underline{r},t) = 0$$

(2.1.16)

Eq. (2.1.16) is the familiar exponential decay law [1,17,39] for excited atomic and molecular states in the absence of an external perturbation. The system of differential equations given by Eq. (2.1.14) corresponds to a time-dependent Hamiltonian that is not self-adjoint. Thus the solution for the time-dependent wave function including decay effects will not be unitary, and the normalization condition given by Eq. (2.1.10) no longer applies [38]. Unless indicated otherwise, decay or relaxation effects will be neglected in what follows.

2.2 Time-Dependent Perturbation Theory

Perturbation theory can be used to obtain approximate solutions to Eq. (2.1.1) which are valid when the perturbation $V(\underline{r},t)$ and the times over which it operates, are small. As a specific example we consider the perturbation representing the interaction of an atom or molecule with a sinusoidal plane polarized time-dependent electric field, $\underline{E}(t)$, given by [43]

$$\underline{E}(t) = \hat{\epsilon}\,\mathcal{E}\cos(\omega t + \delta) \qquad (2.2.1)$$

where $\hat{\epsilon}$ is the unit vector in the direction of the polarization of the field; $\mathcal{E}$, ω and δ are the amplitude, circular frequency and phase, respectively, of the electromagnetic field, and μ is the electric dipole moment operator for the atom or molecule. The perturbation is given by $V(\underline{r};t) = -\mu\cdot\underline{E}(t)$. In order to identify the resonances in the transition probabilities it is often convenient to write $V(\underline{r},t)$ as

$$V(\underline{r},t) = -\tfrac{1}{2}\,\mu\cdot\hat{\epsilon}\mathcal{E}[\exp(i[\omega t+\delta]) + \exp(-i[\omega t+\delta])] \qquad (2.2.2)$$

Following the standard methods of time-dependent perturbation theory [13,16], a perturbation expansion of the coefficients $b_g(t)$ occurring in the interaction representation expansion of the time-dependent wave

function, Eq. (2.1.6), is made,

$$b_\ell(t) = \sum_{n=0}^{\infty} b_\ell^{(n)}(t) \quad , \ \ell = 1,2,... \tag{2.2.3}$$

where n is a perturbation counter associated with the perturbation $V(\underline{r},t)$ and $b_\ell^{(n)}(t)$ depends on the product of n terms involving $V(\underline{r},t)$. Substitution of Eqs. (2.2.2) and (2.2.3) into Eq. (2.1.8) leads to coupled differential equations for the $b_\ell^{(n)}(t)$,

$$\frac{d}{dt}b_\ell^{(n)}(t) = \frac{1}{2}\varepsilon\hat{e}\cdot\sum_{m=1}^{\infty}\mu_{\ell m}b_m^{(n-1)}(t)[\exp(i\delta)\exp(i[E_{\ell m}+\omega]t) + \exp(-i\delta)\exp(i[E_{\ell m}-\omega]t)] \tag{2.2.4}$$

where

$$E_{\ell m} = E_\ell - E_m \tag{2.2.5}$$

represents the energy separation between states ℓ and m and

$$\mu_{\ell m} = \langle\phi_\ell|\underline{\mu}|\phi_m\rangle \tag{2.2.6}$$

where $\mu_{\ell m}$ is taken to be real in what follows. If $\ell \neq m$, Eq. (2.2.6) corresponds to a transition dipole connecting the two states ℓ and m; if $\ell = m$, Eq. (2.2.6) corresponds to the permanent dipole of state m. Until very recently [3], most perturbation treatments of the time-dependent

wave equation have been carried out with $\mu_{\ell\ell} = 0$ and thus have implicitly corresponded to solutions for atoms in which each energy state involved in the transition has a definite parity. Much of this thesis will be concerned with the effects on single and multi photon spectra arising from non-zero permanent dipole moments, see Chapters 3 and 4. In what directly follows, the permanent dipole moments are set equal to zero.

Consider the atom or molecule to be in the pure ground state 1 before the perturbation is switched on at $t = 0$. This leads to the initial conditions

$$b_m(0) = \delta_{m,1} \quad , \quad m = 1,2, \qquad (2.2.7)$$

which, when substituted into Eq. (2.2.3), leads to

$$b_m^{(0)} = \delta_{m,1} \quad ; \quad b_m^{(s)} = 0 \quad , \quad s \neq 0 \qquad (2.2.8)$$

Solving Eq. (2.2.4), subject to Eqs. (2.2.7) and (2.2.8), for $n = 1$ gives [13-15]

$$b_\ell^{(1)}(t) = \tfrac{1}{2}\mu_{\ell 1}\mathcal{E}\{\exp(i\delta)(E_{\ell 1}-\omega)^{-1}(\exp(i(E_{\ell 1}+\omega)t)-1) + \exp(-i\delta)(E_{\ell 1}-\omega)^{-1}(\exp(i(E_{\ell 1}-\omega)t)-1)\} \qquad (2.2.9)$$

Often it is the resonant or near resonant ($E_{\ell 1} \approx \omega$) absorption of electromagnetic radiation that is of interest. This absorption corresponds to the transition of a photon of frequency ω from the initial state 1 to state ℓ with $E_{\ell 1} > 0$. Under this condition the second term in Eq. (2.2.9) is much larger than the first term. Hence the first term can be discarded and the transition probability, for the transition from state 1 to state ℓ by the absorption of a photon of circular frequency $\omega \approx E_{\ell 1}$, is approximately given by

$$P_\ell^{(1)}(t) \approx |b_\ell^{(0)} + b_\ell^{(1)}(t)|^2 = |b_\ell^{(1)}(t)|^2$$

$$\approx |\underline{\mu}_{\ell 1} \cdot \hat{e}\varepsilon|^2 (E_{\ell 1}-\omega)^{-2} \sin^2(\tfrac{1}{2}[E_{\ell 1}-\omega]t) \qquad (2.2.10)$$

When the absorption is exactly on resonance, $E_{\ell 1}-\omega = 0$, and Eq. (2.2.10) simplifies further to

$$P_\ell^{(1)}(t) \approx \tfrac{1}{4}|\underline{\mu}_{\ell 1} \cdot \hat{e}\varepsilon|^2 t^2 \qquad (2.2.11)$$

The transition probability given in Eq. (2.2.11) is directly proportional to t^2 and hence tends to infinity for long times. This is an example of the secular divergences [13] which arise in time-dependent perturbation theory; they are present even if all terms are retained when calculating $P_\ell^{(1)}(t)$ and cannot be removed by going to higher orders in perturbation theory [44,45]. Quasi

secular divergences [45] arise when $E_{\ell 1} \sim \omega$ in the denominator of Eq. (2.2.10) and are unique to the oscillating field perturbation problem. These divergences are generally handled by introducing the radiative width of the excited state, see Eq. (2.1.11), and making the appropriate modifications to the perturbation equations [46].

The solution for $b_\ell^{(n)}(t)$ becomes very complicated as n becomes large, but by retaining only terms that have denominators involving $(E_{\ell 1}-n\omega)$ a generalized approximate expression for the n-photon induced transition probability from state 1 to state ℓ can be obtained and is given by [1,3]

$$P_\ell^{(n)}(t) = 4(\tfrac{1}{2}\varepsilon)^{2n}|C^{(n)}|^2(E_{\ell 1}-n\omega)^{-2}\sin^2[\tfrac{1}{2}(E_{\ell 1}-n\omega)t] \tag{2.2.12}$$

where

$$C^{(n)} = \sum_{k_1}\sum_{k_2}\cdots\sum_{k_{n-1}\neq 1}^{\infty}\frac{(\hat{e}\cdot\mu_{\ell k_1})(\hat{e}\cdot\mu_{k_1 k_2})\cdots(\hat{e}\cdot\mu_{k_{n-1}1})}{[E_{k_1 1}-(n-1)\omega][E_{k_2 1}-(n-2)\omega]\cdots[E_{k_{n-1}1}-\omega]} \tag{2.2.13}$$

Thus multi-photon transitions are predicted when perturbation theory is carried to higher orders [21,47]. These higher order perturbation results are necessary to help understand some of the effects observed with intense monochromatic light sources. Some of these include multi-photon ionization (MPI) of atoms and collisionless

multi-photon dissociation (MPD) and excitation (MPE) of polyatomic molecules upon interaction with intense electromagnetic fields [48,49].

The basic types of level configurations needed to observe the n-photon non-linear transitions can be predicted by using Eq. (2.2.I3) and the parity selection rules for the dipole matrix elements, μ_{ij}. For example, consider a two-level system with states of opposite parity. The selection rules indicate that only odd transitions can occur between the two states. To observe even photon transitions, one needs three states with the initial and final states of the same parity and the remaining state with opposite parity.

Eq. (2.2.12) is useful for predicting n-photon transitions but is restricted to small couplings and small times and still has the inherent problem of secular and quasi secular divergences. One method for removing these divergences is to make use of the rotating wave approximation.

2.3 The Rotating Wave Approximation

The need for more reliable solutions, free of the problems caused by the secular divergences present in perturbation theory, lead Rabi [18] to develop a different approach for solving the time-dependent Schrödinger equation. In this so-called rotating wave approximation (RWA) [17,19,20], all off-resonance or counter-rotating

terms are discarded before the differential equations are solved. Originally, Rabi developed the RWA to solve, exactly, the problem of a two-level, spin ½ system interacting with a rotating magnetic field. The RWA was later applied as a zeroth order approximation in a perturbation treatment of the oscillating field problem of particular interest in this thesis [22]. Since this approximation is restricted to interactions on or near resonance, where $E_{\ell m} \approx \omega$, the analysis of systems with more than two levels becomes highly specific to the actual level configuration [31,40,50-52]. Thus only the two-level RWA is examined here.

The two-level atomic system ($\mu_{11} = 0$) is described by two coupled time-dependent differential equations obtained from Eq. (2.1.8), with $j = 1,2$ and $k = 1,2$, through the use of Eq. (2.2.2);

$$i\frac{db_j(t)}{dt} = -\frac{1}{2}\sum_{k=1}^{2}\mu_{jk}\cdot\hat{\varepsilon}\,b_k(t)\left[\exp(-i[E_{kj}-\omega]t)\exp(i\delta)\right.$$

$$\left. + \exp(-i[E_{kj}+\omega]t)\exp(-i\delta)\right] \quad , \quad j = 1,2 \tag{2.3.1}$$

A solution of these equations is sought for frequencies near resonance with E_{21}, that is for $\omega \approx E_{21} > 0$. The problem of secular or quasi secular divergences does not arise in an approximate solution to Eq. (2.3.1) if the rapidly varying terms $\exp(\pm i[E_{21}+\omega]t)$ are neglected

relative to the slowly varying terms $\exp(\pm i[E_{21}-\omega]t)$ before attempting to obtain the solution. The resulting differential equations are given by

$$i\frac{db_1(t)}{dt} = -\frac{1}{2}\,\underline{\mu}_{12}\cdot\hat{e}\varepsilon\exp(-i[E_{21}-\omega]t)\exp(i\delta)b_2(t) \tag{2.3.2}$$

$$i\frac{db_2(t)}{dt} = -\frac{1}{2}\,\underline{\mu}_{12}\cdot\hat{e}\varepsilon\exp(i[E_{21}-\omega]t)\exp(-i\delta)b_1(t) \tag{2.3.3}$$

and their solution can be obtained as a special case of the solution of a more complicated problem, which retains the effects of $\underline{\mu}_{ii} \neq 0$, discussed in Chapter 3. The result for $b_2(t)$, subject to the initial conditions $b_1(0) = 1$, $b_2(0) = 0$ (see Eq. (2.2.7)), is given by

$$b_2(t) = i\left[\frac{\underline{\mu}_{12}\cdot\hat{e}\varepsilon}{p}\right]\exp(\tfrac{i}{2}[E_{21}-\omega]t)\exp(-i\delta)\sin(\tfrac{1}{2}pt) \tag{2.3.4}$$

where

$$p^2 = (E_{21}-\omega)^2 + |\underline{\mu}_{12}\cdot\hat{e}\varepsilon|^2 \tag{2.3.5}$$

and $\underline{\mu}_{12}\cdot\hat{e}\varepsilon$ is the coupling between the atoms and the applied sinusoidal field.

The time-dependent population of state 2 is then given by

$$|b_2(t)|^2 = \frac{|\mu_{12}\cdot\hat{e}\varepsilon|^2}{p^2}\sin^2(\tfrac{1}{2}pt) \qquad (2.3.5)$$

which is well behaved for long times. The population of state 1 is $|b_1(t)|^2 = 1 - |b_2(t)|^2$, see Eq. (2.1.10).

The RWA removes the problem of secular divergences. When $E_{21} = \omega$, the RWA solution given by Eq. (2.3.6), is bounded and oscillates with time. The first order perturbation solution, given by Eq. (2.2.10) with $f = 2$, is not well behaved for long times, see for example Eq. (2.2.11). If $|\mu_{12}\cdot\hat{e}\varepsilon| << (E_{21}-\omega)$, then Eq. (2.2.10) is recovered from Eq. (2.3.6) by retaining only the first term in the Taylor series expansion of $|b_2(t)|^2$, again indicating that the perturbation result is restricted to small couplings and small times.

While the RWA solution successfully treats the problem of secular and quasi secular divergences, it is applicable in its initial form only for the one-photon transition in atoms. To treat an N-photon transition, one needs to extract resonant terms of the form $\exp(i[E_{jk}-N\omega]t)$ where $N = 1,3,5,\ldots$. This work is discussed more generally for atoms and molecules in Chapter 3, and contains the RWA for atoms as a special case.

Bloch and Siegert [22] included the contributions of the off-resonance or counter-rotating terms in a first

order perturbation treatment of the one-photon atomic problem using the RWA as the zeroth order problem. These terms did not greatly affect the shape of the observed spectra but they did cause a shift from the RWA resonance position, $\omega_{res} = E_{21}$. The shift, through second order in the atom-electromagnetic field coupling, is given by

$$\omega_{res} = E_{21} + \frac{|\mu_{12} \cdot \theta\varepsilon|^2}{4 E_{21}} \qquad (2.3.7)$$

Higher order corrections have since been obtained [23,53-56] and will be discussed further in Chapter 4.

The problems associated with using the usual time-dependent perturbation theory approaches to solve the time-dependent wave equation, and with methods such as the RWA for treating the secular and quasi secular divergences arising in perturbation theory, can be avoided by solving the problem exactly.

2.4 Exact Solutions for the Time-Dependent Wave Equation

The exact numerical calculations discussed in this work are based on the Riemann product integral [11,24,57] or time-slicer [58] representation of the evolution operator for the system, see also [25], coupled with the use of Floquet's theory [23,26] which enables solutions to be obtained for all relevant times from those for the first period of the Hamiltonian. The use of Floquet theory assumes that the time-dependent Hamiltonian for the problem

is periodic in time and is the case of interest in this thesis. The approach outlined here replaces a previous method [27,28,59] in which a (matching) power series technique was employed to obtain the solution to the time-dependent wave equation over the first period of the Hamiltonian.

2.4.1 Matrix Formulation of the Time-Dependent Schrodinger Equation

In what follows, it is more convenient to use the Schrodinger representation of the time-dependent wave function. Using

$$b_j(t) = a_j(t)\exp(iE_jt) \tag{2.4.1}$$

transforms the Schrodinger equation from the interaction representation, see Eq. (2.1.8), into the Schrodinger representation. The resulting time-dependent Schrodinger equation for an N-level atom or molecule interacting with both static and time-dependent electric fields can be written in matrix form [60] as

$$i\frac{d}{dt}\underline{\underline{a}}(t) = \underline{\underline{H}}(t)\underline{\underline{a}}(t) \tag{2.4.2}$$

The corresponding result for the time-dependent wave equation, obtained by substituting Eq. (2.4.1) into Eq. (2.1.6), is given by

where $\hat{e}_S$ is the field unit vector and ε_S is the static field magnitude.

In what follows, a solution to Eq. (2.4.2) will be obtained by a numerical technique based on the Riemann product integral representation of the evolution operator.

2.4.2 The Riemann Product Integral Technique

The solution of Eq. (2.4.2) can be written in terms of the evolution operator in the following manner [26,61]:

$$\underline{a}(t) = \underline{U}(t;t_0)\underline{a}(t_0) \qquad (2.4.7)$$

where t_0 is the time the perturbation is switched on and $\underline{U}(t;t_0)$ is the time evolution operator or, as it is often called, the solution or integral matrix, that takes the solution from $t = t_0$ to the final time t. Substituting Eq. (2.4.7) into Eq. (2.4.2) yields

$$\frac{d}{dt}\underline{U}(t;t_0) = \underline{C}(t)\underline{U}(t;t_0) \qquad (2.4.8)$$

where

$$\underline{C}(t) = -i\underline{H}(t) \qquad (2.4.9)$$

and

$$\underline{U}(t_0;t_0) = \underline{I} \qquad (2.4.10)$$

where $\hat{e}_S$ is the field unit vector and ε_S is the static field magnitude.

In what follows, a solution to Eq. (2.4.2) will be obtained by a numerical technique based on the Riemann product integral representation of the evolution operator.

2.4.2 The Riemann Product Integral Technique

The solution of Eq. (2.4.2) can be written in terms of the evolution operator in the following manner [26,61]:

$$\underline{a}(t) = \underline{U}(t;t_0)\underline{a}(t_0) \qquad (2.4.7)$$

where t_0 is the time the perturbation is switched on and $\underline{U}(t;t_0)$ is the time evolution operator or, as it is often called, the solution or integral matrix, that takes the solution from $t = t_0$ to the final time t. Substituting Eq. (2.4.7) into Eq. (2.4.2) yields

$$\frac{d}{dt}\underline{U}(t;t_0) = \underline{C}(t)\underline{U}(t;t_0) \qquad (2.4.8)$$

where

$$\underline{C}(t) = -i\underline{H}(t) \qquad (2.4.9)$$

and

$$\underline{U}(t_0;t_0) = \underline{I} \qquad (2.4.10)$$

The time interval $[t_0,t]$ can be subdivided into n subintervals and, by making use of the group property of $\underline{\underline{U}}(t;t_0)$ [26,61], one obtains

$$\underline{\underline{U}}(t;t_0) = \underline{\underline{U}}(t,t_{n-1})\underline{\underline{U}}(t_{n-1},t_{n-2})\ldots\underline{\underline{U}}(t_2,t_1)\underline{\underline{U}}(t_1,t_0)$$

$$= T\prod_{k=1}^{n}\underline{\underline{U}}(t_k,t_{k-1}) \qquad (2.4.11)$$

where T is a time-ordering operator that arranges the product in chronological order from right to left.

If n is sufficiently large then each subinterval $[t_{k-1}, t_k]$ of length $\Delta t_k = t_k - t_{k-1}$ is small and $\underline{\underline{C}}(t)$ can be assumed to be constant over this interval with a value $\underline{\underline{C}}(t_k')$ where t_k' is an arbitrary point chosen in this subinterval. The solution of Eq. (2.4.8) for such a subinterval is

$$\underline{\underline{U}}(t_k,t_{k-1}) = \exp(\underline{\underline{C}}(t_k')\Delta t_k) \qquad (2.4.12)$$

The arbitrary point, t_k', in the interval $[t_k,t_{k-1}]$ can be chosen, by applying the mean value theorem [62], such that

$$\underline{\underline{C}}(t_k') = \frac{1}{\Delta t_k}\int_{t_{k-1}}^{t_k}\underline{\underline{C}}(t)dt \qquad (2.4.13)$$

Using Eqs. (2.4.12) and (2.4.13) in Eq. (2.4.11) yields

$$\underline{\underline{U}}(t;t_0) = T \prod_{k=1}^{n} \exp(\underline{\underline{C}}^{(k)}) \qquad (2.4.14)$$

where

$$\underline{\underline{C}}^{(k)} = \int_{t_{k-1}}^{t_k} \underline{\underline{C}}(t)dt \qquad (2.4.15)$$

Eq. (2.4.14) is the Riemann product integral representation of the evolution operator. The formal definition [63] of the Riemann product integral of $\underline{\underline{C}}(t)$ over $[t_0,t]$ is given by

$$\underline{\underline{U}}(t;t_0) = \lim_{m>0} T \prod_{k=1}^{n} \exp(\underline{\underline{C}}^{(k)}) \qquad (2.4.16)$$

where $m = \max \Delta t_k$ is the length of the longest subinterval $[t_{k-1},t_k]$ and the limit $m > 0$ implies limit $n > \infty$. The actual number of subintervals used depends on the problem, on the nature of $\underline{\underline{C}}(t)$ as a function of t, and on the desired accuracy of the solution.

In this thesis, a typical matrix element of $\underline{\underline{C}}(t)$, see Eqs. (2.4.9) and (2.4.5), is given by

$$C_{\ell m}(t) = i[E_\ell \delta_{\ell m} - \mu_{\ell m} \hat{e}_E \cos(\omega t+\delta) - \mu_{\ell m} \hat{e}_S \varepsilon_S] \qquad (2.4.17)$$

Substituting Eq. (2.4.17) into Eq. (2.4.15) yields

$$C_{\ell m}(k) = \frac{-i}{\omega}[(E_\ell \delta_{\ell m} - \underline{\mu}_{\ell m}\cdot\hat{e}_s\varepsilon_s)(\theta_k-\theta_{k-1}) - \underline{\mu}_{\ell m}\cdot\hat{e}\varepsilon(\sin(\theta_k)-\sin(\theta_{k-1}))] \quad (2.4.18)$$

which can be rewritten as

$$C_{\ell m}(k) = \frac{-i}{\omega}(\theta_k-\theta_{k-1})\left[E_\ell \delta_{\ell m} - \underline{\mu}_{\ell m}\cdot\hat{e}_s\varepsilon_s - 2\underline{\mu}_{\ell m}\cdot\hat{e}\varepsilon\cos(\tfrac{1}{2}[\theta_k+\theta_{k-1}])\ \frac{\sin(\tfrac{1}{2}[\theta_k-\theta_{k-1}])}{(\theta_k-\theta_{k-1})}\right] \quad (2.4.19)$$

where

$$\theta_n = \omega t_n + \delta \quad (2.4.20)$$

In the next section, the Riemann product integral representation of the evolution operator given by Eq. (2.4.14) will be used with Floquet theory to obtain solutions to Eq. (2.4.2) which are convenient for the evaluation of the absorption spectra for atoms or molecules.

2.4.3 Sinusoidal Electromagnetic Fields and the Floquet Method

Since $\underline{E}(t)$, and hence $\underline{H}(t)$ and $\underline{\underline{C}}(t)$, is periodic for all $t > t_0$, the evaluation of $\underline{\underline{U}}(t;t_0)$ and the transition probabilities for all t requires determining $\underline{\underline{U}}(t;t_0)$ over the time interval $[0,2\pi/\omega]$ only where $t_p = 2\pi/\omega$ is the

period of the electric field and we choose $t_0 = 0$ for this sinusoidal electric field problem. Only a brief discussion of the working equations for the evaluation of the transition probabilities will be given in this section. Complete derivations can be found in the literature [9,10,23,27-30,59].

Since the Hamiltonian in Eq. (2.4.2) is periodic such that

$$\underline{\underline{H}}(t + t_p) = \underline{\underline{H}}(t) \quad \text{where} \quad t_p = \frac{2\pi}{\omega} , \tag{2.4.21}$$

Floquet theory can be applied and the general solution of the time-dependent Schrodinger equation can be written as [26]

$$\underline{\underline{G}}(t) = \underline{\underline{Z}}(t)\exp(i\underline{\underline{Q}}t) \tag{2.4.22}$$

$\underline{\underline{G}}(t)$ is the general solution matrix of Eq. (2.4.2), $\underline{\underline{Z}}(t)$ is a periodic matrix such that

$$\underline{\underline{Z}}(t) = \underline{\underline{Z}}(t + t_p) \tag{2.4.23}$$

and $\underline{\underline{Q}}$ is a constant diagonal matrix. The Floquet form of the solution proves to be very useful in evaluating the steady state absorption spectrum of an atom or molecule [28]. It is discussed and applied further in Chapter 4.

By making use of the periodicity of $\underline{\underline{H}}(t)$, it can be shown that

$$\underline{\underline{a}}(\theta+2s\pi) = \underline{\underline{U}}(\theta,0)[\underline{\underline{U}}(2\pi,0)]^{s}\underline{\underline{c}}_0(\delta);\ 0 \leq \theta \leq 2\pi \tag{2.4.24}$$

with

$$\theta = \omega t + \delta \quad ; \quad s = 0,1,2,... \tag{2.4.25}$$

and

$$\underline{\underline{c}}_0(\delta) = \underline{\underline{U}}^{-1}(\delta,0)\underline{\underline{a}}(0) \tag{2.4.26}$$

where $\underline{\underline{a}}(0)$ is the initial $t = 0$ value of the coefficient matrix $\underline{\underline{a}}(t)$. It is clear from Eq. (2.4.24) that the evaluation of $\underline{\underline{a}}(t)$ requires knowledge of $\underline{\underline{U}}(\theta,0)$ only on the θ-interval $[0,2\pi]$.

While the time-evolution of a molecular system is important, it is the steady state or long time behaviour that is considered later in this thesis. The expression for the state amplitudes $\underline{\underline{a}}(\theta)$, given in Eq. (2.4.24), can be written [28], in Floquet form, as

$$\underline{\underline{a}}(\theta+2s\pi) = \underline{\underline{Z}}(\theta)\exp(i\underline{\underline{\Lambda}}[\theta+2s\pi])\underline{\underline{b}}_0(\delta) \tag{2.4.27}$$

where

$$\underline{\underline{b}}_0(\theta) = \underline{\underline{S}}^{-1}\underline{\underline{c}}_0(\theta) \qquad (2.4.28)$$

and

$$\underline{\underline{Z}}(\theta) = \underline{\underline{U}}(\theta,0)\ \underline{\underline{S}}\ \exp(-i\underline{\underline{\Delta}}\theta) = \underline{\underline{Z}}(\theta+2s\pi) \qquad (2.4.29)$$

$\underline{\underline{\Delta}}$ is a diagonal characteristic exponent matrix that is related to the complex eigenvalues, $\underline{\underline{\lambda}}$, of the unitary matrix $\underline{\underline{U}}(2\pi,0)$ in the following manner [28,64]

$$i\Delta_{jj} = -i\pi\ln(\lambda_j) \qquad (2.4.30)$$

$\underline{\underline{S}}$ is a square matrix whose columns are the orthonormal eigenvectors $(\underline{\underline{S}})_j$ of $\underline{\underline{U}}(2\pi,0)$, which correspond to the eigenvalues λ_j; $\underline{\underline{S}}^{-1}$ is the inverse of $\underline{\underline{S}}$. The advantage of working in the Schrodinger representation instead of in the interaction representation is that in the former the characteristic exponents correspond to dressed atom energies [23,28,65,66].

The time- and phase-dependent population (transition probability) for state j is given by $|a_j(t)|^2$. The phase-averaged temporal, and the phase- and long time-averaged, transition probabilities are defined by

$$\bar{P}_j(t) = \frac{1}{2\pi}\int_0^{2\pi} |a_j(t)|^2 d\theta \qquad (2.4.31)$$

and

$$\bar{P}_j = \lim_{T\to\infty} \frac{1}{T} \int_0^T P_j(t)dt \qquad (2.4.32)$$

respectively. The physically meaningful time-dependent behaviour of the transition probability is normally independent of the phase δ and corresponds to Eq. (2.4.31). The physically observed spectrum of the atom or molecule often corresponds to the phase- and long time-averaged transition probability given by Eq. (2.4.32) if the effects of the perturbation occur over time intervals which are short relative to the important relaxation times involved in the system [1,23,66-70]. If this condition is not satisfied damping effects must be included; see Sec. 2.1.

From Eq. (2.4.27) one obtains

$$|a_j(t)|^2 = \sum_{q=1}^{N} \sum_{s=1}^{N} Z_{jq}(\theta)\beta_{qs}(\theta,\delta)(Z_{js}(\theta))^* \qquad (2.4.33)$$

with N being the number of energy levels considered and

$$\beta_{qs}(\theta,\delta) = b_{0q}(\delta)(b_{0s}(\delta))^* \exp(i[\Delta_q-\Delta_s]\theta) \qquad (2.4.34)$$

Thus, from Eq. (2.4.31), the phase-averaged transition probability is

$$\bar{P}_j(t) = \sum_{q=1}^{N} \sum_{s=1}^{N} \exp(i[\Delta_q - \Delta_s]\omega t)\beta_{qs}^{j}(\omega t) \qquad (2.4.35)$$

where

$$\beta_{qs}^{j}(\omega t) = \tfrac{1}{2}\pi \int_0^{2\pi} Z_{jq}(\omega t+\theta)(Z_{js}(\omega t+\theta))^* b_{0q}(\theta)(b_{0s}(\theta))^* \times \exp(i[\Delta_q - \Delta_s]\theta)d\theta \qquad (2.4.36)$$

and, since $\underline{Z}(\theta)$ is periodic (see Eq. (2.4.29)),

$$\beta_{qs}^{j}(\omega t) = \beta_{qs}^{j}(\omega t+2s\pi) \qquad (2.4.37)$$

Using Eqs. (2.4.35) and (2.4.37) in Eq. (2.4.32) yields the following expression for the phase- and long time-averaged transition probability [28]

$$\bar{P}_j = \sum_{q=1}^{N} \tfrac{1}{2}\pi \int_0^{2\pi} \beta_{qq}^{j}(\theta')d\theta' , \qquad (2.4.38)$$

where $\theta' = \omega t$, since terms with $q \neq s$ in Eq. (2.4.35) average to zero in the long time-average; see, for example, Sec. 3.2. It is clear from Eq. (2.4.24) and Eqs. (2.4.35)-(2.4.38) that the phase- and time-dependent, the time-dependent phase-averaged, and the phase- and long time-averaged transition probabilities can all be evaluated once the evolution operator is obtained over the first period of the Hamiltonian.

Computational Aspects

The calculations for a given set of parameters defining the problem are carried out using the following procedure:

(1) The evolution operator is evaluated on the interval $[0,2\pi]$ by making use of Eq. (2.4.14). First $\underline{\underline{C}}^{(k)}$ is diagonalized and written as

$$\underline{\underline{C}}^{(k)} = \underline{\underline{L}}^{(k)} \underline{\underline{\Lambda}}^{(k)} (\underline{\underline{L}}^{(k)})^{-1} \tag{2.4.39}$$

where $\underline{\underline{L}}^{(k)}$ contains the eigenvectors of $\underline{\underline{C}}^{(k)}$, $(\underline{\underline{L}}^{(k)})^{-1}$ is the inverse matrix of $\underline{\underline{L}}^{(k)}$, and $\underline{\underline{\Lambda}}^{(k)}$ is a diagonal matrix containing the eigenvalues of $\underline{\underline{C}}^{(k)}$. By using the Taylor series expansion for exp(x), one can show that

$$\exp(\underline{\underline{C}}^{(k)}) = \sum_{n=0}^{\infty} \frac{1}{n!} (\underline{\underline{L}}^{(k)} \underline{\underline{\Lambda}}^{(k)} (\underline{\underline{L}}^{(k)})^{-1})^n$$

$$= \underline{\underline{L}}^{(k)} \exp(\underline{\underline{\Lambda}}^{(k)}) (\underline{\underline{L}}^{(k)})^{-1} \tag{2.4.40}$$

Substituting Eq. (2.4.40) into Eq. (2.4.14) yields

$$\underline{\underline{U}}(t;t_0) = T \prod_{k=1}^{n} [\underline{\underline{L}}^{(k)} \exp(\underline{\underline{\Lambda}}^{(k)}) (\underline{\underline{L}}^{(k)})^{-1}] \tag{2.4.41}$$

which is used to evaluate the evolution operator.

(2) Once $\underline{U}(2\pi,0)$ is calculated it is diagonalized in order to obtain the eigenvalues, λ_j, and eigenvectors $(\underline{S})_j$ from which $\underline{S}$ and $\underline{S}^{-1}$ are constructed.

(3) The λ_j are used to evaluate the characteristic exponents through [28,64,66]

$$\Delta_{jj} = \tfrac{1}{2\pi} \tan^{-1}\left[\frac{\text{Im } \lambda_j}{\text{Re } \lambda_j} \right] \qquad (2.4.42)$$

(4) $\underline{b}_0(\delta)$ and $\underline{Z}(\theta)$ are determined from Eqs. (2.4.28) and (2.4.29) respectively.

(5) The various transition probabilities are obtained from Eqs. (2.4.33), (2.4.35) and (2.4.38).

The above procedure was used to evaluate the "exact" absorption spectra discussed in subsequent chapters of this thesis. When using the Riemann product integral method in step (1), the $[0,2\pi]$ interval in θ was subdivided into 180 subintervals. Simpson's rule [71] with 30 quadrature points was used to evaluate the phase- and time-averages occurring in Eqs. (2.4.36) and (2.4.38). This lead to much more than graphical accuracy for the resulting absorption spectra [72]. The diagonalization process was performed using the Eispack library with the subroutines RS and CG [75].

CHAPTER 3

TWO-LEVEL ROTATING WAVE APPROXIMATION INCLUDING THE EFFECTS OF PERMANENT DIPOLES AND A STATIC ELECTRIC FIELD

In this chapter rotating wave types of approximations (RWA's) are derived for the single- and multi-photon absorption spectra or resonance profiles for a two-level system, with non-zero diagonal dipole matrix elements or "permanent dipole moments", interacting with both applied static and sinusoidal electric fields (see Eqs. (2.4.6) and (2.2.1) respectively). In the appropriate limit the results reduce to the usual atomic two-level RWA expressions discussed in Sec. 2.3. The analytic expressions for the resonance profiles derived in Sec. 3.2, which are particularly simple in the absence of an applied static field, are used to explain and illustrate some of the effects of permanent dipole moments and static electric fields on the absorption spectra of atoms and molecules in Sec. 3.3. Comparison with exact two-level calculations, carried out using the techniques outlined in Sec. 2.4, are used to help assess the validity of the RWA results for the resonance profiles as a function of the parameters specifying the atom/molecule-applied fields interaction. Some mathematical preliminaries are outlined in what follows.

3.1 Preliminaries

In the Schrodinger representation the two-level problem is described by the wave function $\Psi(\underline{r},t) = \sum_{i=1}^{2} a_i(t)\phi_i(\underline{r})$ such that $|a_1(t)|^2 + |a_2(t)|^2 = 1$. The time-evolution of this system, upon interaction with both static and time-dependent electric fields, is determined by the solution of

$$i\frac{d}{dt}\underline{a}(t) = \underline{H}(t)\underline{a}(t)$$

$$= \left[\begin{bmatrix} E_1 & 0 \\ 0 & E_2 \end{bmatrix} - (\hat{e}_S\varepsilon_S + \underline{E}(t)) \cdot \begin{bmatrix} \mu_{11} & \mu_{12} \\ \mu_{21} & \mu_{22} \end{bmatrix}\right]\begin{bmatrix} a_1(t) \\ a_2(t) \end{bmatrix} \qquad (3.1.1)$$

where E_1 and E_2 are the energies of states 1 and 2, $\hat{e}_S$ is the unit vector in the direction of the static field, ε_S is the magnitude of the static field, $\underline{E}(t)$ is the time dependent field and μ_{ij} is defined in Eq. (2.2.6).

Since multiples of the unit matrix additive within $\underline{H}(t)$ do not affect the probabilities, $|a_j(t)|^2$, of finding the system in state j as a function of time, a simplification is obtained by removing the traces in $\underline{\mu}$ and $\underline{E}$ from the other terms [4].

By defining

$$\underline{m} = \tfrac{1}{2}(\underline{\mu}_{11} + \underline{\mu}_{22}) \; ; \; \underline{d} = (\underline{\mu}_{22} - \underline{\mu}_{11}) \qquad (3.1.2)$$

$$E_0 = \tfrac{1}{2}(E_1 + E_2) \quad ; \Delta E = (E_2 - E_1) > 0 \,, \qquad (3.1.3)$$

The Hamiltonian occurring in Eq. (3.1.1) can be written as follows

$$\underline{\underline{H}}(t) = \begin{bmatrix} E_0 - \frac{1}{2}\Delta E & 0 \\ 0 & E_0 + \frac{1}{2}\Delta E \end{bmatrix} - (\hat{e}_S \varepsilon_S + \underline{E}(t)) \cdot \begin{bmatrix} \underline{m} - \frac{1}{2}\underline{d} & \underline{\mu}_{12} \\ \underline{\mu}_{21} & \underline{m} + \frac{1}{2}\underline{d} \end{bmatrix}$$

$$= [E_0 - (\hat{e}\varepsilon_S + \underline{E}(t)) \cdot \underline{m}] \begin{bmatrix} 1 & 0 \\ 0 & 1 \end{bmatrix}$$

$$+ \tfrac{1}{2}[\Delta E - \underline{d} \cdot (\hat{e}_S \varepsilon_S + \underline{E}(t))] \begin{bmatrix} -1 & 0 \\ 0 & 1 \end{bmatrix} - [\hat{e}_S \varepsilon_S + \underline{E}(t)] \cdot \underline{\mu}_{12} \begin{bmatrix} 0 & 1 \\ 1 & 0 \end{bmatrix}, \qquad (3.1.4)$$

where we take $\underline{\mu}_{21} = \underline{\mu}_{12}$. The substitution

$$a_j(t) = c_j(t) \exp(-i[E_0 t - \hat{e}_S \varepsilon_S \cdot \underline{m} t - \underline{m} \cdot \int_0^t E(t')dt']) \qquad (3.1.5)$$

is then made where $c_j(t)$ satisfies

$$i\frac{d}{dt}\,\underline{c}(t) = \underline{\underline{\mathcal{H}}}(t)\underline{c}(t) \qquad (3.1.6)$$

$\underline{\underline{\mathcal{H}}}(t)$ is that part of $\underline{\underline{H}}(t)$ not involving the unit matrix and clearly

$$|a_j(t)|^2 = |c_j(t)|^2 \qquad (3.1.7)$$

In what follows, $\underline{\underline{\mathcal{H}}}(t)$ is transformed to a static Hamiltonian diagonalized representation following [4].

The effective Hamiltonian matrix $\underline{\underline{\mathcal{H}}}(t)$ can be written as a static field dependent term and a time-dependent field dependent term as follows

$$\underline{\underline{\mathcal{H}}}(t) = \left[\tfrac{1}{2}(\Delta E - \underline{d}\cdot\hat{e}_S\mathcal{E}_S)\begin{bmatrix}1 & 0\\ 0 & 1\end{bmatrix} \quad \mu_{12}\cdot\hat{e}_S\mathcal{E}_S\begin{bmatrix}0 & 1\\ 1 & 0\end{bmatrix}\right]$$
$$+ \left[-\tfrac{1}{2}\underline{d}\cdot\underline{E}(t)\begin{bmatrix}1 & 0\\ 0 & 1\end{bmatrix} - \mu_{12}\cdot\underline{E}(t)\begin{bmatrix}0 & 1\\ 1 & 0\end{bmatrix}\right]$$
$$= \underline{\underline{H}}_S + \underline{\underline{V}}(t) \qquad (3.1.8)$$

The solution of Eq. (3.1.6) can be further simplified by diagonalizing $\underline{\underline{H}}_S$ by a rotation through an angle θ [4,76] defined by

$$\underline{\underline{R}}_\theta = \begin{bmatrix}\cos\theta & \sin\theta\\ \sin\theta & \cos\theta\end{bmatrix} \qquad (3.1.9)$$

Thus

$$\underline{\underline{H}}_\theta(t) = \underline{\underline{R}}_\theta\underline{\underline{\mathcal{H}}}(t)\underline{\underline{R}}_\theta^{-1}$$
$$= \underline{\underline{H}}_{S,\theta} + \underline{\underline{V}}_\theta(t) \qquad (3.1.10)$$

The static field dependent term is now given by

$$\underline{\underline{H}}_{s,\theta} = \underline{\underline{R}}_{\theta}\underline{\underline{H}}_{s}\underline{\underline{R}}_{\theta}^{-1}$$

$$= \tfrac{1}{2}(\Delta E - \underline{d}\cdot\hat{e}_s\varepsilon_s)\begin{bmatrix} -\cos 2\theta & \sin 2\theta \\ \sin 2\theta & \cos 2\theta \end{bmatrix} - \underline{\mu}_{12}\cdot\hat{e}_s\varepsilon_s\begin{bmatrix} \sin 2\theta & \cos 2\theta \\ \cos 2\theta & -\sin 2\theta \end{bmatrix} \qquad (3.1.11)$$

Requiring $\underline{\underline{H}}_{s,\theta}$ to be diagonal gives

$$\tfrac{1}{2}(\Delta E - \underline{d}\cdot\hat{e}_s\varepsilon_s)\sin 2\theta - \underline{\mu}_{12}\cdot\hat{e}_s\varepsilon_s\cos 2\theta = 0 \qquad (3.1.12)$$

which yields

$$\tan 2\theta = (2\underline{\mu}_{12}\cdot\hat{e}_s\varepsilon_s)(\Delta E - \underline{d}\cdot\hat{e}_s\varepsilon_s)^{-1} \qquad (3.1.13)$$

and then

$$\cos 2\theta = \gamma^{-1}(\Delta E - \underline{d}\cdot\hat{e}_s\varepsilon_s) \; ; \; \sin 2\theta = \gamma^{-1}(2\underline{\mu}_{12}\cdot\hat{e}_s\varepsilon_s) \qquad (3.1.14)$$

where

$$\gamma = [(\Delta E - \underline{d}\cdot\hat{e}_s\varepsilon_s)^2 + 4(\underline{\mu}_{12}\cdot\hat{e}_s\varepsilon_s)^2]^{\frac{1}{2}} \qquad (3.1.15)$$

$\underline{\underline{H}}_{s,\theta}$ can be simplified by using Eqs. (3.1.14) and (3.1.15) to yield

$$\underline{\underline{H}}_{s,s} = \tfrac{1}{2}\gamma\begin{bmatrix} -1 & 0 \\ 0 & 1 \end{bmatrix} \qquad (3.1.16)$$

The time-dependent term in $\underline{\underline{H}}_\theta(t)$ is then given by

$$\underline{\underline{V}}_\theta(t) = \underline{\underline{R}}_\theta \underline{\underline{V}}(t) \underline{\underline{R}}_\theta^{-1}$$

$$= -\tfrac{1}{2}\underline{d}\cdot\underline{E}(t)\begin{bmatrix} \cos 2\theta & \sin 2\theta \\ \sin 2\theta & \cos 2\theta \end{bmatrix}$$

$$\mu_{12}\cdot\underline{E}(t)\begin{bmatrix} \sin 2\theta & \cos 2\theta \\ \cos 2\theta & \sin 2\theta \end{bmatrix} \qquad (3.1.17)$$

which can be written, using Eqs (3.1.14) and (3.1.15), as

$$\underline{\underline{V}}_S(t) = \tfrac{1}{2} D\cdot\underline{E}(t)\begin{bmatrix} 1 & 0 \\ 0 & 1 \end{bmatrix} - M\, E(t)\begin{bmatrix} 0 & 1 \\ 1 & 0 \end{bmatrix} \qquad (3.1.18)$$

where

$$D = d\cos 2\theta \quad 2\mu_{12}\sin 2\theta \qquad (3.1.19)$$

and

$$M = \mu_{12}\cos 2\theta + \tfrac{1}{2}d\sin 2\theta \qquad (3.1.20)$$

The matrix representation of the coupled differential equations, given by Eq (3.1.6), in the static Hamiltonian diagonalized representation is

$$i\frac{d}{dt}\underline{c}_S(t) = (\underline{\underline{H}}_{S\,\mathrm{diag}} + \underline{\underline{V}}_S(t))\underline{c}_S(t) \qquad (3.1.21)$$

where

$$\underline{c}_S(t) = \begin{bmatrix} c_{S-}(t) \\ c_{S+}(t) \end{bmatrix} \qquad (3.1.22)$$

The transformation from the static diagonal representation to the original (1,2) representation is given by

$$\underline{c}(t) = \underline{R}_S^{-1}\, \underline{c}_S(t) \qquad (3.1.23)$$

where $\underline{R}_S$ is given by Eq. (3.1.9) with the angle 2θ defined by Eq. (3.1.4). The angle θ is selected such that in the limit that $\theta \to 0$ (i.e. $\varepsilon_S \to 0$), the state $|s-\rangle \to |1\rangle$ and $|s+\rangle \to |2\rangle$. Thus

$$\cos\theta = \frac{1}{\sqrt{2}}\,(1 + \cos 2\theta)^{\frac{1}{2}} > 0 \; ; \; \sin\theta = \frac{1}{\sqrt{2}}\,(1 - \cos 2\theta)^{\frac{1}{2}} S \qquad (3.1.24)$$

where S is the sign of $\sin\theta$ and is determined from the expression given for $\sin 2\theta$ in Eq. (3.1.14) with $-\frac{\pi}{2} \leq \theta \leq \frac{\pi}{2}$ [4].

Mathematically convenient expressions for the spectra in the (1,2) representation, that are useful for the analysis of the effects of permanent dipole moments and static electric fields on the single- and multi-photon spectra of atoms and molecules, can be obtained by using the following initial conditions to solve Eq. (3.1.21);

$$a_1(0) = 1 \quad ; \quad a_2(0) = 0 \tag{3.1.25}$$

These conditions are such that state 2 is not populated before the time-dependent perturbation is switched on at $t = 0$. More general results, for arbitrary initial conditions, can be obtained in an analogous manner; the corresponding results for the $|a_j(t)|^2$ are tedious and not particularly helpful.

Since several transformations have been used in obtaining Eq. (3.1.21), the initial conditions must be transformed as well. Putting $t = 0$ in the transformation given by Eq. (3.1.5) yields

$$c_1(0) = 1 \quad ; \quad c_2(0) = 0 \tag{3.1.26}$$

Finally, putting $t = 0$ in Eq. (3.1.23) and making use of Eq. (3.1.26) shows that [4]

$$c_{s-}(0) = \cos\theta \quad ; \quad c_{s+}(0) = -\sin\theta \tag{3.1.27}$$

The temporal populations associated with finding the system in states 1 and 2 are given by Eq. (3.1.7). Similarly the probabilities of finding the system in states - or + are given by

$$|a_+(t)|^2 = |c_{s+}(t)|^2 \tag{3.1.28}$$

The populations in the (1,2) representation are easily expressed as a function of the solutions to Eq. (3.1.21). This is done by noting that (see Eq. (3.1.23))

$$c_1(t) = \cos\theta\, c_{S-}(t) - \sin\theta\, c_{S+}(t) \tag{3.1.29}$$

$$c_2(t) = \sin\theta\, c_{S-}(t) + \cos\theta\, c_{S+}(t) \tag{3.1.30}$$

and

$$|c_1(t)|^2 = \tfrac{1}{2} - \tfrac{1}{2}\cos 2\theta(|c_{S+}(t)|^2 - |c_{S-}(t)|^2) - \tfrac{1}{2}\sin 2\theta(c_{S-}(t)c_{S+}^*(t) + c_{S-}^*(t)c_{S+}(t)) \tag{3.1.31}$$

$$|c_2(t)|^2 = \tfrac{1}{2} + \tfrac{1}{2}\cos 2\theta(|c_{S+}(t)|^2 - |c_{S-}(t)|^2) + \tfrac{1}{2}\sin 2\theta(c_{S-}(t)c_{S+}^*(t) + c_{S-}^*(t)c_{S+}(t)) \tag{3.1.32}$$

where of course

$$|c_1(t)|^2 + |c_2(t)|^2 = 1 \tag{3.1.33}$$

The time-dependent populations of states 1 and 2 are related to the absorption spectrum for the two-level atom or molecule through the phase- and long time-averaging procedures discussed in Sec. 2.4.3.

Once $c_{s+}(t)$ and $c_{s-}(t)$ are found by solving Eq. (3.1.21) with the conditions given in Eq. (3.1.27), Eq. (3.1.30) is used to construct the transition probability $|c_2(t)|^2$ for the $1 \rightarrow 2$ transition. However, Eq. (3.1.21) cannot be solved exactly in closed form except in very special cases, see [4]. Reliable approximate analytic expressions for the transition probabilities that are capable of exhibiting the essential features of single- and multi-photon two-level spectra would be very useful in understanding and predicting some of the effects due to static fields and permanent dipoles that occur in such spectra. Also, a systematic examination of the spectra as a function of the parameters of the problem (i.e. ΔE, $\underline{\mu}_{12} \cdot \hat{e}_s \mathcal{E}_s$, $\underline{\mu}_{12} \cdot \hat{e} \mathcal{E}$, $\underline{d} \cdot \hat{e}_s \mathcal{E}_s$, etc.) is possible using closed form results for the transition probability. One way of obtaining an analytic solution to Eq. (3.1.21) is to make use of rotating wave type approximations.

3.2 The Static Field RWA Including Effects of Permanent Dipole Moments

When the perturbation is the sum of a static electric field and a plane-polarized sinusoidal electric field (given by Eq. (2.2.1)) relatively simple closed form solutions for Eq. (3.1.21), and hence Eq. (3.1.1), can be obtained by making an "on resonance" or rotating wave type approximation for those coupled differential equations.

The resonances in the transition probabilities are located more easily if Eq. (3.1.21) is transformed to an interaction representation defined by

$$c_{s(-,+)}(t) = b_{(-,+)}(t)\exp(\pm\tfrac{i}{2}[\gamma t - \underline{D}\cdot\int_0^t \underline{E}(t')dt']) \qquad (3.2.1)$$

Substitution of Eq. (3.2.1) into Eq. (3.1.21) shows that the coefficients $b_{(-,+)}(t)$ satisfy

$$i\frac{d}{dt}\underline{\underline{b}}(t) = i\frac{d}{dt}\begin{bmatrix} b_-(t) \\ b_+(t) \end{bmatrix} = \underline{\underline{H}}_I(t)\underline{\underline{b}}(t) \qquad (3.2.2)$$

where

$$H_{I,--}(t) = H_{I,++}(t) = 0 \qquad (3.2.3)$$

and

$$H_{I,-+}(t) = H_{I,+-}^{*}(t) = -\underline{M}\cdot\underline{E}(t)\exp(-i[\gamma t - \underline{D}\cdot\int_0^t \underline{E}(t')dt']) \qquad (3.2.4)$$

This can be written explicitly, for the interaction of the two-level system with a plane-polarized sinusoidal electric field, and a static field by making use of Eq. (2.2.1),

$$H_{I,-+}(t) = H_{I,+-}^{*}(t) = -\underline{M}\cdot\hat{\epsilon}\mathcal{E}\cos(\omega t+\delta)\exp(-i\gamma t)$$
$$\times \exp\left(i\underline{D}\cdot\int_0^t \hat{\epsilon}\mathcal{E}\cos(\omega t'+\delta)dt'\right)$$
$$= -\tfrac{1}{2}\underline{M}\cdot\hat{\epsilon}\mathcal{E}[\exp(i\delta)\exp(-i[\gamma-\omega]t)$$
$$+ \exp(-i\delta)\exp(-i[\gamma+\omega]t)]$$
$$\times \exp\left(i\underline{D}\cdot\int_0^t \hat{\epsilon}\mathcal{E}\cos(\omega t'+\delta)dt'\right) \qquad (3.2.5)$$

This is further expanded by noting that

$$i\underline{D}\cdot\int_0^t \hat{\epsilon}\mathcal{E}\cos(\omega t'+\delta)dt' = \frac{1}{\omega}\,\underline{D}\cdot\hat{\epsilon}\mathcal{E}[\sin(\omega t+\delta)-\sin(\delta)] \qquad (3.2.6)$$

and thus

$$\exp\left(i\underline{D}\cdot\int_0^t \hat{\epsilon}\mathcal{E}\cos(\omega t'+\delta)dt'\right)$$
$$= \exp(iY\sin(\omega t+\delta))\exp(-iY\sin\delta) \qquad (3.2.7)$$

where

$$Y = \frac{\underline{D}\cdot\hat{\epsilon}\mathcal{E}}{\omega} \qquad (3.2.8)$$

By making use of the relationship [77]

$$\exp(iz\sin x) = \sum_{k=-\infty}^{\infty} J_k(z)\exp(ikx) \qquad (3.2.9)$$

where $J_k(z)$ is a Bessel function of integer order k, one obtains

$$\exp(i\underline{D}\cdot\int_0^t \hat{\epsilon}\mathcal{E}\cos(\omega t'+\delta)dt')$$

$$= \exp(-iY\sin\delta)\sum_{k=-\infty}^{\infty} J_k(Y)\exp(ik[\omega t+\delta]) \qquad (3.2.10)$$

Using Eq. (3.2.10) in Eq. (3.2.5) yields

$$H_{I,-+}(t) = H_{I,+-}^{*}(t) = -\tfrac{1}{2}\underline{M}\cdot\hat{\epsilon}\mathcal{E}\exp(-iY\sin\delta)$$

$$\times \sum_{k=-\infty}^{\infty} J_k(Y)[\exp(i[k+1]\delta)\exp(-i[\gamma-(k+1)\omega]t)$$

$$+ \exp(i[k-1]\delta)\exp(-i[\gamma-(k-1)\omega]t)] \qquad (3.2.11)$$

Eq. (3.2.11) contains terms that are slowly varying functions of time at certain frequencies. The resonances in the transition probability occur approximately at these frequencies and these terms are identified by $\omega = \gamma/N$, with $N = 1,2,3,\ldots$ The on-resonance terms occur when $k = N - 1$ in the first term in Eq. (3.2.11) and $k = N + 1$ in the second one. All other terms in Eq. (3.2.11) are rapidly varying off-resonance or counter-rotating terms that tend

to average to zero. Neglecting these off-resonance terms leads to a simple RWA type expression for $\underline{H}_I(t)$ in Eq. (3.2.2) where Eq. (3.2.4) is replaced by

$$H_{I,-+}(t) = H_{I,+-}^{*}(t) = -\tfrac{1}{2}\underline{M}\cdot\hat{\theta}\varepsilon\exp(-iY\sin\delta)\exp(iNS) \times \exp(-i[\gamma-N\omega]t) \times [J_{N-1}(Y) + J_{N+1}(Y)] \qquad (3.2.12)$$

This is further simplified by making use of [78]

$$J_{p-1}(x) + J_{p+1}(x) = \frac{2p}{x}J_p(x) \qquad (3.2.13)$$

and by defining

$$C(N) = 2\underline{M}\cdot\hat{\theta}\varepsilon N(Y)^{-1}J_N(Y) \qquad (3.2.14)$$

and

$$\xi = \exp(-i[Y\sin\delta - N\delta]) \qquad (3.2.15)$$

to obtain

$$H_{I,-+}(t) = H_{I,+-}^{*}(t) = -\tfrac{1}{2}C(N)\xi\exp(-i[\gamma-N\omega]t) \qquad (3.2.16)$$

C(N) is the effective coupling between the sinusoidal field and the atom or molecule for the N-photon resonance involving the $1 \rightarrow 2$ transition. It contains the effects of the static electric field and permanent dipole moments and reduces to the coupling $\mu_{12} \cdot \hat{\epsilon}$ associated with the usual RWA for atoms (see Sec. 2.3) in the limit that $\epsilon_s = 0$ and $\underline{d} = 0$.

Eq. (3.2.2), in the RWA where matrix elements of $\underline{H}_I(t)$ are given by Eqs. (3.2.3) and (3.2.16), represents the following set of coupled differential equations

$$i\frac{d}{dt}b_-(t) = -\tfrac{1}{2}C(N)\xi\exp(-i[\gamma-N\omega]t)b_+(t) \qquad (3.2.17)$$

$$i\frac{d}{dt}b_+(t) = -\tfrac{1}{2}C(N)\xi^*\exp(i[\gamma-N\omega]t)b_-(t) \qquad (3.2.18)$$

Solving these equations yields expressions for $b_-(t)$ and $b_+(t)$ that will be used to construct the temporal populations of states 1 and 2 through the use of Eqs. (3.2.1), (3.1.31) and (3.1.32). In what follows several standard techniques [79] are used to help solve Eqs. (3.2.17) and (3.2.18).

To begin Eq. (3.2.17) is rearranged to give

$$b_+(t) = -2i(\xi C(N))^{-1}\exp(i[\gamma-N\omega]t)\frac{d}{dt}b_-(t) \qquad (3.2.19)$$

Substituting this expression into Eq. (3.2.18) yields

$$\frac{d^2}{dt^2}b_-(t) + i(\gamma-N\omega)\frac{d}{dt}b_-(t) + \tfrac{1}{4}C^2(N)b_-(t) = 0 \qquad (3.2.20)$$

The solutions of this second order differential equation have the form $b_-(t) = \exp(\lambda t)$, where λ is a constant, and the characteristic equation associated with this differential equation is given by

$$\lambda^2 + i(\gamma-N\omega)\lambda + \tfrac{1}{4}C^2(N) = 0 \qquad (3.2.21)$$

Solving Eq.(3.2.21) yields the following roots

$$\lambda_1 = -\tfrac{1}{2}(\gamma-N\omega-p) \quad , \quad \lambda_2 = -\tfrac{1}{2}(\gamma-N\omega+p) \qquad (3.2.22)$$

where

$$p^2 = (\gamma-N\omega)^2 + C^2(N) \qquad (3.2.23)$$

Since the roots of Eq. (3.2.21) are distinct, the solution to Eq. (3.2.20) is

$$b_-(t) = A\exp(\lambda_1 t) + B\exp(\lambda_2 t)$$
$$= A\exp(-\tfrac{1}{2}[\gamma-N\omega-p]t) + B\exp(-\tfrac{1}{2}[\gamma-N\omega+p]t) \qquad (3.2.24)$$

An expression for $b_+(t)$ is found by substituting Eq. (3.2.24) into Eq. (3.2.19) yielding

$$b_+(t) = -\xi^*(C(N))^{-1}[A(\gamma-N\omega-p)\exp(\tfrac{i}{2}[\gamma-N\omega+p]t) + B(\gamma-N\omega+p)\exp(\tfrac{i}{2}[\gamma-N\omega-p]t)] \tag{3.2.25}$$

The constants A and B are found by noting that $b_-(0) = c_{s-}(0)$ and $b_+(0) = c_{s+}(0)$, see Eq. (3.2.1), and by making use of the initial conditions given in Eq. (3.1.27). Hence

$$A = \frac{1}{2p}[(p+\gamma-N\omega)\cos\theta - C(N)\xi\sin\theta] \tag{3.2.26}$$

and

$$B = \frac{1}{2p}[(p-(\gamma-N\omega))\cos\theta + C(N)\xi\sin\theta] \tag{3.2.27}$$

The expressions for $b_-(t)$ and $b_+(t)$ are further simplified by defining

$$A_- = \tfrac{1}{2}(\cos\theta-\beta) \quad ; \quad B_- = \tfrac{1}{2}(\cos\theta+\beta) \tag{3.2.28}$$

$$A_+ = -\tfrac{1}{2}(\sin\theta+\alpha) \quad ; \quad B_+ = -\tfrac{1}{2}(\sin\theta-\alpha) \tag{3.2.29}$$

where

$$\alpha = \frac{-1}{p}[(\gamma-N\omega)\sin\theta + C(N)\xi^*\cos\theta] \qquad (3.2.30)$$

and

$$\beta = \frac{-1}{p}[(\gamma-N\omega)\cos\theta - C(N)\xi\sin\theta] \qquad (3.2.31)$$

Thus the solutions of Eqs. (3.2.17) and (3.2.18) are given by

$$b_{(-,+)}(t) = [A_{(-,+)}\exp(\tfrac{1}{2}pt) + B_{(-,+)}\exp(\tfrac{-1}{2}pt)] \times \exp((-,+)\tfrac{1}{2}[\gamma-N\omega]t) \qquad (3.2.32)$$

Eq. (3.2.32) is easily transformed back into the static Hamiltonian diagonalized representation by substitution into Eq. (3.2.1) and the resulting expressions are used in Eq. (3.1.32) to give $|c_2(t)|^2$; $|c_1(t)|^2$ is then obtained from Eq. (3.1.33). It is convenient to separately examine the terms dependent on $c_{s(-,+)}(t)$ in Eq. (3.1.32) when evaluating the transition probability $|c_2(t)|^2$.

It is easy to show that

$$|c_{s+}(t)|^2 = |b_+(t)|^2$$

$$= |A_+|^2 + |B_+|^2 + A_+B_+^*\exp(ipt)$$

$$+ A_+^*B_+\exp(-ipt)$$

$$= \tfrac{1}{2}(\sin^2\theta + |\alpha|^2) + \tfrac{1}{2}(\sin^2\theta - |\alpha|^2)\cos(pt)$$

$$- \tfrac{i}{2}(\alpha^* - \alpha)\sin\theta\,\sin(pt) \qquad (3.2.33)$$

and

$$|c_{s-}(t)|^2 = |b_-(t)|^2$$

$$= |A_-|^2 + |B_-|^2 + A_-B_-^*\exp(ipt)$$

$$+ A_-^*B_-\exp(-ipt)$$

$$= \tfrac{1}{2}(\cos^2\theta + |\beta|^2) + \tfrac{1}{2}(\cos^2\theta - |\beta|^2)\cos(pt)$$

$$+ \tfrac{i}{2}(\beta^* - \beta)\cos\theta\,\sin(pt) \qquad (3.2.34)$$

Further

$$c_{s-}(t)c_{s+}^{*}(t) = \exp(-i\underline{D}\cdot\int_0^t d\cdot\hat{e}\varepsilon\cos(\omega t'+\delta)dt')$$

$$\times [\exp(iN\omega t)(A_-A_+^{*} + B_-B_+^{*}) + \exp(i[N+p/\omega]\omega t)A_-B_+^{*}$$

$$+ \exp(i[N-p/\omega]\omega t)A_+^{*}B_-] \qquad (3.2.35)$$

Making use of Eq. (3.2.10) yields

$$c_{s-}(t)c_{s+}^{*}(t) = \exp(iY\sin\delta)$$

$$\times \sum_{k=-\infty}^{\infty} J_k(Y)\exp(-ik\delta)[(A_-A_+^{*} + B_-B_+^{*})\exp(-i[k-N]\omega t)$$

$$+ A_+^{*}B_-\exp(-i[k-N+p/\omega]\omega t) + A_-B_+^{*}\exp(-i[k-N-p/\omega]\omega t)]$$

$$= \exp(iY\sin\delta)\sum_{k=-\infty}^{\infty} J_k(Y)\exp(-ik\delta)\exp(-i[k-N]\omega t)$$

$$\times [\beta\alpha^{*}\sin^2(\tfrac{1}{2}pt) - \tfrac{1}{2}\sin 2\theta\cos^2(\tfrac{1}{2}pt)$$

$$+ i(\alpha^{*}\cos\theta + \beta\sin\theta)\sin(\tfrac{1}{2}pt)\cos(\tfrac{1}{2}pt)] \qquad (3.2.36)$$

The expression for $c_{s-}^{*}(t)c_{s+}(t)$ is obtained by taking the complex conjugate of Eq. (3.2.36).

Substituting Eqs. (3.2.33), (3.2.34) and (3.2.36) into Eq. (3.1.32) yields an analytical, but complicated, expression for the phase and time-dependent transition probability $|c_2(t)|^2$. However, the long time- and phase-

average of $|c_2(t)|^2$ obtained from this result, which yields the absorption spectra of the two-level system (see Sec. 2.4), is markedly simpler than $|c_2(t)|^2$ itself.

In calculating the phase-independent steady state result for the population of state 2 one can evaluate the time-average first, followed by the phase-average, or vice versa. In the derivation that follows, the long time-average is taken first since it greatly simplifies the calculation. The same result has been obtained by carrying out the analogous derivation, which is not given here explicitly, resulting from performing the phase-average first.

First consider the long time-average of Eq. (3.2.33). It follows that

$$\lim_{T\to\infty} \frac{1}{T} \int_0^T |c_{S+}(t)|^2 dt$$

$$= \lim_{T\to\infty} \frac{1}{T}[\tfrac{1}{2}(\sin^2\theta + |\alpha|^2)T + \frac{1}{2p}(\sin^2\theta - |\alpha|^2)\sin(pT)$$

$$+ \frac{i}{2p}(\alpha^* - \alpha)\sin\theta(\cos(pT) - 1)]$$

$$= \tfrac{1}{2}(\sin^2\theta + |\alpha|^2) \qquad (3.2.37)$$

since both $\sin(pT)/pT$ and $((\cos/pT)-1)/pT$ tend to zero as $T \to \infty$. In a similar manner, the time-average of Eq. (3.2.34) is

$$\lim_{T\to\infty} \frac{1}{T} \int_0^T |c_{s-}(t)|^2 dt = \tfrac{1}{2}(\cos^2\theta + |\beta|^2) \qquad (3.2.38)$$

The evaluation of the long time-average of $c_{s-}(t)c_{s+}^*(t)$ is somewhat more complicated and is most readily carried out by using the first expression for $c_{s-}(t)c_{s+}^*(t)$ given in Eq. (3.2.36). First one obtains

$$\lim_{T\to\infty} \frac{1}{T} \int_0^T c_{s-}(t)c_{s+}^*(t)dt$$

$$= \exp(i Y \sin\delta)$$

$$\times \lim_{T\to\infty}\{(A_-A_+^* + B_-B_+^*)[i \sum_{\substack{k=-\infty \\ k\neq N}}^{\infty} J_k(Y)\exp(-ik\delta)\left[\frac{1}{[k-N]\omega T}\right]$$

$$\times (\exp(-i[k-N]\omega T)-1) + J_N(Y)\exp(-iN\delta)]$$

$$+ A_+^*B_-[i \sum_{k=-\infty}^{\infty} J_k(Y)\exp(-ik\delta)\left[\frac{1}{[k-N+p/\omega]\omega T}\right]$$

$$\times (\exp(-i[k-N+p/\omega]\omega T)-1)]$$

$$+ A_-B_+^*[i \sum_{k=-\infty}^{\infty} J_k(Y)\exp(-ik\delta)\left[\frac{1}{[k-N-p/\omega]\omega T}\right]$$

$$\times (\exp(-i[k-N-p/\omega]\omega T)-1)]\} \qquad (3.2.39)$$

If p/ω is an integer, the last two terms in Eq. (3.2.39) contribute to the time-average when $k = N - p/\omega$ in the second term and $k = N + p/\omega$ in the third term. However, physically, p/ω is rarely an integer and when it is the

contribution of these terms is small (see Appendix A for more details). Thus only the first term in Eq. (3.2.28) is carried through in what follows and one obtains

$$\lim_{T\to\infty} \frac{1}{T} \int_0^T c_{s-}(t)c_{s+}^*(t)dt$$

$$= \exp(iY\sin\delta)(A_-A_+^* + B_-B_+^*)J_N(Y)\exp(-iN\delta)$$

$$= -\tfrac{1}{2} \exp(iY\sin\delta)(\tfrac{1}{2}\sin 2\theta - \beta\alpha^*)J_N(Y)\exp(-iN\delta) \qquad (3.2.40)$$

Combining all the results of this paragraph yields an expression for the long time-average of $|c_2(t)|^2$:

$$\lim_{T\to\infty} \frac{1}{T} \int_0^T |c_2(t)|^2 dt = \tfrac{1}{2} + \tfrac{1}{2}(|\alpha|^2 - |\beta|^2 - \cos 2\theta)\cos 2\theta$$

$$- \tfrac{1}{2}J_N(Y)\sin 2\theta\{\xi(\tfrac{1}{2}\sin 2\theta - \alpha\beta^*) + \text{c.c.}\} \qquad (3.2.41)$$

Eq. (3.2.41) is simplified by using Eqs. (3.2.30) and (3.2.31) and doing some algebra;

$$\lim_{T\to\infty} \frac{1}{T} \int_0^T |c_2(t)|^2 dt$$

$$= \frac{1}{2} - \frac{1}{2p^2}[(\gamma-N\omega)^2\cos^2 2\theta - J_N(Y)(\gamma-N\omega)C(N)\sin 2\theta\cos 2\theta]$$

$$+ \frac{1}{4p^2}(\xi^*+\xi)[(\gamma-N\omega)C(N)\sin 2\theta\cos 2\theta$$

$$- J_N(Y)C^2(N)\sin^2 2\theta] \qquad (3.2.42)$$

The phase-average of Eq. (3.2.42) is easy to evaluate. The first two terms are independent of phase and therefore contribute directly to the phase-average. In the last term in Eq. (3.2.42), all the phase dependence is contained in ξ and ξ^* and the relevant phase integral is therefore

$$I = \frac{1}{2\pi}\int_0^{2\pi} (\xi^* + \xi)d\delta \qquad (3.2.43)$$

By using Eq. (3.2.9) in Eq. (3.2.15), ξ can be written as

$$\xi = \sum_{k=-\infty}^{\infty} J_k(Y)\exp(-i[k-N]\delta) \qquad (3.2.44)$$

and substituting this into Eq. (3.2.43) gives

$$I = 2J_N(Y) + \sum_{\substack{k=-\infty \\ k\neq N}}^{\infty} \{J_k(Y)\left[\frac{1}{k-N}\right](\exp(-i[k-N]2\pi)-1) + c.c.\}$$

$$= 2J_N(Y) \qquad (3.2.45)$$

since

$$\exp(\pm is2\pi) = 1 \quad , \ s \text{ integer.} \qquad (3.2.46)$$

Thus the phase- and long time-averaged transition probability is given by

$$\bar{P}_2^N = \lim_{T\to\infty} \frac{1}{2\pi T} \int_0^T \int_0^{2\pi} |c_2(t)|^2 dt d\theta$$

$$= \frac{1}{2} - \frac{1}{2p^2}[(\gamma - N\omega)\cos 2\theta - C(N)J_N(Y)\sin 2\theta]^2 \qquad (3.2.47)$$

When there is no sinusoidal time-dependent electric field, i.e. $\varepsilon = 0$ and hence $C(N) = 0$, Eq. (3.2.47) reduces to

$$\bar{P}_2(\text{stat}) = \tfrac{1}{2}[1 - \cos^2 2\theta] \qquad (3.2.48)$$

which vanishes when the static field $\varepsilon_s = 0$, see Eq. (3.1.14). This is the static background in the N-photon resonance profile that arises from a frequency independent contribution to the transition probability [59,80].

The absorption spectra obtained from examining $\bar{P}_2^N$ as a function of frequency will be discussed next.

3.3 Examples Showing Some of the Effects of Permanent Dipole Moments and Static Electric Fields

The features of single- and multi-photon absorption spectra of atoms and molecules can depend markedly on the presence of non-zero diagonal dipole matrix elements (permanent dipole moments) and/or static electric fields. This will be illustrated in this section for two-level systems where the use of the analytic RWA expressions for the resonance profiles makes predictions and/or the interpretation of the spectra readily tractable. Comparison

with exact two-level results will be used to illustrate the validity of the RWA expressions.

3.3.1 The Usual Rotating Wave or Rabi Approximation ($\underline{d} = 0$, $\varepsilon_s = 0$)

When $\varepsilon_s = 0$, $\cos 2\theta = 1$, $\sin 2\theta = 0$, $\underline{D} = \underline{d}$, $Y = \frac{\underline{d}\cdot\hat{e}\varepsilon}{\omega}$, $\gamma = \Delta E$, and $\underline{M} = \underline{\mu}_{12}$ (see Eqs. (3.1.14), (3.1.15), (3.1.19), (3.1.20) and (3.2.8)) and when $\underline{d} = 0$ as well, $Y = 0$. Using these limits, and Eq. (3.2.13), in Eq. (3.2.14) gives the following expression for the atom-electromagnetic field (EMF) coupling

$$C(N) = \underline{\mu}_{12}\cdot\hat{e}\varepsilon[J_{N-1}(0) + J_{N+1}(0)] = \underline{\mu}_{12}\cdot\hat{e}\varepsilon\delta_{N,1} \tag{3.3.1}$$

since $J_k(0) = \delta_{k,0}$ [78]. Substitution of this result into Eq. (3.2.47) then yields

$$\bar{P}_2^N = \frac{1}{2p^2}\,|\underline{\mu}_{12}\cdot\hat{e}\varepsilon|^2\delta_{N,1} \tag{3.3.2}$$

where

$$p^2 = (\Delta E-\omega)^2 + |\underline{\mu}_{12}\cdot\hat{e}\varepsilon|^2 \tag{3.3.3}$$

This is the original Rabi or rotating wave approximation (RWA) [17-20,23], see also Sec. 2.3, for the one-photon absorption spectra of two-level atoms and also applies to two-level molecules with no permanent dipole moments.

In order to discuss the validity of the RWA result for the one-photon absorption spectra, it is useful to define the coupling strength parameter

$$b = \frac{|\mu_{12} \cdot \hat{e}\varepsilon|}{\Delta E} \tag{3.3.4}$$

The RWA is valid for weak coupling cases where $b < < 1$ and under these conditions the atom-electromagnetic field coupling is given by $\mu_{12} \cdot \hat{e}\varepsilon$. Figure 3.1 illustrates the absorption spectrum obtained from examining Eq. (3.3.2) as a function of $\omega/\Delta E$ when the coupling strength is relatively small, $b = 0.2$. The peak is Lorentzian in shape with resonance frequency $\omega_{res} = \Delta E$ and the full width at half-maximum (FWHM), which is the width of the absorption spectrum when $\bar{P}_2^N = 0.25$, is given by $2|\mu_{12} \cdot \hat{e}\varepsilon|$.

As the coupling strength increases to $b \leq 1$ or $b > 1$, the counter-rotating terms neglected in deriving the RWA become more important and as a result the RWA becomes more and more unreliable. There are many examples of exact atomic two-level calculations of resonance profiles in the literature [10,23,27-30,58,59,73,81] and comparison of them with the analogous RWA results leads to an understanding of the breakdown of the RWA expression for the one-photon

Figure 3.1. The single-photon RWA resonance profile for atoms or molecules with no permanent dipoles; $\bar{P}_2^{\,1}$, given by Eq. (3.3.2), versus $\omega/\Delta E$ for $b = |\underline{\mu}_{12}\cdot\hat{e}\mathcal{E}|/\Delta E = 0.2$. The resonance occurs at $\omega/\Delta E = 1.0$ where $\bar{P}_2^{\,1} = 0.5$ and the profile, as a function of $\omega/\Delta E$, has a full width at half maximum (FWHM) of 2b.

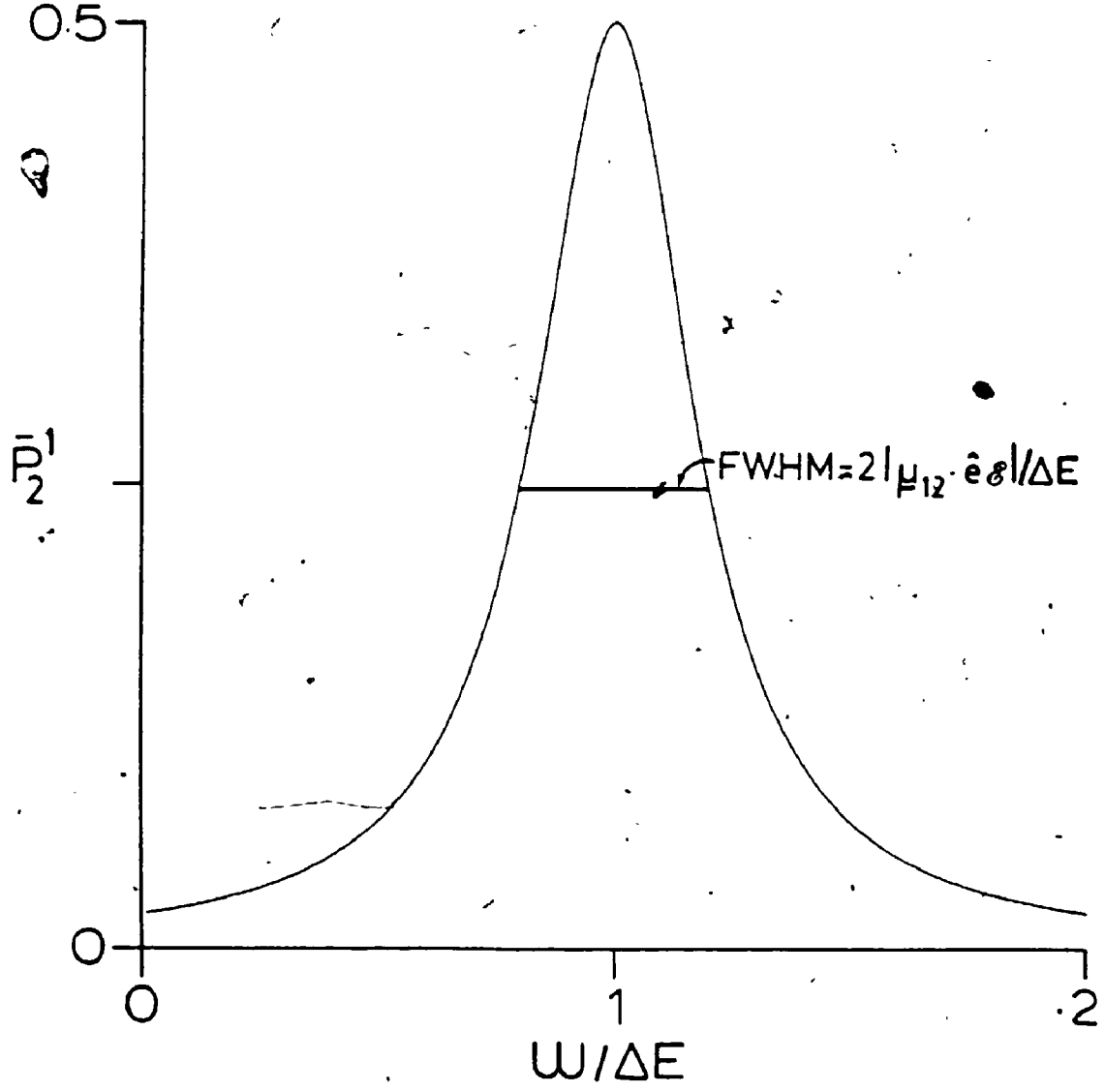
0.5
$\bar{P}_2^1$
0
0
1
2
$\omega/\Delta E$
FWHM=$2|\mu_{12}\cdot\hat{e}\mathcal{E}|/\Delta E$

resonance profile as a function of b.

As b increases, the widths of the spectral resonances become broader, the spectra become asymmetric as a function of frequency, and the FWHM is no longer given by $2|\mu_{12}\cdot\delta\varepsilon|$. In exact two-level calculations of the spectra the one-photon resonance positions shift from $\omega = \Delta E$ to higher frequencies - this is the Bloch-Siegert shift (see Sec. 2.3) - and dynamic backgrounds occur that are not predicted by the RWA.

Expressions analogous to Eq. (3.3.2) have also been derived [23,68,82] for atomic multi-photon resonances and comments analogous to the N = 1 case apply for these higher photon resonances. For weak fields ($b << 1$), $\omega_{res}^{N} = \Delta E/N$ for the N-photon transition and for atoms N = 1,3,5,... assuming the energy states involved in the transition have a definite parity. Bloch-Siegert shifts to higher frequency and deformation of the Lorentzian type profiles occur, as in the N = 1 problem, as b increases [23,28,53-56,81].

The RWA expressions for N = 3,5,..., analogous to Eq. (3.3.2), can be derived [23,82] by a perturbation treatment of the Floquet secular equation, see Sec. 4.2. The single-photon result of Eq. (3.3.2) arises from a first order treatment of the secular equation around a zeroth order energy ΔE; in Sec. 4.3 perturbative corrections to Eq. (3.3.2), which include some of the effects missing in the RWA result, will be discussed as a special case of a

more general treatment for molecules. In order to obtain atomic RWA results for N = 3,5,..., Shirley [23] developed perturbative treatments about zeroth order energies $\Delta E/N$, obtained expressions for the first non-zero results which are of N-th order, and rewrote the results in RWA form.

3.3.2 RWA with $\underline{d} \neq 0$, $\varepsilon_s = 0$

When $\varepsilon_s = 0$ in Eq. (3.2.47), the following RWA type expression for the N-photon resonance profile, that includes the effects of permanent dipole moments, is obtained;

$$\bar{P}_2^N = \frac{[C(N)]^2}{2[(\Delta E - N\omega)^2 + [C(N)]^2]} \tag{3.3.5}$$

where

$$C(N) = |2\underline{\mu}_{12}\cdot\hat{e}\varepsilon N(Y)^{-1}J_N(Y)| \tag{3.3.6}$$

with

$$Y = \frac{\underline{d}\cdot\hat{e}\varepsilon}{\omega} \tag{3.3.7}$$

Eq. (3.3.5) was originally [83] obtained by solving Eq. (3.1.6) with $\varepsilon_s = 0$ in $\underline{x}(t)$ and a recent derivation in the literature agrees with this result for N = 1 and 2 [84]. This yields a simpler Hamiltonian that does not need

to be diagonalized by a rotation through θ. However, $\underline{\underline{\kappa}}(t)$ still needs to be transformed to an interaction representation and the rest of the derivation is analogous to, but much simpler than, that given in Sec. 3.2 for $\varepsilon_S \neq 0$ (when $\varepsilon_S = 0$, γ, $\underline{D}$, $\underline{M}$ and the states $|-\rangle$ and $|+\rangle$ are replaced by ΔE, $\underline{d}$, $\underline{\mu}_{12}$, $|1\rangle$ and $|2\rangle$ respectively). When $\varepsilon_S \neq 0$ the explicit expression for $|b_2(t)|^2$, the time-dependent population of state 2, is tedious (see Sec. 3.2). For $\varepsilon_S = 0$, $|b_2(t)|^2 = |c_{S+}(t)|^2$, and using $\cos\theta = 1$ and $\sin\theta = 0$ (see Eq.(3.1.24) with $\cos 2\theta = 1$) in Eqs. (3.2.30) and (3.2.33), it is easy to show that

$$|b_2^N(t)|^2 = \frac{|C(N)|^2}{p^2} \sin^2(\tfrac{1}{2}pt) \qquad (3.3.8)$$

with

$$p = [(\Delta E - N\omega)^2 + |C(N)|^2]^{\frac{1}{2}} \qquad (3.3.9)$$

When $\underline{d} \neq 0$ the atom-EMF coupling is given by Eq. (3.3.1) and Eq. (3.3.8) becomes

$$\left|b_2^N(t)\right|^2_{\underline{d}=0} = \frac{1}{p^2}|\underline{\mu}_{12}\cdot\underline{\varepsilon}|^2\delta_{N,1}\sin^2(\tfrac{1}{2}pt) \qquad (3.3.10)$$

with p^2 given by Eq. (3.3.3). The $\underline{d} \to 0$ limit of the molecular $\underline{d} \neq 0$ result is the usual RWA expression [23] for the single-photon time-dependence of the population of

state 2. The temporal population $|b_2^N(t)|^2$ is independent of the phase of the electromagnetic field and taking its long time-average yields Eq. (3.3.5). When $\underline{d} = 0$, Eq. (3.3.5) reduces to Eq. (3.3.2).

Eq. (3.3.5) is valid for two-level atoms or molecules and since molecules are not isotropic their spectra will depend on the orientation of the molecule relative to the direction of the applied electromagnetic field. Thus, in some cases, averaging over the allowed orientations of the molecule relative to the field direction should be included in calculations of the absorption spectra [73,85] (see Sec. 3.3.3B). Unless mentioned otherwise all results discussed in what follows will be for fixed molecule-EMF configurations where $\underline{\mu}_{12} \| \underline{d} \| \hat{e} \| \hat{e}_s$.

The similarity between the atomic RWA result of Eq. (3.3.2) and the more general molecular resonance profile of Eq. (3.3.5) is striking; the usual expression for the coupling between the atom and the electromagnetic field, $\underline{\mu}_{12} \cdot \hat{e}\mathcal{E}$, occurring in the former, is simply replaced by the new molecule-EMF coupling term C(N) in the latter. The coupling C(N), given by Eq. (3.3.6), depends on frequency and is an oscillating function of the argument, Y, of the Bessel function J_N. Figure 3.2 is a plot of C(N), as a function of Y, for N = 1,2 and 3 showing this behaviour. When permanent dipole moments are present the coupling between the system and the applied time-dependent field can

Figure 3.2. The RWA molecule-electromagnetic field coupling $C(N)$, given by Eq. (3.3.6), as a function of Y for N = 1, 2 and 3. Plotted is $C(N)/(\mu_{12} \cdot \hat{e}\varepsilon)$ as a function of $\underline{d} \cdot \hat{e}\varepsilon/\omega$.

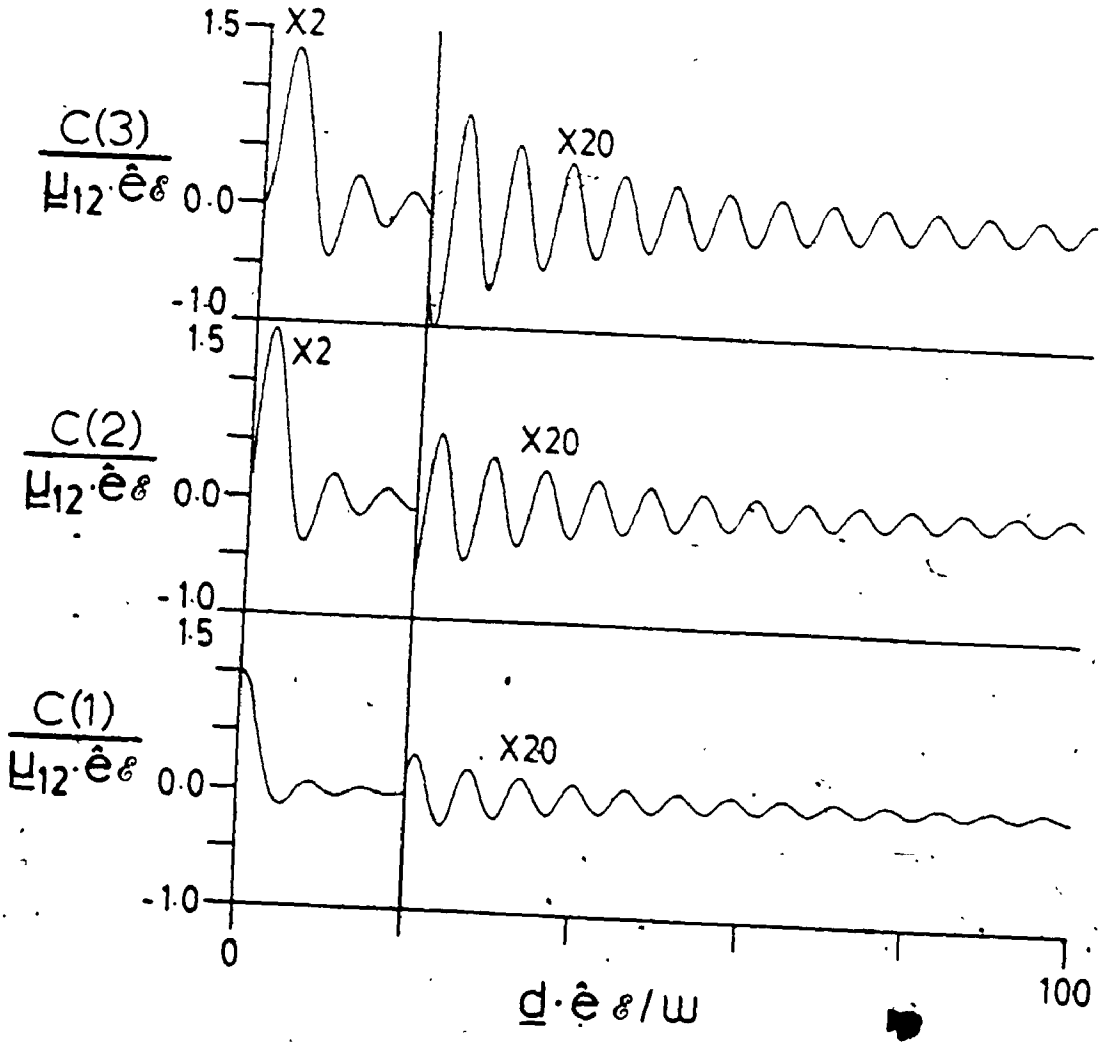
1.5
X2
C(3)
μ12·êℰ
0.0
X20
-1.0
1.5
X2
C(2)
μ12·êℰ
0.0
X20
-1.0
1.5
C(1)
μ12·êℰ
0.0
X20
-1.0
0
d·êℰ/ω
100

be much less than $\underline{\mu}_{12}\cdot\hat{e}\mathcal{E}$.

When $\underline{d} \neq 0$ at least one of the states of the system must have no definite (i.e. mixed) parity; that is $\underline{\mu}_{ii} = \langle\phi_i|\underline{\mu}|\phi_i\rangle = 0$ if ϕ_i has a definite parity since $\underline{\mu}$ is an odd operator. Thus for a two-level molecule with $\underline{d} \neq 0$ even (N = 2,4,...) as well as the usual odd (N = 1,3,5,...) photon transitions can occur [35,59,86] and the RWA supports both for $\underline{d} \neq 0$.

Additional effects of permanent dipoles on the spectra can be discussed qualitatively by comparing the resonance profiles predicted by the molecular RWA expression given by Eq. (3.3.5) with the Lorentzian profile predicted by the atomic result of Eq. (3.3.2). The "usual" system-EMF coupling $\underline{\mu}_{12}\cdot\hat{e}\mathcal{E}$ in the atomic result is replaced by the frequency dependent coupling C(N) for $\underline{d} \neq 0$. Hence for a molecule with $\underline{d} \neq 0$ the N-photon resonance profile will not be given by a pure Lorentzian like that in Figure 3.1. The Lorentzian profile will be modified by oscillating fringes and asymmetries as a function of ω. The zeros of the fringes will occur at the zeros of the Bessel function occurring in C(N), see Eq. (3.3.5). However the general molecular result for the resonance profiles still predicts that the N-photon (main) resonance will occur at $\omega = \omega_{res}^{N} = \Delta E/N$ where $\bar{P}_2^N$ has its maximum value of 0.5.

Eq. (3.3.5) can also be used to obtain an approximate expression for the FWHM of the N-photon main

resonance by assuming that C(N) does not vary appreciably over the width of the resonance, that is that C(N) is essentially a constant over the relevant frequency range. The result for $(FWHM)^N$ is obtained by solving Eq. (3.3.5) with $\bar{P}_2^N = 0.25$ for its roots, ω_1 and ω_2, taking C(N) independent of ω. The difference between these two frequencies gives the width of the main resonance at its half maxima. Thus when the main resonances do not vary appreciably with ω, that is when they are narrow, the roots are

$$\omega_1 = \frac{1}{N}[\Delta E - |C(N)|]_{\omega=\omega_{res}^N} \qquad (3.3.11)$$

and

$$\omega_2 = \frac{1}{N}[\Delta E + |C(N)|]_{\omega=\omega_{res}^N} \qquad (3.3.12)$$

Therefore

$$(FWHM)^N = \omega_2 - \omega_1 = \frac{2}{N}\{|C(N)|\}_{\omega=\omega_{res}^N}$$

$$= 4\mu_{12}\cdot\hat{e}\varepsilon \left[\frac{-\Delta E}{Nd\cdot\hat{e}\varepsilon}\right] J_N\left[\frac{Nd\cdot\hat{e}\varepsilon}{\Delta E}\right] \qquad (3.3.13)$$

This RWA result indicates that the width of the N-photon resonance decreases as N increases through the factor of N^{-1} in Eq. (3.3.13) and since the Bessel function, $J_N\left[\frac{Nd\cdot\hat{e}\varepsilon}{\Delta E}\right]$, often decreases as N increases. This prediction will often be reliable but it is not rigorous. For example it is not correct if $Y = \frac{Nd\cdot\hat{e}\varepsilon}{\Delta E}$ is near a zero of J_N for N small relative to N large (typical plots of C(N) versus Y are shown in Figure 3.2).

A related effect of the presence of permanent dipoles is the reduction of the width of a resonance relative to the atomic result with $\underline{d} = 0$. This point is best illustrated by comparing the FWHM for the one-photon resonance in the atomic case versus that for molecules. In the former, FWHM $= 2|\mu_{12}\cdot\hat{e}\varepsilon|$ and in the latter $(\text{FWHM})^1 = 2|C(1)|_{\omega=\omega_{res}}^{-1}$. Since, in general, the molecule-EMF coupling can be significantly smaller than that for an atom, the widths can be much narrower. Similar comments hold for $N > 1$ and examples will be discussed later. The reduction in peak width can be considerable if the argument of the Bessel function J_N occurring in C(N) is large for $\omega \sim \omega_{res}^N$ and especially if the argument is near a zero of the Bessel function.

While the molecular RWA expression for the N-photon resonance profile has proved and will prove to be very useful, there are some obvious problems associated with it. It is clearly not correct as $\underline{d} > 0$ since $C(N) > 0$ (see Eq. (3.3.1)) and hence $P_2^N > 0$ for $N = 3,5,7,\ldots$ and it is

known that all N odd transitions occur in a two-level atom with no permanent dipole moments. The RWA result also predicts that the N-photon (main) resonances will occur at $\omega = \omega_{res}^{N} = \Delta E/N$. Exact calculations (see what follows) show that when $\underline{d} \neq 0$ the frequencies of the main resonances can shift to the low frequency side of $\omega = \Delta E/N$ in contrast to the Bloch-Siegert shifts to the high frequency side observed in the atomic case.

Like all RWA type approximations, Eq. (3.3.5) is more reliable as the coupling C(N) becomes small, that is as $\underline{\mu}_{12} \cdot \hat{e}\mathcal{E}$ decreases, and usually as $\underline{d} \cdot \hat{e}\mathcal{E}$ increases, for fixed ΔE. For molecules the RWA type expressions can be used with larger applied fields than one would normally expect since C(N) is generally less than $\underline{\mu}_{12} \cdot \hat{e}\mathcal{E}$. Since the RWA expression involves a near resonance approximation it breaks down when the N-photon resonances begin to overlap appreciably. Indeed, as in the atomic case, the molecular RWA is not capable of supporting the dynamic spectral background characteristic of this type of behaviour as the molecule-EMF coupling becomes large. In general, the RWA predicts the overall structure of the absorption spectra and is a useful analytical expression that can be used to interpret and predict the effects of permanent dipole moments on absorption spectra as a function of the parameters of the problem. Illustrations of its use and validity follow.

Numerical Examples

In order to examine several examples of single- and multi-photon spectra obtained from the RWA result of Eq. (3.3.5), and to compare them with the corresponding exact results, it is useful to define the parameters

$$\eta(N) = \frac{N}{\Delta E}|\underline{d}\cdot\hat{e}\varepsilon| \qquad (3.3.14)$$

$$\beta(N) = \left[\frac{C(N)}{\Delta E}\right]_{\omega=\omega_{res}^{N}} \qquad (3.3.15)$$

$\eta(N)$ is the argument of the Bessel functions occurring in $C(N)$ when $\omega = \omega_{res}^{N} \approx \Delta E/N$ and $\beta(N)$ takes into account the effect of permanent dipole moments in the molecule-EMF coupling strength. The parameter $\beta(N)$ is the N-photon and $\underline{d} \neq 0$ analogue of the often used atom-EMF coupling strength parameter, b, defined by Eq. (3.3.4). These parameters are also useful in interpreting exact single- and multi-photon spectra and in discussing the validity of the RWA results.

In Figure 3.3 the exact spectra for a two-level model system, both with and without $\underline{d}$ (Figure 3.3d), are compared to the corresponding spectra (Figure 3.3a-c) obtained from Eq. (3.3.5) for the N = 1,2 and 3 photon resonances. In addition the $\underline{d} = 0$ RWA "atomic" spectrum obtained from Eq. (3.3.2) is included with the one-photon

Figure 3.3. The absorption spectra or resonance profile, $\bar{P}_2^N$ as a function of $\omega/\Delta E$, for a two-level model molecule specified by $\mu_{12} = 1.0$, $d = \mu_{22} - \mu_{11} = 20.0$, $\Delta E = 1.0$ and $\varepsilon = 0.5$. Parts a-c correspond to the RWA result of Eq. (3.3.5), with N = 1,2 and 3 respectively, and d to the exact result. The relevant d = 0 results are also included for comparative purposes.

Figure 3.4. As in Figure 3.3 except for the two-level model molecule specified by $\mu_{12} = -0.5072$, $d = 2.0$, $\Delta E = 3.706 \times 10^{-5}$ and $\varepsilon = 5.0 \times 10^{-4}$.

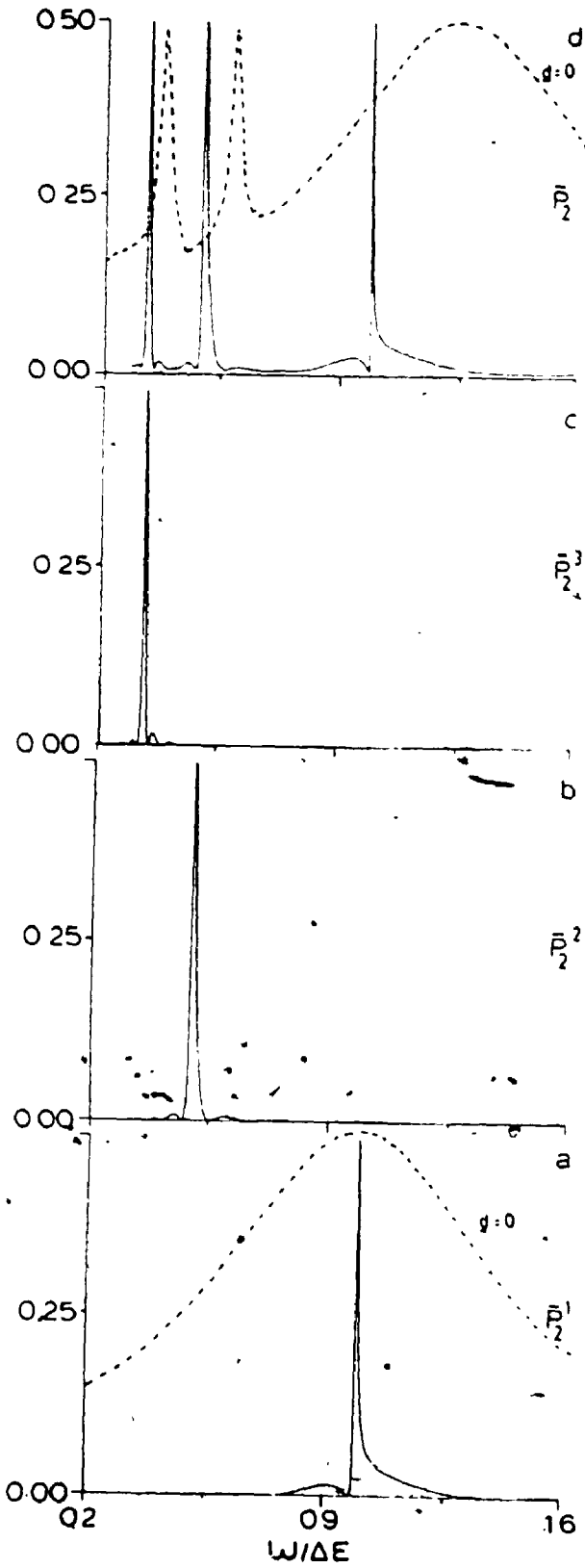

Figure 33

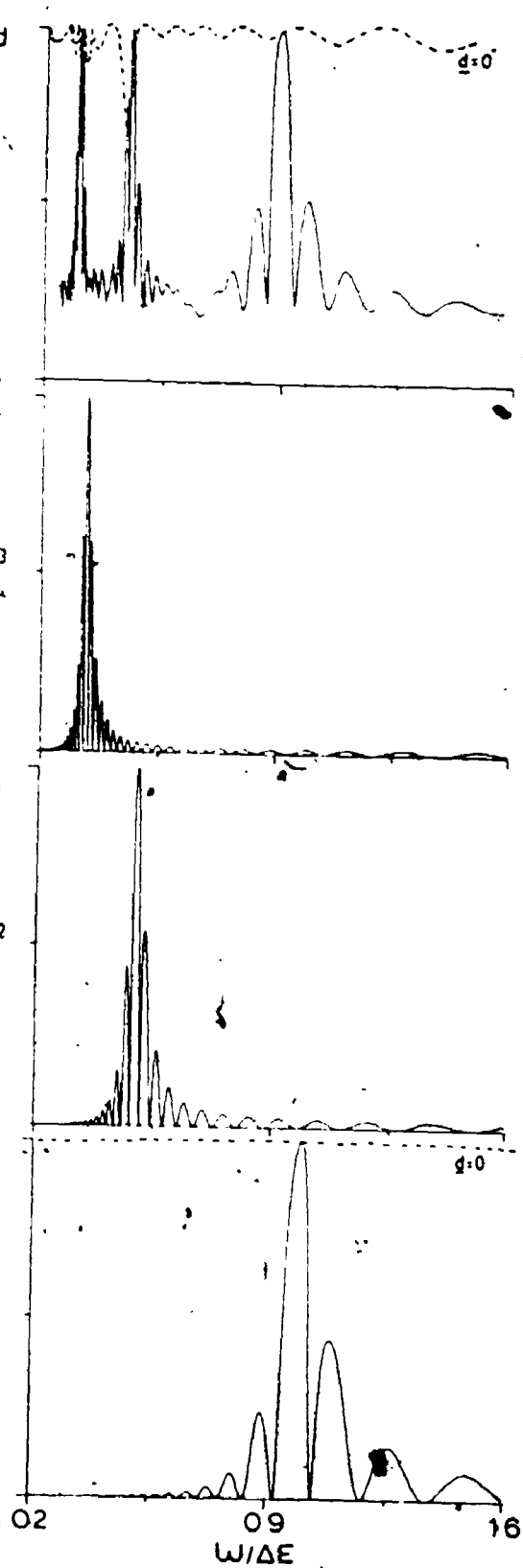

Figure 34

RWA molecular spectrum. The parameters characterizing the one-photon resonance are $\eta(1) = 10.0$ and $\beta(1) = 4.35 \times 10^{-3}$ and $b = 0.5$.

Figures 3.3a and 3.3d illustrate the considerable effect that permanent dipole moments can have on the widths of the resonance profiles. For example, the $\underline{d} \neq 0$ one-photon resonances are narrow spikes whereas the $\underline{d} = 0$ resonances are much broader. This is due to the considerable reduction in the coupling between the molecule and the EMF caused by the presence of non-zero permanent dipoles relative to the atom-EMF coupling; $\beta(1)$ is approximately 100 times smaller than b. The molecular one-photon resonance is very narrow and is not surrounded by many oscillatory fringes. The narrowness of the resonance arises because the argument, $\eta(1) = 10.0$, of the molecule-EMF coupling is near the third zero of the Bessel function $J_1(Y)$ occurring in $C(1)$. The range of ω covered in Figure 3.3 corresponds to a relatively narrow range of Y values $(6.25 \leq Y \leq 50.0)$ in the plot of $C(1)$ versus Y in Figure 3.2 and since many maxima and minima are located on either side of $Y = \eta(1)$ one would expect several oscillatory fringes around the one-photon peak. However only one fringe is significant since the heights of the others are "damped" through both the relatively small value of b^2 and the factor of $(\Delta E - \omega)^2$ occurring in the denominator of Eq. (3.3.5) with $N = 1$ which, in this example, is usually much larger than $|C(1)|^2$ for

off-resonance frequencies. Rewriting Eq. (3.3.5) in the following form aids in the understanding of these trends;

$$\bar{P}_2^N = \frac{|C'(N)|^2 b^2}{2[(1-N\omega/\Delta E)^2 + |C'(N)|^2 b^2]} \qquad (3.3.16)$$

where $C'(N) = C(N)/(\mu_{12}\cdot\hat{e}\varepsilon)$ is the quantity plotted in Figure 3.2.

In the exact $\underline{d} = 0$ spectrum the one-photon resonance occurs at $\omega/\Delta E = 1.06$ (see Figure 3.3d) and the Bloch-Siegert shift is fairly large for this example. When permanent dipole moments are present the one-photon resonance occurs at a value of $\omega/\Delta E$ insignificantly less than unity in essential agreement with the prediction of the molecular RWA. The elimination of the Bloch-Siegert shift is also due to the drastic reduction in the molecular-EMF coupling by the presence of permanent dipole moments relative to the atomic-EMF coupling.

An analogous discussion applies for the $N > 1$ photon resonances. In the $\underline{d} = 0$ exact spectrum the two-photon resonance is absent, as expected, and the three-photon resonance is shifted significantly to the high frequency side of $\omega = \Delta E/3$ ($\omega/\Delta E = 1/3$) and occurs at $\omega/\Delta E = 0.41$. For $\underline{d} \neq 0$ the exact two- and three-photon resonances occur at essentially $\omega/\Delta E = 0.50$ and 0.33 respectively and the three-photon resonance is very narrow relative to the atomic result. In all cases the presence of permanent dipoles suppresses the dynamic spectral background


2
1.0
1.1
1.25
1.4
1.6
1.8
2.0
2.2
2.5
2.8
3.2
3.6
4.0
MicroD

associated with the strongly coupled atomic resonance profiles. In contradistinction to the atomic case the RWA predicts the exact molecular spectrum very well in this example since the coupling between the molecule and the EMF is weak.

Two-level model RWA (N = 1,2,3) and exact spectra, characterized by b = 6.84, $\beta(1) = 6.85 \times 10^{-2}$ and $\eta(1) = 26.98$, analogous to those presented in Figure 3.3, are shown in Figure 3.4a-3.4d. The coupling parameters for this set of calculations are much larger than those for the more weakly coupled example of Figure 3.3.

When $\underline{d} = 0$ both the one-photon RWA and the exact spectra (see Figures 3.4a and 3.4d respectively) are completely saturated and the resonances in the latter cannot be easily identified. This is to be expected with such a large atomic coupling strength b. When $\underline{d} \neq 0$ the effective coupling strength $\beta(1)$ is approximately 100 times smaller than b and the molecular one- and higher photon resonances are markedly narrower than in the atomic case.

Since $\eta(1) = 26.98$ occurs near the fifth maximum of the Bessel function $J_1(Y)$ contained in C(1) (see Figure 3.2), the one-photon resonance is relatively broad (see Figures 3.4a and 3.4d). Also the range of ω in Figure 3.4 corresponds to a large range of Y values ($17 \leq Y \leq 135$) in Figure 3.2 and thus the one-photon resonance is surrounded by many oscillatory fringes with their zeros and maxima occurring at the zero and maxima (or minima) surrounding Y

$= \eta(1) = -26.98$. In this example b^2 is quite large and $|C(1)|^2$ is often comparable to the $(\Delta E-\omega)^2$ term occurring in the denominator of Eq. (3.3.5) for off-resonance frequencies. Thus the fringes are significantly higher than those in the previous example and are observable on the scale of Figure 3.4.

The atomic Bloch-Siegert shifts, easily seen in Figure 3.3d, cannot be easily determined in Figure 3.4d ($\underline{d} = 0$) for any of the resonances; precise numerical investigations show they are very large. However, when $\underline{d} \neq 0$ the exact resonances are easily recognized and occur at $\omega/\Delta E = 0.87$, 0.44 and 0.31 for N = 1,2 and 3 respectively. These are shifted significantly to the low frequency side of the positions predicted from the RWA; $\omega/\Delta E = 1.0$, 0.5 and 0.33. Thus one of the effects of $\underline{d} \neq 0$ in this strongly coupled example, relative to Figure 3.3, is the occurrence of "negative Bloch-Siegert shifts" for the molecule. Another effect of the marked reduction of the molecule-EMF coupling strength, relative to the atomic-EMF coupling, caused by the presence of permanent dipoles is the narrowing of the resonance profiles and the significant suppression of the spectral dynamic background for the molecule relative to the atom (see the exact spectra of Figure 3.4d).

A comparison of the $\underline{d} \neq 0$ exact spectrum with the $\underline{d} \neq 0$ RWA spectra illustrates some of the features that may be missing in the molecular RWA spectra. The RWA spectra

have oscillatory fringes but the heights of these fringes are not in quantitive agreement with those in the exact spectrum since the RWA does not support a dynamic spectral background. Also the shifts of the main resonances to the low frequency side of $\Delta E/N$ present in the exact spectrum are absent in the RWA results. This example illustrates a situation where the RWA predicts the gross features of the structure of single- and multi-photon spectra but not some of the important details (discussed above).

The argument of the Bessel function J_N at $\omega = \omega_{res}^N$, $\eta(N)$ (see Eq. (3.3.14)), increases with N and hence the magnitude of $J_N(\eta(N))$ occurring in C(N) usually decreases as N increases. The usual effect of this is to decrease the resonance widths as N increases as discussed earlier in this subsection. This effect is seen in the series of spectra in Figure 3.4 where $\eta(N)$ occurs near a maximum in C(N) (see Figure 3.2) for N = 1,2 and 3 and as the argument increases the coupling decreases. However, this trend is not observed in Figure 3.3. The one-photon resonance is narrower than the two-photon resonance because $\eta(1)$ is near a zero of C(1), while $\eta(2)$ and $\eta(3)$ are near minima and maxima of C(2) and C(3) respectively.

In Figure 3.5, the parameters b = 1.5, $\eta(1)$ = 3.25 and $\beta(1)$ = 0.223 of the spectra are characteristic of a two-energy level configuration in substituted aromatic molecules that exhibit intense one-photon transitions [87]. In this example, parts (a) and (b) correspond to the

Figure 3.5 Comparison of RWA and exact results for the absorption spectrum or resonance profile, $\bar{P}_2^N$ as a function of $\omega/\Delta E$, for a two-level model specified by $\Delta E = 0.1$, $\mu_{12} = 3.0$, $\mu_{11} = 2.35$, $\mu_{22} = 8.85$, $d = 6.5$ and $\varepsilon = 5.0 \times 10^{-2}$. RWA resonance profiles for N = 1,2 and 3 are illustrated in (a) and (b), as evaluated from Eq. (3.3.5). The exact multi-photon spectra is illustrated in (c) which also contains the d = 0 exact spectra for comparative purposes.

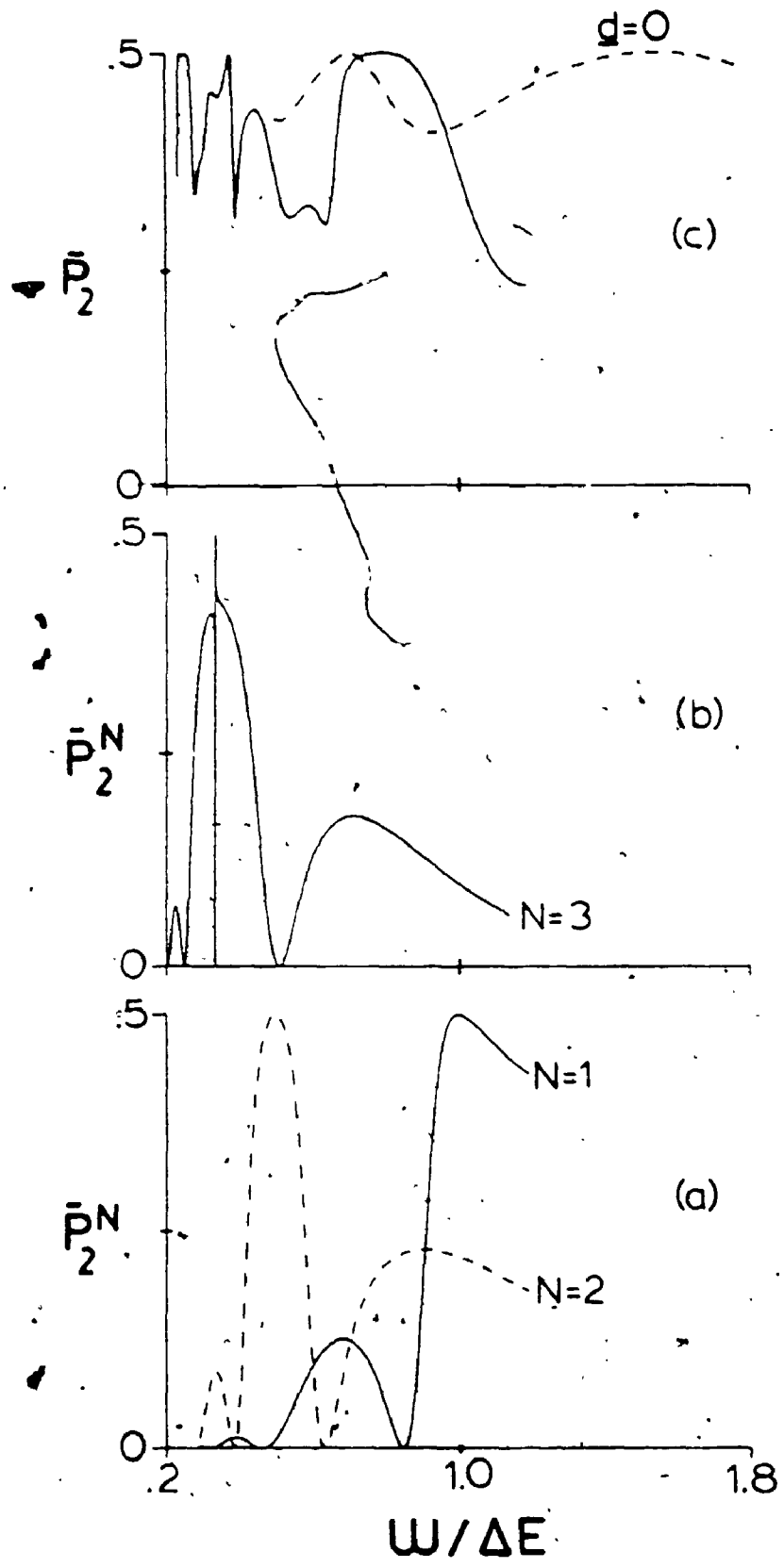
d=0
.5
0
(c)
$\bar{P}_2$
.5
0
(b)
$\bar{P}_2^N$
N=3
.5
0
(a)
$\bar{P}_2^N$
N=1
N=2
.2
1.0
1.8
W/ΔE

RWA spectra (N = 1,2,3) and (c) to the exact molecular ($\underline{d} \neq 0$) and atomic ($\underline{d} = 0$) spectra.

Once again the $\underline{d} \neq 0$ one-photon resonance is considerably narrower than the $\underline{d} = 0$ resonance, see the exact spectra. However, the molecule-EMF coupling is much larger than that in the previous examples and as a result the one-photon resonance is still quite broad. A huge Bloch-Siegert shift is evident when $\underline{d} = 0$, the one-photon resonance occurs at $\omega/\Delta E \approx 1.50$. When $\underline{d} \neq 0$ this resonance occurs at $\omega/\Delta E \approx 0.80$ providing another example of a shift to low frequency caused by non-zero permanent dipole moments.

Oscillatory fringes occur on the low frequency side of the one-photon RWA spectrum since $\eta(1)$ occurs between the first maximum and the first zero occurring in C(1) (see Figure 3.2); see also the previous discussions. The fringes occurring around the one-photon resonance in the exact spectrum have been largely suppressed by the high dynamic background present due to the strong molecule-EMF coupling.

Similar discussions apply to the $N > 1$ photon resonances. When $\underline{d} = 0$ the two-photon resonance does not occur and the three-photon resonance is very broad and is shifted to $\omega/\Delta E \approx 0.69$. When $\underline{d} \neq 0$ the three-photon resonance occurs at $\omega/\Delta E \approx 0.24$ which corresponds to a negative Bloch-Siegert shift. The two-photon resonance occurs at $\omega/\Delta E \approx 0.38$. The oscillatory fringes are partially

suppressed by the dynamic background associated with the two- and three-photon resonances.

The molecular RWA results do not show the dynamic background on the shifts from the zero-field resonance frequency $\omega_{res}^{N} = \Delta E/N$, but they do suggest the oscillations seen in the exact spectra as a function of frequency and the narrowing of the resonance widths as N increases. The coupling parameters $\beta(N)$ can vary over the widths of the resonances in this strongly coupled example where $\beta(N) =$ 0.22, 0.28 and 0.0025 for N = 1,2 and 3, particularly for N = 1, and so the $(FWHM)^N$ do not necessarily follow Eq. (3.3.13), that is $\beta(N)$, as a function of N.

3.3.3 RWA with $\varepsilon_s \neq 0$

The Schrödinger time-dependent wave equation given by Eqs. (2.4.2) and (2.4.5), and for the two-level problem by Eq. (3.1.1), is in the representation defined by the stationary states of the unperturbed Hamiltonian H_o, where $H_o\Phi_i = E_i\Phi_i$. In the presence of a static electric field $e_s\varepsilon_s$, it is convenient to transform the time-dependent wave equation into the static diagonalized Hamiltonian representation. This transformation was done for the two-level problem in Sec. 3.1 by diagonalizing the static part of the Hamiltonian operator with respect to Φ_1 and Φ_2 to obtain the eigenfunctions, Φ_- and Φ_+, and eigenvalues, E_- and E_+, for the new representation. The influence of the static field causes the original stationary state

energies E_1 and E_2 to be shifted to E_- and E_+ by mixing the wave functions Φ_1 and Φ_2 to form Φ_- and Φ_+. Since the static field mixes the original states, Φ_- and Φ_+ are of mixed parity and hence both even and odd photon transitions can occur [3,59,86] even if $\underline{d} = 0$. In what follows the basis functions (Φ_1,Φ_2) and (Φ_-,Φ_+) are denoted as the (1,2) and (-,+) representations respectively.

The spectra for the two-level model system are readily interpreted in the static diagonalized Hamiltonian, or (-,+), representation in an analogous fashion to the interpretation of a spectrum in the (1,2) representation in the absence of a static field, with several obvious exceptions [59,80,86,88]. These include the additional static background, see Eq. (3.2.48), and the mixing of states of different parity caused by the application of the static field. In the (-,+) representation the energy level separation is γ which is given by Eq. (3.1.15). For weak electromagnetic fields $\omega_{res}^{N} \approx \gamma/N$, $N = 1,2,3\ldots$. When $\underline{d} = 0$, γ is always greater than ΔE and the main resonances will occur at frequencies greater than $\Delta E/N$ even for weak electromagnetic fields. However, this is not the Bloch-Siegert shift disoussed in Secs. 2.3 and 3.3.1. For stronger electromagnetic fields $\omega_{res}^{N} > \gamma/N$ and the difference between ω_{res}^{N} and γ/N contains the Bloch-Siegert shift for the static field problem. If $\underline{d} \neq 0$, γ can be greater or less than ΔE depending on the orientation of the molecule with respect to the static field and ω_{res}^{N} can be

greater or less than $\Delta E/N$. In addition the resonance frequencies can be either to the low or high frequency side of γ/N depending on the size of $\underline{d} \neq 0$ and the magnitude of the electromagnetic field.

The molecular RWA expression for the resonance profiles obtained when $\varepsilon_s \neq 0$ is given by Eq. (3.2.47) with $\cos 2\theta$ and $\sin 2\theta$, γ, Y, C(N) and p^2 given by Eqs. (3.1.14), (3.1.15), (3.2.8), (3.2.14) and (3.2.23) respectively. The (main) resonance frequencies are obtained by equating Eq. (3.2.47) to 0.5 and solving for ω. Thus the main resonances occur when

$$X(\omega) = [(\gamma - N\omega)\cos 2\theta - C(N)J_N(X)\sin 2\theta] = 0 \qquad (3.3.17)$$

If the applied static field is non-zero the spectrum obtained from Eq. (3.2.47) consists of a static background $\bar{P}_2(\text{stat})$, given by Eq. (3.2.48), and a frequency-dependent part given by

$$\delta\bar{P}_2^N = \bar{P}_2^N - \bar{P}_2(\text{stat}) = \frac{1}{2}\cos^2 2\theta - \frac{1}{2p^2}X^2(\omega) \qquad (3.3.18)$$

The FWHM associated with the height of the resonance profile above the static background, $\delta(\text{FWHM})^N$, is obtained by equating Eq. (3.3.18) to $\frac{1}{4}\cos^2 2\theta$ to obtain

$$X^2(\omega) - \tfrac{1}{4}p^2\cos^2 2\theta = 0 \qquad (3.3.19)$$

Solving this equation for its roots ω_- and ω_+ such that $\omega_- < \omega_{res}^N < \omega_+$, where ω_- and ω_+ are the roots of Eq. (3.3.19) lying closest to $\omega = \omega_{res}^N$, yields

$$\omega_\pm = \frac{1}{N}[\gamma - 2C(N)J_N(Y)\tan 2\theta \pm |C(N)|\{1 + 2(J_N(Y))^2\tan^2 2\theta\}^{\frac{1}{2}}]_{\omega=\omega_{res}^N} \tag{3.3.20}$$

and

$$\delta(FWHM)^N = \omega_+ - \omega_- = \frac{2}{N}[|C(N)|\{1 + 2(J_N(Y))^2\tan^2 2\theta\}^{\frac{1}{2}}]_{\omega=\omega_{res}^N} \tag{3.3.21}$$

where for the moment we take $\cos 2\theta \neq 0$. In obtaining ω_+ and ω_- it has been assumed, see also Sec. 3.3.2, that $J_N(Y)$ and hence $C(N)$, do not vary appreciably as functions of ω across the main resonances. It is interesting to note that in this approximation $\delta(FWHM)^N \sim \frac{2}{N}|C(N)|_{\omega=\omega_{res}^N}$ for the static field problem whereas if $\varepsilon_s = 0$ the same approximation yields $(FWHM)^N = \frac{2}{N}|C(N)|_{\omega=\omega_{res}^N}$. The zeros of δP_2^N around $\omega = \omega_{res}^N$, occur for frequencies that satisfy

$$X^2(\omega) - p^2\cos^2 2\theta = 0 \tag{3.3.22}$$

When $\varepsilon_s = 0$ Eq. (3.3.21) reduces to the expression given

for the $(FWHM)^N$ in Eq. (3.3.13).

Eq. (3.3.21) is not valid when $\cos 2\theta = 0$ which corresponds to originally degenerate energy levels ($\Delta E = 0$) when $\underline{d} = 0$ or to $\Delta E = \underline{d}\cdot\hat{e}_s\varepsilon_s$ (see Eq. (3.1.14)). Under this condition the RWA resonance profile given in Eq. (3.2.47) reduces to

$$\bar{P}_2^N = \frac{1}{2} - \frac{1}{2p^2}\,|C(N)|^2 (J_N(Y))^2 \qquad (3.3.23)$$

where

$$p^2 = (\gamma - N\omega)^2 + |C(N)|^2 \qquad (3.3.24)$$

$$C(N) = \underline{d}\cdot\hat{e}\varepsilon N(Y)^{-1} J_N(Y) \qquad (3.3.25)$$

and

$$Y = \frac{-2\underline{\mu}_{12}\cdot\hat{e}\varepsilon}{\omega} \qquad (3.3.26)$$

The "static" background, obtained by setting $\varepsilon = 0$ in Eq. (3.3.23), is 0.5. Thus the spectra consists of a saturating background with a series of dips whose minima occur at frequencies such that the second term in Eq. (3.3.23) is a maximum. This will often correspond to $\omega = \gamma/N$ ($\omega = \gamma/N$ if $C(N)$ and $J_N(Y)$ do not vary across the widths of the "resonances") provided $Y = \frac{-2N\underline{\mu}_{12}\cdot\hat{e}\varepsilon}{\gamma}$ does not occur near

a zero of J_N. Such resonances have been discussed for the one-photon degenerate case with $\Delta E = 0$, $\underline{d} = 0$ and $\varepsilon_s = 0$, and for problems corresponding to the condition $\underline{M}\cdot\underline{E}(t) = 0$ in Eq. (3.1.18); both of these problems are exactly soluble [4,88,89-91]. Analogous effects have been discussed in the context of exact Floquet type calculations involving Stark tuning ($\Delta E \neq 0$, $\varepsilon_s \neq 0$, $\underline{d} = 0$) and magnetic resonance problems [91,92]. The RWA result given in this paragraph will hopefully prove to be a useful analytical expression for suggesting and interpreting such spectral effects for more general situations involving permanent dipole moments.

In order to discuss the single- and multi-photon spectra obtained from the RWA type expression given by Eq. (3.2.47) it is useful to define the coupling strength parameter

$$\beta_\gamma(N) = \left[\frac{C(N)}{\gamma}\right]_{\omega=\omega_{res}^N} \qquad (3.3.27)$$

$\beta_\gamma(N)$ is the N-photon molecule-EMF coupling strength parameter, for the static field problem, that is analogous to $\beta(N)$ used in Sec. 3.3.2.

3.3.3A RWA with $\underline{d} = 0, \varepsilon_s \neq 0$

When $\underline{d} = 0$ the RWA type expression is still given by Eq. (3.2.47) where C(N), Y and p^2 are given by Eqs. (3.2.14), (3.2.8) and (3.2.23) but now (see Eqs. (3.1.14),

(3.1.15), (3.1.19) and (3.1.20))

$$\cos 2\theta = \gamma^{-1}(\Delta E) \; ; \; \sin 2\theta = \gamma^{-1}(2\underline{\mu}_{12}\cdot\hat{e}_S\varepsilon_S) \qquad (3.3.28)$$

$$\underline{D} = -2\underline{\mu}_{12}\sin 2\theta \; ; \; \underline{M} = \underline{\mu}_{12}\cos 2\theta \qquad (3.3.29)$$

and

$$\gamma = [(\Delta E)^2 + 4(\underline{\mu}_{12}\cdot\hat{e}_S\varepsilon_S)^2]^{\frac{1}{2}} \qquad (3.3.30)$$

Here the roles of $\underline{D}$ and $\underline{M}$ in the coupling parameter $C(N)$ are analogous to that of $\underline{d}$ and $\underline{\mu}_{12}$ in the $\underline{d} \neq 0$, $\varepsilon_S = 0$ problem of Sec. 3.3.2.

In Figure 3.6 the exact spectra both with and without ε_S are given for an example that corresponds to the $J = 0$ to $J = 1$ rotational transition in the ground vibrational level of CsI [93]. The coupling strengths are quite weak, $\beta_\gamma(N) = 0.038$, 0.0025, 0.00017 for the $N = 1, 2$, and 3 photon resonances. The static background is 0.194 (see Eq. (3.2.48) with $\cos 2\theta = \Delta E/\gamma$). In this example the RWA spectra and the exact spectrum agree to much better than graphical accuracy; the resonance frequencies for both coincide with $\omega_{res}^{N} = \gamma/N > \Delta E/N$ to four significant figures ($\gamma/\Delta E = 1.28$). When $\varepsilon_S = 0$ the exact spectrum and the one- and three-photon RWA spectra also agree precisely, with the main resonances occurring at $\omega_{res}^{N} = \Delta E/N$, and the two-photon resonance is absent as expected. For $\varepsilon_S \neq 0$, $\delta(FWHM)^N$

Figure 3.6. The absorption spectrum or the steady state transition probability, $\bar{P}_2$ as a function of $\omega/\Delta E$, for a two-level model system characterized by $\Delta E = 2.151 \times 10^{-7}$, $d = 0$, $\mu_{12} = 2.6398$, $\varepsilon = 5.0 \times 10^{-9}$ and $\varepsilon_s = 3.24 \times 10^{-8}$. The spectrum with $\varepsilon_s = 0$ is included for comparative purposes. The molecular parameters correspond to the $J = 0 \rightarrow J = 1$ rotational transition in CsI [93].

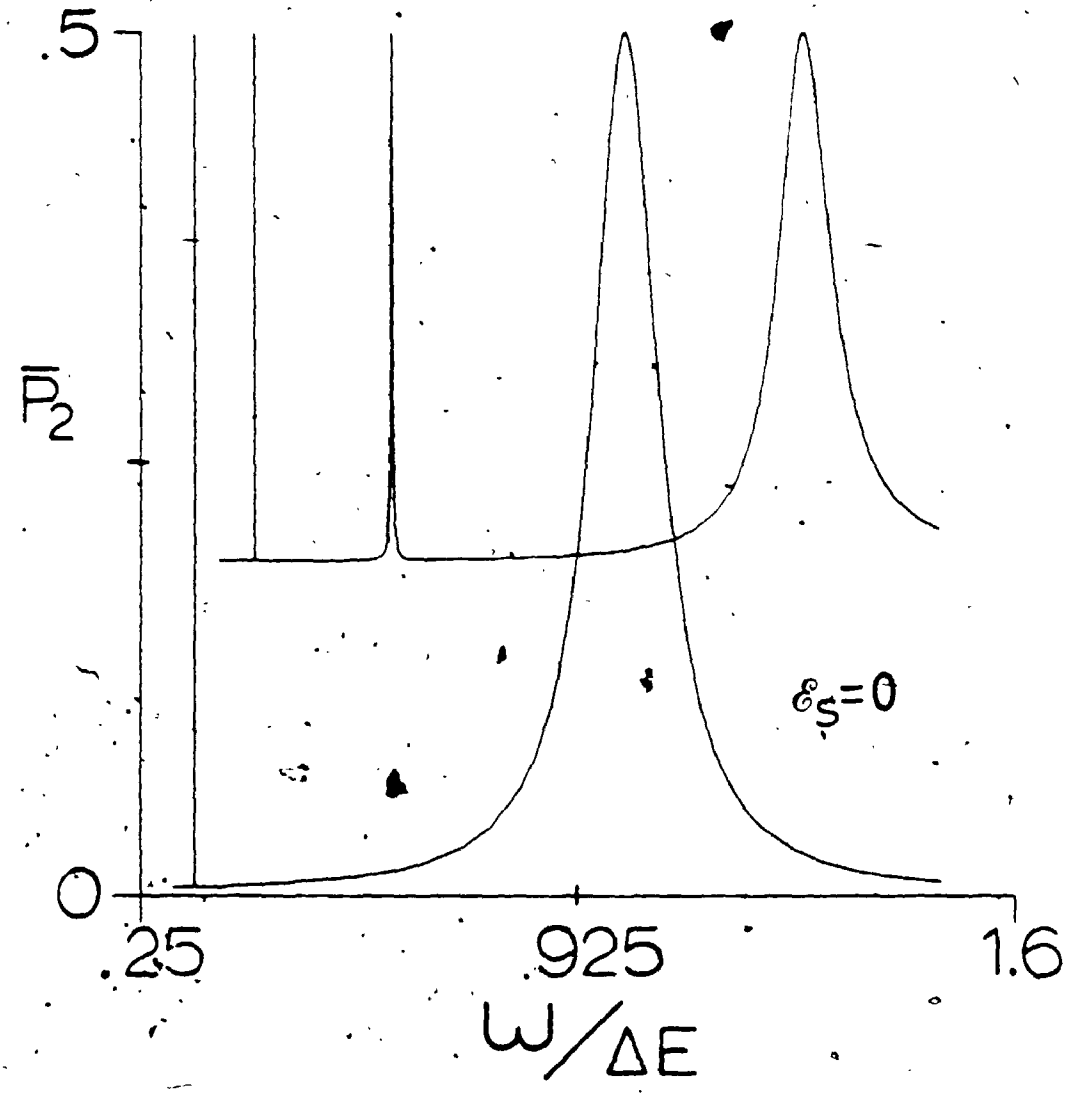
.5
$\bar{P}_2$
0
.25
.925
1.6
$W/\Delta E$
$\varepsilon_S=0$

predicted from Eq. (3.3.21) are 2.07×10^{-8}, 6.2×10^{-10} and 2.7×10^{-11} for N = 1,2 and 3 respectively and these agree precisely with those measured from the data used to construct Figure 3.6.

In Figure 3.7 spectra with molecular parameters identical to those of the previous example are examined. However the applied fields, and hence the couplings, are larger since $\beta(N) = 0.34$, 0.21 and 0.14 for N = 1,2 and 3. The exact spectra both with and without ε_s (Figure 3.7c) are compared to the RWA spectra (Figure 3.7a) obtained from Eq. (3.2.49), and Eqs. (3.3.28)-(3.3.30), for the N = 1,2 and 3 photon resonances. The spectrum obtained by adding the RWA results for N = 1,2 and 3 is given in Figure 3.7b together with the RWA one-photon spectrum with $\varepsilon_s = 0$. The static background is $\bar{P}_2(\text{stat}) = 0.25$ for this problem.

In the exact spectrum with $\varepsilon_s \neq 0$ (see Figure 3.7c) the one-photon resonance is shifted to $\omega = 2.4 \times 10^{-7}$ ($\omega/\Delta E = 1.1$) from the zero field prediction of $\omega = 2.151 \times 10^{-7}$ ($\omega/\Delta E = 1.0$). When $\varepsilon_s \neq 0$ the one-photon resonance is shifted even further to $\omega = 3.44 \times 10^{-7}$ ($\omega/\Delta E = 1.6$) which is considerably greater than the weak EMP limit of $\gamma/1 = 3.04 \times 10^{-7}$ ($\omega/\Delta E = 1.41$). The RWA one-photon resonance (see Figure 3.7a) is also shifted to a higher frequency than γ; it occurs at $\omega = 3.36 \times 10^{-7}$ ($\omega/\Delta E = 1.56$).

Similarly, when N > 1 the three-photon resonance occurring in the exact $\varepsilon_s = 0$ spectrum is shifted to $\omega = 1.03 \times 10^{-7}$ ($\omega/\Delta E = 0.48$) relative to the zero field

Figure 3.7. Comparison of RWA and exact results for the absorption spectrum, $\bar{P}_2$ as a function of $\omega/\Delta E$, for the two-level model specified by $\Delta E = 2.151 \times 10^{-7}$, $d = 0$, $\mu_{12} = 2.6398$, $\varepsilon = 5.76 \times 10^{-8}$ and $\epsilon_s = 4.07 \times 10^{-8}$. RWA resonance profiles for $N = 1,2$ and 3 are illustrated in (a), as evaluated from Eqs. (3.2.47) and (3.3.28)-(3.3.30). The sum of the RWA profiles in (a) is given in (b), together with the analogous RWA result for $\epsilon_s = 0$. The exact multi-photon spectra are illustrated in (c) which contains the exact spectra for $\epsilon_s = 0$ for comparative purposes.

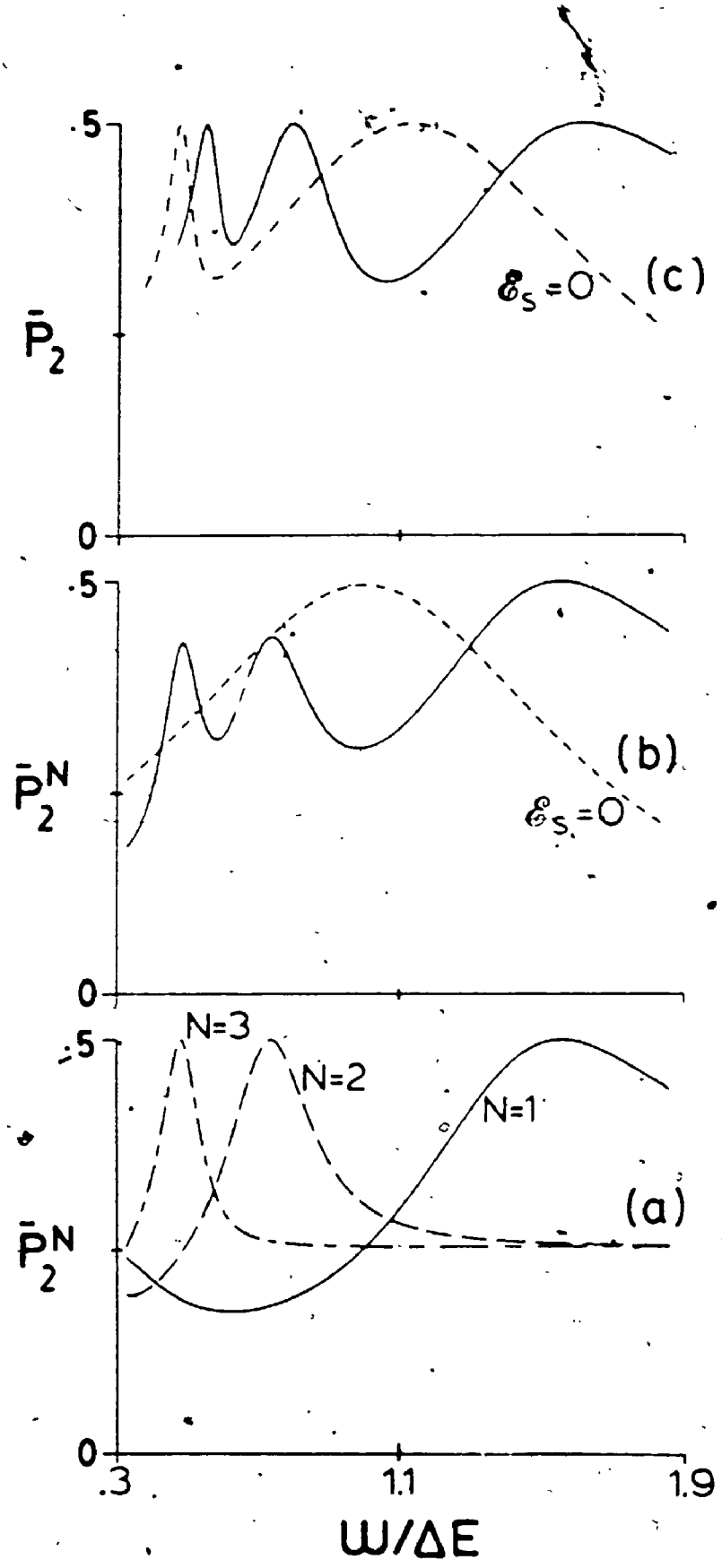
.5
$\bar{P}_2$
0
$\mathcal{E}_s = 0$
(c)
.5
$\bar{P}_2^N$
(b)
$\mathcal{E}_s = 0$
0
N=3
N=2
N=1
.5
$\bar{P}_2^N$
(a)
0
.3
1.1
1.9
$W/\Delta E$

limit of $\omega = 7.17 \times 10^{-8}$ ($\omega/\Delta E = 0.33$). The two-photon resonance does not occur when $\varepsilon_s = 0$. When $\varepsilon_s \neq 0$ the two- and three-photon resonances frequencies are $\omega = 1.7 \times 10^{-7}$ ($\omega/\Delta E = 0.79$) and 1.2×10^{-7} ($\omega/\Delta E = 0.55$) respectively. The values of γ/N are 1.52×10^{-7} ($\omega/\Delta E = 0.71$) and 1.013×10^{-7} ($\omega/\Delta E = 0.47$) for $N = 2$ and 3. The RWA resonances also occur at frequencies greater than γ/N; they are $\omega = 1.57 \times 10^{-7}$ ($\omega/\Delta E = 0.73$) and $\omega = 1.03 \times 10^{-7}$, ($\omega/\Delta E = 0.48$) for the two- and three-photon resonances. Thus for $N = 1,2$ and 3 the RWA accounts for some of the shift from the zero EMF limit of γ/N that occurs in the exact spectra. The $\delta(\text{FWHM})^N$ predicted by Eq. (3.3.21) for this strongly coupled example are 2.2×10^{-7}, 6.7×10^{-8} and 3.1×10^{-8} for $N = 1,2$ and 3 respectively. These agree reasonably well with the numerical values used to obtain Figure 3.7; 1.6×10^{-7}, 5.5×10^{-8} and 2.6×10^{-8} for the one-, two- and three-photon resonances. The one-photon resonance, in particular, is quite broad and in general the assumption that $C(N)$ and hence $J_N(Y)$ do not vary across the resonances is not particularly good.

The RWA is a near resonance approximation and the off-resonance difficulties associated with it are evident in Figure 3.7b where the sum of the RWA resonance profiles is presented. The one-photon resonance is slightly above 0.5 and the two- and three-photon resonances are considerably below 0.5. This is largely due to the resonance overlap present in this strongly coupled example (see

Figure 3.7a) which includes the dips in the RWA resonance profiles below the static background for frequencies sufficiently off-resonance. Adding the RWA results for the resonance profiles is not generally an accurate representation of the exact spectrum unless the applied fields are quite weak (see the example of Figure 3.6).

The effect of the static field is clearly illustrated in Figure 3.6 and is accurately predicted by the RWA for this weakly coupled example. When the effective coupling between the molecule or atom and the applied fields is larger, as in Figure 3.7, the RWA predicts the general structure of the exact spectrum and some of the shifts of the main resonances from $\omega = \gamma/N$.

3.3.3B RWA with $d \neq 0$, $\varepsilon_s \neq 0$

As pointed out earlier (Sec. 3.3.2), molecules are not isotropic and therefore their spectra depend on the orientation of the molecule relative to the direction of the applied EMF. For molecular problems it is often important to average the transition probabilities or absorption spectra with respect to the molecule-applied field orientations. For example, many experiments are carried out in the gas phase, in the absence of applied static fields, and in order to relate calculations to such experiments it is necessary to take into account the equally probable random orientations of the molecule when calculating observables [73]. In the presence of static

electric fields all orientations are not equally probable and the averaging of spectral observables requires weighting each orientation with the appropriate Boltzmann factor (see for example [74,85]).

Orientationally averaged transition probabilities have been evaluated for perturbation theory results where they can be performed analytically [3,94,95]. Apparently little analogous work has been done for orientational averages in the exact approaches for solving the time-dependent wave equation, and in this section we give a simple example of how to carry out such calculations. This comment does not apply to rotational calculations which involve explicit inclusion of rotational energy levels, such as in IR multi-photon absorption spectrum caloulations involving the Floquet secular equation approach [6,7].

In what follows, the rotating wave approximation will be used to calculate the absorption spectra for a two-level molecular system as a function of the orientation of the molecule with respect to the applied field directions. The resulting spectra will then be orientationally averaged with respect to the direction of the applied fields. The problem selected is such that $\underline{\mu}_{12} \| \underline{d}$ defines the molecular z axis and $\hat{\epsilon} \| \hat{e}_z$ defines the space-fixed z axis. The EMF amplitude is such that the RWA results and the exact calculations agree to far better than graphical accuracy for all frequencies in this example [74]. Several fixed configuration spectra will be considered as well as

the orientationally averaged spectra.

When $\underline{d} \neq 0$ and $\varepsilon_s \neq 0$ the RWA type expression for the single- and multi-photon resonances is given by Eq. (3.2.47) where cos2θ and sin2θ, γ, $\underline{D}$, $\underline{M}$, C(N), Y and p^2 are given by Eqs. (3.1.14), (3.1.15), (3.1.19), (3.1.20), (3.2.14), (3.2.8) and (3.2.23) respectively. The orientational average $\langle \bar{P}_2^N \rangle_{rot}$ of the steady state population of excited state 2, via the N-photon transition, is obtained by weighting the contribution of each orientation by a Boltzmann factor. The energies, E_- and E_+, of the molecule perturbed by the static field are the roots obtained from diagonalizing the static Hamiltonian matrix given by Eq. (3.1.4) with $\varepsilon = 0$ [4]. From Sec. 3.1 it follows that

$$E_\mp = \tfrac{1}{2}[E_1+E_2 - (\underline{\mu}_{11}+\underline{\mu}_{22})\cdot\theta_s\varepsilon_s \mp \gamma] \qquad (3.3.31)$$

These energies, and the fixed configuration transition probability, depend only on the angle θ between the space- and body-fixed z axes where $0 \leq \theta \leq \pi$ and

$$\underline{\mu}_{12}\cdot\theta\varepsilon = \mu_{12}\varepsilon x \; ; \; \underline{d}\cdot\theta\varepsilon = d\varepsilon x \qquad (3.3.32)$$

$$\underline{\mu}_{12}\cdot\theta_s\varepsilon_s = \mu_{12}\varepsilon_s x \; ; \; \underline{d}\cdot\theta_s\varepsilon_s = d\varepsilon_s x \qquad (3.3.33)$$

where

$$x = \cos\theta \qquad (3.3.34)$$

The orientationally averaged absorption spectrum is given by

$$\langle \bar{P}_2^N \rangle_{rot} = \frac{\int_0^{2\pi} \int_0^{\pi} \bar{P}_2^N \exp\left[\frac{-\Delta W}{kT}\right] \sin\theta \, d\phi \, d\theta}{\int_0^{2\pi} \int_0^{\pi} \exp\left[\frac{-\Delta W}{kT}\right] \sin\theta \, d\phi \, d\theta}$$

$$= \frac{\int_{-1}^{1} \bar{P}_2^N \exp\left[\frac{-\Delta W}{kT}\right] dx}{\int_{-1}^{1} \exp\left[\frac{-\Delta W}{kT}\right] dx} \qquad (3.3.35)$$

where $\exp\left[\frac{-\Delta W}{kT}\right]$ is the Boltzmann weighting factor, k is the Boltzmann constant, T is the absolute temperature and

$$\Delta W = E_- - E_1$$
$$= \tfrac{1}{2}[\Delta E - (\mu_{11}+\mu_{22}) \cdot e_s \varepsilon_s - \gamma] \qquad (3.3.36)$$

is the interaction energy arising from the interaction of the molecule, in ground state 1, with the applied static field in the absence of the time-dependent oscillating field. E_1 is the energy of the isolated molecule and E_- is the energy of the molecule, originally in the ground state 1, perturbed by the static field. This choice of ΔW is appropriate for initial conditions specifying that the molecule is in the ground energy state 1 at time $t = 0$. ΔW can be written in a more recognizable form by expanding γ (see Eq. (3.1.15)) as follows

$$\gamma = (\Delta E)[1-2(\Delta E)^{-1}(\underline{d}\cdot\hat{e}_s\varepsilon_s) + (\Delta E)^{-2}(\underline{d}\cdot\hat{e}_s\varepsilon_s)^2$$

$$+ 4(\Delta E)^{-2}(\underline{\mu}_{12}\cdot\hat{e}_s\varepsilon_s)^2]^{\frac{1}{2}}$$

$$\approx \Delta E - \underline{d}\cdot\hat{e}_s\varepsilon_s + 2(\Delta E)^{-1}(\underline{\mu}_{12}\cdot\hat{e}_s\varepsilon_s)^2 + \ldots \quad (3.3.37)$$

assuming $|\underline{d}\cdot\hat{e}_s\varepsilon_s|$ and $|\underline{\mu}_{12}\cdot\hat{e}_s\varepsilon_s|$ are small relative to ΔE. Substitution into Eq. (3.3.36) gives

$$\Delta W \approx -\underline{\mu}_{11}\cdot\hat{e}_s\varepsilon_s - (\Delta E)^{-1}(\underline{\mu}_{12}\cdot\hat{e}_s\varepsilon_s)^2 + \ldots \quad (3.3.38)$$

The first term on the right-hand side of Eq. (3.3.38) represents the interaction of the permanent dipole with the applied static field and the second term is the field induced dipole induction energy [96,97]. The free orientationally averaged spectrum is obtained when $\frac{\Delta W}{kT} \neq 0$ and can correspond to either $\varepsilon_s = 0$ or to large T. In this case, all the orientations are weighted equally, see Eq. (3.3.35).

The method of evaluating orientationally averaged spectra described above is designed for use when the rotational motion of the molecule is much slower than the time it takes for the transition from state 1 to state 2 to occur. Different techniques will be required for calculations of the microwave or rotational spectra of a molecule [6,7].

The one-photon resonance of a two-level molecular model representative of the (linear) pentadienal molecule [2] is examined in Figure 3.8. Figure 3.8a consists of the

Figure 3.8. The orientationally averaged one-photon resonance profiles, $\langle \bar{P}_2 \rangle_{rot}$ as a function of $\omega/\Delta E$, for a two-level model characterized [2] by $\Delta E = 0.1899$, $\mu_{12} = 2.486$, $\mu_{11} = 4.760$, $\mu_{22} = 8.415$ and $d = 3.655$. The amplitude of the oscillating electric field is $\varepsilon = 10^{-3}$ and that of the static electric field is $\varepsilon_s = 10^{-3}$: (a) corresponds to the fixed configuration spectra with $\underline{\mu}_{12} \| \underline{d} \| \hat{e} \| \hat{e}_s (x = 1)$ and $\underline{\mu}_{12} \| \underline{d}$ antiparallel to $\hat{e} \| \hat{e}_s (x = -1)$ as well as the free orientationally averaged spectra with $d = 3.655$ and, for comparative purposes, with $d = 0$. (b)-(e) correspond to the Boltzmann orientationally averaged spectra for $T = 7000\text{-}100$ K.

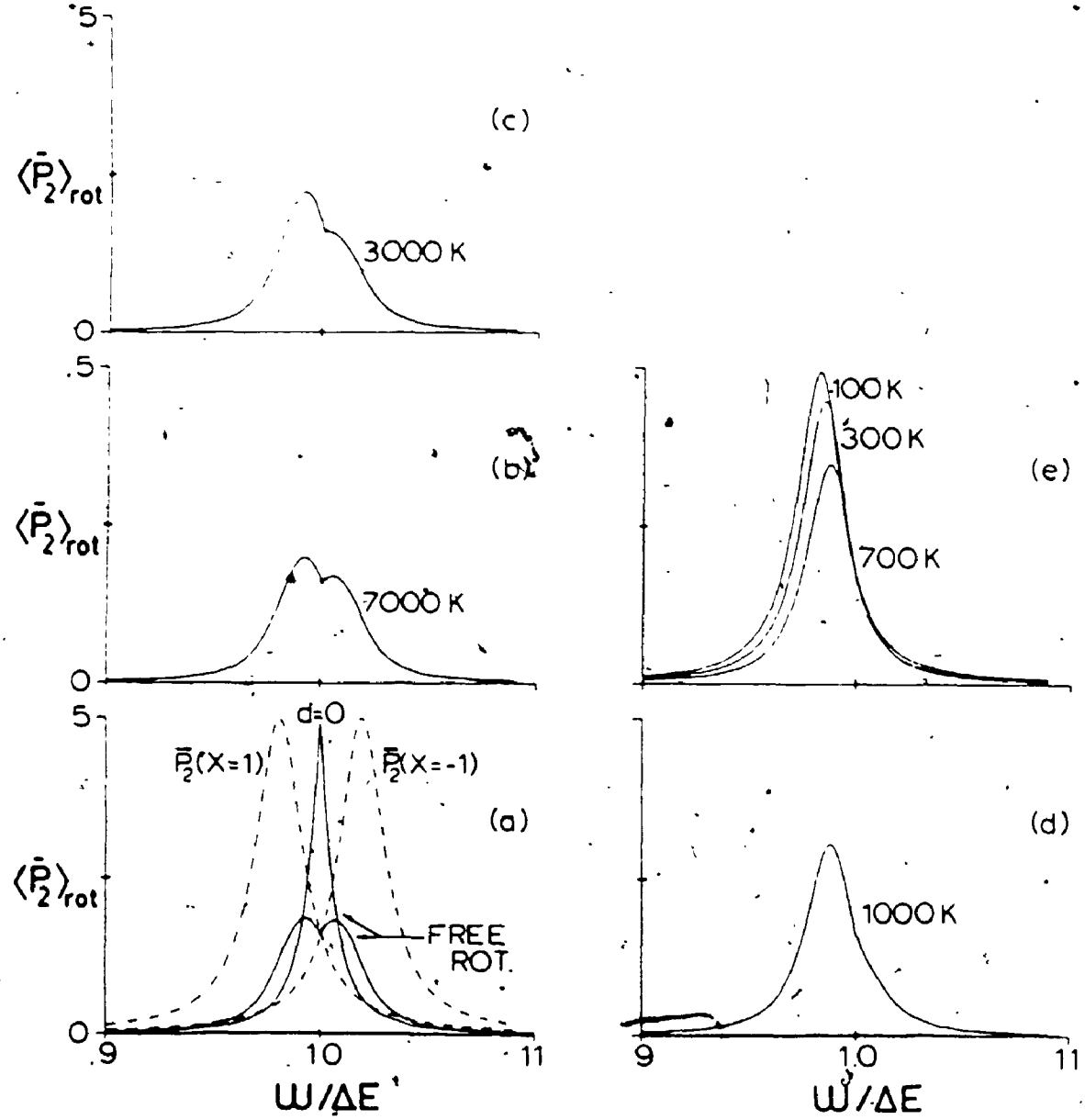
.5
(c)
$\langle \bar{P}_2 \rangle_{rot}$
3000 K
0
.5
(b)
$\langle \bar{P}_2 \rangle_{rot}$
7000 K
0
5
d=0
$\bar{P}_2(X=1)$
$\bar{P}_2(X=-1)$
(a)
$\langle \bar{P}_2 \rangle_{rot}$
FREE ROT.
0
.9
10
11
$\omega/\Delta E$
100 K
300 K
(e)
700 K
(d)
1000 K
9
1.0
11
$\omega/\Delta E$

fixed configuration results, obtained from Eq. (3.2.47), for the one-photon resonance corresponding to $(\underline{\mu}_{12},\underline{d})\,||\,(\hat{e},\hat{e}_S)$ and to $(\underline{\mu}_{12},\underline{d})$ antiparallel to $(\hat{e},\hat{e}_S)$; $\varepsilon = \varepsilon_S = 10^{-3}$. The coupling strength parameters for these configurations are $\beta_\gamma(1) = 0.0137$ and -0.0124 (see Eq. (3.3.27) respectively. The resonances occur at $\omega = \gamma = 0.1863$ ($\omega/\Delta E = 0.981$) and $\omega = \gamma = 0.1937$ ($\omega/\Delta E = 1.020$) for the parallel and antiparallel configurations respectively, where $\gamma < \Delta E$ in the former and $\gamma > \Delta E$ in the latter. The free orientationally ("$T = \infty$") averaged spectra, both with and without $\underline{d}$, are also included in Figure 3.8a and can be related to the fixed configuration spectra by considering the coupling parameter for each of the configurations included in the orientationally averaged spectrum.

The coupling between the molecule and the EMF is given by $C(1) = \underline{\mu}_{12}\cdot\hat{e}\varepsilon$, see Eq. (3.2.14), and can be explicitly written as a function of x by making use of Eqs. (3.3.32) and (3.3.33) in Eqs. (3.1.19), (3.1.20), (3.2.8) and (3.2.14) . Analyzing C(1), at $\omega_{res} = \gamma$, shows that it has a maximum value of $\simeq 0.253 \times 10^{-2}$ when $x = 1$ (the parallel configuration), decreases smoothly to zero at $x = 0$ (where $(\underline{\mu}_{12},\underline{d}) \perp (\hat{e},\hat{e}_S)$) and then increases in size to $\simeq 0.244 \times 10^{-2}$ when $x = -1$ (the antiparallel configuration). $|C(1)|$ is almost symmetrical about $x = 0$; it is slightly smaller in magnitude for $x < 0$ than for $x > 0$. The one-photon resonance occurs at $\omega_{res} = \gamma$ for any given configuration of the molecule with respect to the

applied fields and since γ can be either greater than or less than ΔE the resonance can occur on the high or low frequency side of $\omega = \Delta E$ (examples are given in the last paragraph). Each configuration included in the orientational average will have a resonance at $\omega_{res} = \gamma$ with a height of 0.5 and a width (above the very small static background of order $\leq 10^{-4}$), given by Eq. (3.3.21), that varies with x essentially through C(1). The free orientationally ("T = ∞") averaged spectrum is obtained from Eq. (3.3.35) with $\frac{\Delta W}{kT} = 0$. This spectrum is the sum of all the fixed configuration spectra divided by the number of fixed configurations used in the average; in this example 41 values of x placed symmetrically around x = 0 were more than sufficient to ensure graphical accuracy [73]. The end points in $\langle \bar{P}_2^N \rangle_{rot}$ are the parallel and the antiparallel configurations and the resonances for all the other configurations occur at frequencies between these two extremes and are narrower as well (C(1) smaller). Thus the free orientationally averaged spectrum lies between the parallel and antiparallel configuration extremes with two maxima significantly lower than 0.5 and a minimum located between the maxima at $\omega = \Delta E$ since C(1) = 0 and $\gamma = \Delta E$ when x = 0. This is in qualitative agreement with Figure 3.8a. The minimum that occurs in the free orientationally averaged spectrum is due to the presence of $\underline{d} \neq 0$ since the term $\underline{d} \cdot \theta_s \varepsilon_s$ in γ, see Eq. (3.1.15), causes the fixed configuration resonances to "shift" to either side of

$\omega = \Delta E$. When $\underline{d} = 0$ the fixed configuration spectra all occur at $\omega = \Delta E$ (since the maximum value of $4(\underline{\mu}_{12} \cdot \hat{e}_S \mathcal{E}_S)^2 = 2.47 \times 10^{-5}$ is very small relative to $(\Delta E)^2 = 3.61 \times 10^{-2}$ in γ) and hence the free orientationally averaged spectrum consists of a single peak centered at $\omega = \Delta E$ (see Figure 3.8a).

The effect of temperature, which occurs in the Boltzmann factor in Eq. (3.3.35), is examined in Figures 3.8b-3.8e, where T = 7000, 3000, 1000 and 700-100 K respectively for the two-level molecular model of Figure 3.8a. As T decreases the attractive configurations of the molecule relative to the directions of the applied fields, which correspond to $x > 0$ and $\gamma < \Delta E$, are favored by the Boltzmann factor over the repulsive configurations where $x < 0$ and $\gamma > \Delta E$. Thus as temperature decreases the Boltzmann weighted orientationally averaged spectra increase in height on the low frequency side of $\omega = \Delta E$ and decrease on the high frequency side. The minimum that occurred at $\omega = \Delta E$ in Figure 3.8a eventually changes to a point of inflection at T = 1000 K (see Figure 3.8d) and then disappears for lower temperatures (see Figure 3.8e) since the molecule rotates less and tends to align itself parallel to the static field as T decreases. The orientationally averaged spectrum obtained at T = 100 K in Figure 3.8e is essentially the fixed configuration spectrum with $x = 1$ given in Figure 3.8a.

The behaviour of the orientationally averaged spectra, as a function of ω and T, can depend on the relative orientation of the transition and permanent dipoles. For example if $\underline{\mu}_{12} \perp \underline{d}$, with $\hat{e} \| \hat{e}_s$, the transition probability will be zero for sufficiently low temperatures where $\underline{d}$ is parallel to $\hat{e}_s$ and hence $\underline{\mu}_{12} \cdot \hat{e} = 0$. Thus instead of increasing with decreasing temperatures as for $\underline{\mu}_{12} \| \underline{d}$, the resonance height will eventually decrease with decreasing T if $\underline{\mu}_{12} \perp \underline{d}$ [98]. The nature of the orientationally averaged spectra can also depend, for example, on the magnitude of the static field. Decreasing ε_s from 10^{-3} to 5×10^{-4} in the calculation associated with Figure 3.8 leads to free orientationally averaged spectra with no minimum [74].

CHAPTER 4

PERTURBATIVE CORRECTIONS TO THE TWO-LEVEL RWA ($d \neq 0$, $\varepsilon_s = 0$) AND A DISCUSSION OF GIANT DIPOLE MOLECULAR SPECTRA

In this chapter perturbative corrections to the two-level rotating wave approximation (RWA) for the absorption spectra and its FWHM, with $d \neq 0$ and $\varepsilon_s = 0$, derived in Sec. 3.2 and discussed with illustrative examples in Sec. 3.3.2, will be obtained to help investigate and explain the effects arising in the exact spectra that are absent from the RWA spectra. These effects include the shifts from the resonance position $\omega_{res}^{N} \Delta E/N$ predicted by the RWA and the dynamic backgrounds seen in the exact spectra. The corrections are obtained by applying Floquet theory [9,10,23,26] to the time dependent wave equation given by Eq. (3.1.1) to obtain a time independent Floquet Hamiltonian matrix for the problem. Perturbation theory is then applied to the resulting Floquet Hamiltonian secular equation and the perturbative corrections are obtained to the desired order, the RWA result corresponds to the zeroth plus first order perturbation solution of the Floquet Hamiltonian secular equation. The Floquet secular equation is derived in Sec. 4.2 and the perturbation treatment of it is discussed in Sec. 4.3 where perturbative corrections to the RWA resonance profiles and full widths at half maximum are obtained and discussed. In the limit that $d \to 0$, the

results obtained here yield "atomic" results in essential agreement with those obtained by Shirley [23] some time ago, see also [82]. The perturbative results are also used in Sec. 4.3 to help analytically explain some of the effects missing in the RWA and in the $\underline{d} = 0$ limit. This discussion is continued in Sec. 4.4 by using the perturbative corrections to explain some of the effects absent in the RWA by using some of the examples discussed earlier in Chapter 3 as models. Due to the slow convergence of the perturbation theory, and to difficulties associated with the definition of the orders of the perturbative corrections to the RWA results for the spectra, its application to problems with large EMF-permanent dipole and/or EMF-transition dipole couplings is rather limited; it is, however, useful from a qualitative point of view. Sec. 4.4 includes a further discussion of the absorption spectra of molecules with large permanent dipole moments with illustrative examples evaluated using the exact approach to the problem discussed in Sec. 2.4. The exact approach avoids the difficulties associated with perturbation approaches. This discussion relates that of Sec. 3.3.2 with recent published material [34,35] on "giant dipole molecules".

4.1 Preliminaries

Rather than begin with the original time-dependent wave equation for the problem, Eq. (3.1.1) with $\varepsilon_s = 0$, it is convenient to start with its interaction energy representation analogue given by Eq. (3.2.2) with $\varepsilon_s = 0$. The Hamiltonian, in the interaction representation, is defined by Eqs. (3.2.3) and (3.2.11) with $\varepsilon_s = 0$ such that γ, $\underline{D}$, $\underline{M}$ and the states $|-\rangle$ and $|+\rangle$ are replaced by ΔE, $\underline{d}$, $\underline{\mu}_{12}$, $|1\rangle$ and $|2\rangle$ respectively. Thus, in summary

$$H_{I,11}(t) = H_{I,22}(t) = 0 \tag{4.1.1}$$

$$H_{I,12}(t) = (H_{I,21}(t))^* = -\tfrac{1}{2}(\underline{\mu}_{12}\cdot\hat{e}\varepsilon)\exp(-i\Upsilon\sin\theta)$$

$$\times \sum_{k=-\infty}^{\infty} J_k(\Upsilon)[\exp(i[k+1]\theta)\exp(-i[\Delta E-(k+1)\omega]t)$$

$$+ \exp(i[k-1]\theta)\exp(-i[\Delta E-(k-1)\omega]t)] \tag{4.1.2}$$

where

$$\Upsilon = \frac{\underline{d}\cdot\hat{e}\varepsilon}{\omega} \tag{4.1.3}$$

The relevant differential equation is

$$i\frac{d}{dt}\underline{b}(t) = i\frac{d}{dt}\begin{bmatrix} b_1(t) \\ b_2(t) \end{bmatrix} = \underline{H}_I(t)\underline{b}(t) \tag{4.1.4}$$

Floquet theory will be applied to Eq. (4.1.4) and perturbation theory will be used to obtain the corrections to the zeroth order RWA solution.

4.2 The Floquet Secular Equation with $\mu_{ii} \neq 0$

In this section the Hamiltonian defined by Eqs. (4.1.1) and (4.1.2) will be transformed to a time-independent Floquet Hamiltonian. The eigenvectors and eigenvalues of the associated secular equation will be used to construct the transition probabilities of interest.

To start, the differential equation given by Eq. (4.1.4) is transformed into a phase factored form [31] by writing,

$$b_{(1,2)}(t) = K_{(1,2)}(t)\exp(-i[\pm\tfrac{1}{2}\Delta E+\alpha_{(1,2)}]t) \qquad (4.2.1)$$

and choosing $\alpha_{(1,2)}$ such that it is useful in identifying the N-photon resonances in the Floquet matrix equations to be derived in what follows. The new Hamiltonian is now back in a Schrödinger-like representation if $\alpha_{(1,2)} = 0$. Substituting Eq. (4.2.1) into Eq. (4.1.4) and choosing

$$\alpha_1 = -\tfrac{1}{2}N\omega \quad ; \quad \alpha_2 = \tfrac{1}{2}N\omega \qquad (4.2.2)$$

gives

$$i\frac{d}{dt}\underline{\underline{K}}(t) = i\frac{d}{dt}\begin{bmatrix}K_1(t)\\K_2(t)\end{bmatrix} = \underline{\underline{H}}(t)\underline{\underline{K}}(t) \qquad (4.2.3)$$

where

$$H_{11} = -H_{22} = -\Delta = -\tfrac{1}{2}(\Delta E - N\omega) \tag{4.2.4}$$

and

$$H_{12}(t) = (H_{21}(t))^* = -\tfrac{1}{2}(\underline{\mu}_{12}\cdot\theta\varepsilon)\exp(-iY\sin\theta)$$

$$\times \sum_{k=-\infty}^{\infty} J_k(Y)[\exp(i[k+1]\theta)\exp(-i[N-(k+1)]\omega t)$$

$$+ \exp(i[k-1]\theta)\exp(-i[N-(k-1)]\omega t)] \tag{4.2.5}$$

Since $\underline{H}(t)$ is a periodic Hamiltonian such that $\underline{H}(t) = \underline{H}(t + t_p)$ where $t_p = 2\pi/\omega$ (see Eq. (3.2.46)), Floquet theory states that the solution of Eq. (4.2.3) can be written as [26]

$$\underline{G}(t) = \underline{Z}(t)\exp(-i\underline{Q}t) \tag{4.2.6}$$

where

$$\underline{G}(t) = \begin{bmatrix} G_{11}(t) & G_{12}(t) \\ G_{21}(t) & G_{22}(t) \end{bmatrix}, \quad \underline{Q} = \begin{bmatrix} q_1 & 0 \\ 0 & q_2 \end{bmatrix},$$

$$\underline{Z}(t) = \begin{bmatrix} Z_{11}(t) & Z_{12}(t) \\ Z_{21}(t) & Z_{22}(t) \end{bmatrix}. \tag{4.2.7}$$

Here $\underline{\underline{G}}(t)$ is the general solution matrix of Eq. (4.2.3) and includes the specific solution of interest; $\underline{\underline{Z}}(t)$ is a periodic matrix such that

$$\underline{\underline{Z}}(t) = \underline{\underline{Z}}(t + t_p) \quad , \tag{4.2.8}$$

and q_1 and q_2 are time-independent constants.

Substitution of Eq. (4.2.6) into Eq. (4.2.3) yields

$$i[\frac{d}{dt}\underline{\underline{Z}}(t) - i\,\underline{\underline{Q}}\,\underline{\underline{Z}}(t)] = \underline{\underline{H}}(t)\underline{\underline{Z}}(t) \tag{4.2.9}$$

and using Eq. (4.2.7) results in the set of coupled differential equations:

$$q_\beta Z_{\alpha\beta}(t) + i\frac{dZ_{\alpha\beta}(t)}{dt} = \sum_{\gamma=1}^{2} H_{\alpha\gamma}(t)Z_{\gamma\beta}(t) \; ; \; \alpha = 1,2, \; \beta = 1,2 \tag{4.2.10}$$

The matrix elements of $\underline{\underline{H}}(t)$ and $\underline{\underline{Z}}(t)$ are periodic and therefore can be expanded as a Fourier series [99] in the following manner:

$$Z_{\sigma\eta}(t) = \sum_{k=-\infty}^{\infty} Z_{\sigma\eta}(k)\exp(ik\omega t), \tag{4.2.11}$$

and

$$H_{\sigma\eta}(t) = \sum_{p=-\infty}^{\infty} H_{\sigma\eta}(p)\exp(ip\omega t) \tag{4.2.12}$$

where $Z_{\sigma\eta}(k)$ and $H_{\sigma\eta}(p)$ are time-independent Fourier coefficients. Substitution of Eqs. (4.2.11) and (4.2.12) into Eq. (4.2.10) yields

$$\sum_{k=-\infty}^{\infty} [q_\beta - k\omega] Z_{\alpha\beta}(k) \exp(ik\omega t)$$

$$= \sum_{\gamma=1}^{2} \sum_{p=-\infty}^{\infty} \sum_{k=-\infty}^{\infty} H_{\alpha\gamma}(p) Z_{\gamma\beta}(k) \exp(i[k+p]\omega t) \qquad (4.2.13)$$

which can be written as

$$\sum_{n=-\infty}^{\infty} [q_\beta - n\omega] Z_{\alpha\beta}(n) \exp(in\omega t)$$

$$= \sum_{\gamma=1}^{2} \sum_{n=-\infty}^{\infty} \sum_{k=-\infty}^{\infty} H_{\alpha\gamma}(n-k) Z_{\gamma\beta}(k) \exp(in\omega t) \qquad (4.2.14)$$

Resolving this into Fourier components leads to

$$q_\beta Z_{\alpha\beta}(n) = \sum_{\gamma=1}^{2} \sum_{k=-\infty}^{\infty} \varkappa_{\alpha\gamma}(n-k) Z_{\gamma\beta}(k) \qquad (4.2.15)$$

where the matrix elements

$$\varkappa_{\alpha\gamma}(n-k) = H_{\alpha\gamma}(n-k) + n\omega\delta_{\gamma\alpha}\delta_{kn} \qquad (4.2.16)$$

define an effective time-independent Hamiltonian matrix

called the Floquet Hamiltonian. Eq. (4.2.15) represents a set of simultaneous homogeneous linear equations which have a non-trivial solution for the eigenvectors $Z_{\gamma\beta}(k)$ only if [100]

$$\det|H_{\alpha\gamma}(n-k) + (n\omega-q_\beta)\delta_{\gamma\alpha}\delta_{kn}| = 0 \qquad (4.2.17)$$

The rows and columns of the Floquet Hamiltonian matrix are denoted by the indices $n\alpha$ and $k\gamma$, respectively, where α and γ are the atomic indices 1 or 2 and n and k are Fourier indices ranging from $-\infty$ to $+\infty$.

The $H_{\alpha\gamma}(n-k)$, occurring in Eq. (4.2.17), can be identified by comparing Eqs. (4.2.4) and (4.2.5) with Eq. (4.2.12) and are given by

$$\left.\begin{aligned} H_{11}(0) &= -H_{22}(0) = -\Delta \\ H_{11}(m) &= -H_{22}(m) = 0, \quad m = n-k \neq 0 \end{aligned}\right\} \qquad (4.2.18)$$

and

$$\begin{aligned} H_{12}(m) &= (H_{21}(-m))^* \\ &= -\tfrac{1}{2}(\underline{\mu}_{12}\cdot\hat{e}\varepsilon)\exp(-iY\sin\delta)\exp(i[N+m]\delta) \\ &\quad \times [J_{N+m-1}(Y) + J_{N+m+1}(Y)] \end{aligned} \qquad (4.2.19)$$

This expression is further simplified by making use of Eq. (3.2.13) to obtain

$$H_{12}(m) = (H_{21}(-m))^* = -\tfrac{1}{2}C(N+m)\xi(N+m) \qquad (4.2.20)$$

where (see Eqs. (3.2.14) and (3.2.15))

$$C(N+m) = 2\underline{\mu}_{12}\cdot\hat{e}\varepsilon(N+m)(Y)^{-1}J_{N+m}(Y) \qquad (4.2.21)$$

and

$$\xi(N+m) = \exp(-i[Y\sin\delta-(N+m)\delta]) \qquad (4.2.22)$$

A portion of the secular equation is given in Figure 4.1.

The eigenvalues, q_β, are obtained by solving the Floquet secular equation given in Eq. (4.2.17) and then the eigenvectors, $Z_{\gamma\beta}(k)$, are determined for each eigenvalue by using the set of simultaneous homogeneous linear equations given in Eq. (4.2.15). Once the eigenvectors are known, the transition probability can be found by using the time-evolution operator [26,61] (see also Sec. 2.4.2) in what follows.

The solution of Eq. (4.2.3) can be written as

$$\underline{K}(t) = \underline{U}(t;t_0)\underline{K}(t_0) \qquad (4.2.23)$$

Figure 4.1. A portion of the Floquet secular equation, for all N, given by Eq. (4.2.17) with the $H_{\alpha\gamma}^{(n-k)}$ defined by Eqs. (4.2.18) and (4.2.20). C(N+m) and ξ(N+m) are defined in Eqs. (4.2.21) and (4.2.22), Δ is given by Eq. (4.2.4), and the q's are the eigenvalues obtained by solving the secular equation.

k,γ→ / n,α↓	-2,2	-1,1	-1,2	0,1	0,2	1,1	1,2	2,1
-2,2	$\Delta-2\omega-q$	$-\frac{1}{2}C(N+1)\times\xi^{*}(N+1)$	0	$-\frac{1}{2}C(N+2)\times\xi^{*}(N+2)$	0	$-\frac{1}{2}C(N+3)\times\xi^{*}(N+3)$	0	$-\frac{1}{2}C(N+4)\times\xi^{*}(N+4)$
-1,1	$-\frac{1}{2}C(N+1)\times\xi(N+1)$	$-\Delta-\omega-q$	$-\frac{1}{2}C(N)\times\xi(N)$	0	$-\frac{1}{2}C(N-1)\times\xi(N-1)$	0	$-\frac{1}{2}C(N-2)\times\xi(N-2)$	0
-1,2	0	$-\frac{1}{2}C(N)\times\xi^{*}(N)$	$\Delta-\omega-q$	$-\frac{1}{2}C(N+1)\times\xi^{*}(N+1)$	0	$-\frac{1}{2}C(N+2)\times\xi^{*}(N+2)$	0	$-\frac{1}{2}C(N+3)\times\xi^{*}(N+3)$
0,1	$-\frac{1}{2}C(N+2)\times\xi(N+2)$	0	$-\frac{1}{2}C(N+1)\times\xi(N+1)$	$-\Delta-q$	$-\frac{1}{2}C(N)\times\xi(N)$	0	$-\frac{1}{2}C(N-1)\times\xi(N-1)$	0
0,2	0	$-\frac{1}{2}C(N-1)\times\xi^{*}(N-1)$	0	$-\frac{1}{2}C(N)\times\xi^{*}(N)$	$\Delta-q$	$-\frac{1}{2}C(N+1)\times\xi^{*}(N+1)$	0	$-\frac{1}{2}C(N+2)\times\xi^{*}(N+2)$
1,1	$-\frac{1}{2}C(N+3)\times\xi(N+3)$	0	$-\frac{1}{2}C(N+2)\times\xi(N+2)$	0	$-\frac{1}{2}C(N+1)\times\xi(N+1)$	$-\Delta+\omega-q$	$-\frac{1}{2}C(N)\times\xi(N)$	0
1,2	0	$-\frac{1}{2}C(N-2)\times\xi^{*}(N-2)$	0	$-\frac{1}{2}C(N-1)\times\xi^{*}(N-1)$	0	$-\frac{1}{2}C(N)\times\xi^{*}(N)$	$\Delta+\omega-q$	$-\frac{1}{2}C(N+1)\times\xi^{*}(N+1)$
2,1	$-\frac{1}{2}C(N+4)\times\xi(N+4)$	0	$-\frac{1}{2}C(N+3)\times\xi(N+3)$	0	$-\frac{1}{2}C(N+2)\times\xi(N+2)$	0	$-\frac{1}{2}C(N+1)\times\xi(N+1)$	$-\Delta+2\omega-q$

$= 0$

where $\underline{\underline{U}}(t;t_0)$ is the time-evolution operator and t_0 is the time the EMF is turned on. The time-evolution operator takes the solution from $t = t_0$ to the final time t and can be constructed [23] in terms of the general solution matrix $\underline{\underline{G}}(t)$,

$$\underline{\underline{U}}(t;t_0) = \underline{\underline{G}}(t)\underline{\underline{G}}^{-1}(t_0) \tag{4.2.24}$$

which implies

$$\underline{\underline{U}}(t_0;t_0) = \underline{\underline{I}} \tag{4.2.25}$$

The time-dependent population of state 2 is given by

$$|b_2(t)|^2 = |K_2(t)|^2 \tag{4.2.26}$$

and the initial conditions are chosen such that state 1 is populated at $t = t_0$ while state 2 is not. This corresponds to $a_1(t_0) = 1$ and $a_2(t_0) = 0$ and thus, using Eqs. (3.1.5), (3.2.1) and (4.2.1),

$$K_1(t_0) = \exp\left(\tfrac{i}{2}[(E_1+E_2-N\omega)t_0]\right)$$

$$\times \exp\left(-i\frac{\mu_{12}\cdot\theta\varepsilon}{\omega}\{\sin(\omega t_0+\delta)-\sin(\delta)\}\right);\ K_2(t_0) = 0 \tag{4.2.27}$$

Using Eq. (4.2.27) in Eq. (4.2.23) shows that

$$K_2(t) = U_{21}(t;t_0)K_1(t_0) \qquad (4.2.28)$$

and hence the time-dependent population of state 2 can be written as

$$|K_2(t)|^2 = |U_{21}(t;t_0)|^2 \qquad (4.2.29)$$

where $U_{21}(t;t_0)$ can be constructed from the eigenvalues and eigenvectors of the Floquet Hamiltonian.

Since $\underline{G}(t)$ is a unitary matrix [26,61], $\underline{G}^{-1}(t) = (\underline{G}^*)^T$ where T denotes the transpose of the matrix $\underline{G}$. Using this, together with Eq. (4.2.6) in Eq. (4.2.24) yields

$$\underline{U}(t;t_0) = [\underline{Z}(t)\exp(-i\underline{Q}t)][(\underline{Z}(t_0))^*\exp(i\underline{Q}t_0)]^T \qquad (4.2.30)$$

This can be simplified by expanding the exponential term in a Taylor series;

$$\exp(-i\underline{Q}t) = \sum_{k=0}^{\infty} \frac{(-1)^k(i\underline{Q}t)^k}{k!} = \sum_{k=0}^{\infty} \frac{1}{k!} \begin{bmatrix} (-iq_1t)^k & 0 \\ 0 & (-iq_2t)^k \end{bmatrix}$$

$$= \begin{bmatrix} \exp(-iq_1t) & 0 \\ 0 & \exp(-iq_2t) \end{bmatrix} \qquad (4.2.31)$$

where use has been made of $(\underline{Q}_{ij})^k = q_i^k \sigma_{ij}$. Substitution of Eqs. (4.2.7) and (4.2.31) into Eq. (4.2.30) yields explicit expressions for the matrix elements of $\underline{U}(t;t_0)$. In particular,

$$U_{21}(t;t_0) = \sum_{\gamma=1}^{2} Z_{2\gamma}(t)(Z_{1\gamma}(t_0))^* \exp(-iq_\gamma[t-t_0]) \qquad (4.2.32)$$

and Eq. (4.2.11) then yields

$$\begin{aligned} U_{21}(t;t_0) &= \sum_{\gamma=1}^{2} \sum_{s=-\infty}^{\infty} \sum_{p=-\infty}^{\infty} Z_{2\gamma}(s)(Z_{1\gamma}(p))^* \exp(is\omega t)\exp(-ip\omega t_0) \\ &\qquad \times \exp(-iq_\gamma[t-t_0]) \\ &= \sum_{\gamma=1}^{2} \sum_{s=-\infty}^{\infty} \sum_{n=-\infty}^{\infty} Z_{2\gamma}(s)(Z_{1\gamma}(n+s))^* \exp(-in\omega t_0) \\ &\qquad \times \exp(-i[q_\gamma - s\omega][t-t_0]) \end{aligned} \qquad (4.2.33)$$

Thus the time-dependent population of state 2 is

$$\begin{aligned} |K_2(t)|^2 &= |U_{21}(t;t_0)|^2 \\ &= \sum_{\gamma,\gamma'=1}^{2} \sum_{n,n'=-\infty}^{\infty} \sum_{s,s'=-\infty}^{\infty} (Z_{2\gamma'}(s'))^* \\ &\quad \times Z_{2\gamma}(s) Z_{1\gamma'}(n'+s')(Z_{1\gamma}(n+s))^* \\ &\quad \times \exp(i[n'-n]\omega t_0)\exp(-i[q_\gamma - q_{\gamma'} - (s-s')\omega][t-t_0]) \end{aligned} \qquad (4.2.34)$$

In the interaction of the EMP with a molecule, the initial time t_0, or equivalently the initial phase of the field seen by the molecule, is not well defined, see Sec. 2.4.3. The time-dependent transition probability of interest corresponds to Eq. (4.2.34) averaged over t_0, while the elapsed time $t - t_0$ is kept constant [23,66]. The initial time-averaged temporal transition probability is then given by

$$P_2^N(t) = \lim_{\Gamma\to\infty} \frac{1}{\Gamma} \int_0^\Gamma |U_{2i}(t;t_0)|^2 dt_0$$

$$= \sum_{\gamma,\gamma'=1}^{2} \exp(i[q_\gamma - q_{\gamma'}](t - t_0))$$

$$\times \sum_{s,s'=-\infty}^{\infty} \sum_{n=-\infty}^{\infty} (Z_{2\gamma'}(s'))^* Z_{2\gamma}(s) Z_{1\gamma'}(n+s') (Z_{1\gamma}(n+s))^*$$

$$\times \exp(i[s - s']](t - t_0)\omega) \qquad (4.2.35)$$

since the integral is zero unless $n' = n$ in Eq. (4.2.34). The initial time and long time averaged transition probability, which corresponds to the absorption spectrum (see Sec. 2.4.3), is given by

$$\bar{P}_2^N = \lim_{\tau\to\infty} \frac{1}{\tau} \int_0^\tau \dot{P}_2^N(t)\,d(t-t_0)$$

$$= \sum_{\gamma=1}^{2} \sum_{s=-\infty}^{\infty} \sum_{n=-\infty}^{\infty} |Z_{2\gamma}(s)|^2 |Z_{1\gamma}(n+s)|^2$$

$$= \sum_{\gamma=1}^{2} \sum_{s=-\infty}^{\infty} \sum_{p=-\infty}^{\infty} |Z_{2\gamma}(s)|^2 |Z_{1\gamma}(p)|^2 \qquad (4.2.36)$$

since the integral yields zero results unless $\gamma = \gamma'$ and $s = s'$, see Eq. (4.2.35).

In the next section, perturbation expansions for the $Z_{\sigma\eta}(s)$ will be obtained from the perturbation theory outlined in Appendix B and the transition probability to the desired perturbation order will then be constructed by making use of Eq. (4.2.36).

4.3 Perturbation Theory

To apply the perturbation theory [32,33] discussed in Appendix B, the set of linear equations given by Eq. (4.2.15) is rearranged as follows

$$\sum_{\gamma=1}^{2} \sum_{k=-\infty}^{\infty} [\varkappa_{\alpha\gamma}(n-k) - q_\beta \delta_{\gamma\alpha}\delta_{kn}] Z_{\gamma\beta}(k) = 0 \qquad (4.3.1)$$

Using Eqs. (4.2.16), (4.2.18) and (4.2.20), the matrix element $\varkappa_{\alpha\gamma}(n-k)$ can be written as

$$\varkappa_{\alpha\gamma}(n-k) = E_{n\alpha,k\gamma}^{(0)} + V_{\alpha\gamma}(n-k) \qquad (4.3.2)$$

where,

$$E_{n\alpha,k\gamma}^{(0)} = ((-1)^{\alpha}\Delta + n\omega)\delta_{\gamma\alpha}\delta_{kn} = E_{n\alpha}^{(0)} \qquad (4.3.3)$$

and

$$\begin{aligned} V_{\alpha\gamma}(n-k) &= -\tfrac{1}{2}C(N+n-k)\xi(N+n-k) \quad , \quad \alpha < \gamma \\ &= -\tfrac{1}{2}C(N-n+k)\xi^{*}(N-n+k) \quad , \quad \alpha > \gamma \\ &= 0 \quad , \quad \alpha = \gamma \end{aligned} \qquad (4.3.4)$$

Eq. (4.3.1) is the same as Eq. (B.79) if the following identifications are made: the $\varkappa_{\alpha\gamma}(n-k) \sim H_{rs}$, $q_{\beta} \sim E_L$, and $Z_{\gamma\beta}(k) \sim c_{sL}$. The r, s and L indices of the Appendix are equivalent to (n,α), (k,γ), and β respectively in the Floquet notation.

The desired resonances can be identified in the Floquet secular equation, see Figure 4.1, by setting $\Delta E = N\omega$, where $N = 1,2,3,\ldots$, and hence $\Delta = \tfrac{1}{2}(\Delta E - N\omega) = 0$. Two of the diagonal Floquet Hamiltonian matrix elements, $\varkappa_{11}^{(0-0)} \sim H_{11}^{(0)} = -\Delta$ and $\varkappa_{22}^{(0-0)} \sim H_{22}^{(0)} = \Delta$, will be almost equal. These two elements together with the corresponding off-diagonal matrix elements define a 2 x 2 matrix. The associated 2 x 2 secular equation will have nearly degenerate roots, q_{β}, and therefore when $\Delta E \sim N\omega$ the zeroth order states $|0,1\rangle$ and $|0,2\rangle$ are nearly

degenerate.

The perturbation theory discussed in Appendix B can be applied to these nearly degenerate states. The $C_{\nu,\pm}$ occurring in Eq. (B.69) are identified as the $Z_{\sigma\beta}(p)$ where ν represents both σ and p, and $\pm$ is denoted by β. The perturbative expansions for $Z_{\gamma\beta}(k)$, through second order, are given by Eqs. (B.71)-(B.76) and application of these to the Floquet system of equations defined by Eq. (4.3.1) yields the following with $\gamma = 1$ and 2:

$$Z_{\gamma,\pm}(0) = (Z_{\gamma,\pm}(0))(0) + (Z_{\gamma,\pm}(0))(2) + O(3) \qquad (4.3.5)$$

and

$$Z_{\gamma,\pm}(u) = (Z_{\gamma,\pm}(u))(1) + (Z_{\gamma,\pm}(u))(2) + O(3) \; ; \; u \neq 0 \qquad (4.3.6)$$

where $(Z_{\gamma,\pm}(p))(m)$ is the mth order perturbation term in the expansion of $Z_{\gamma,\pm}(p)$ and only non-zero terms are kept in these expansions. These perturbation terms are given by

$$(Z_{\gamma,\pm}(0))(0) = d_{0\gamma,\pm}F_{0\gamma}(0) \qquad (4.3.7)$$

$$(Z_{\gamma,\pm}(0))(2) = \sum_{p=1}^{2} d_{0p,\pm}F_{0\gamma,p}(2)$$

and

$$(Z_{\gamma,\pm}(u))^{(1)} = \sum_{p=1}^{2} d_{0p,\pm} F_{u\gamma,p}^{(1)}$$

$$(Z_{\gamma,\pm}(u))^{(2)} = \sum_{p=1}^{2} d_{0p,\pm} F_{u\gamma,p}^{(2)};\ u \neq 0 \qquad (4.3.8)$$

where $F_{j\gamma}^{(m)}$ and the $F_{j\gamma,p}^{(m)}$ are the m-th order perturbation coefficients in the expansions of the $(Z_{\gamma,\pm}(p))^{(m)}$. Identifying the perturbation matrix elements V_{ab} and the zeroth order energies $E_a^{(0)}$ of the Appendix with the $V_{\alpha\gamma}^{(n-k)}$ matrix elements and the zeroth order energies $E_{n\gamma}^{(0)}$ associated with the Floquet secular equation yields

$$F_{01}^{(0)} = F_{02}^{(0)} = 1\ ;\ F_{u1,1}^{(1)} = F_{u2,2}^{(1)} = 0 \qquad (4.3.9)$$

$$F_{u1,2}^{(1)} = -\left[\frac{C(N+u)\xi(N+u)}{2(2\Delta-u\omega)}\right] \qquad (4.3.10)$$

$$F_{u2,1}^{(1)} = \left[\frac{C(N-u)\xi^{*}(N-u)}{2(2\Delta+u\omega)}\right] \qquad (4.3.11)$$

$$F_{01,2}^{(2)} = F_{02,1}^{(2)} = 0$$

$$F_{01,1}^{(2)} = F_{02,2}^{(2)} = -1/8 \sum_{s\neq 0}\left[\frac{C(N+s)}{(2\Delta-s\omega)}\right]^{2} \qquad (4.3.12)$$

$$F_{u2,1}^{(2)} = F_{u1,2}^{(2)} = 0 \tag{4.3.13}$$

$$F_{u1,1}^{(2)} = -\left[\frac{C(N+u)C(N)\xi(N+u)\xi^*(N)}{(4u\omega)(2\Delta-u\omega)}\right]$$

$$+\sum_{s\neq 0}\left[\frac{C(N+u-s)C(N-s)\xi(N+u-s)\xi^*(N-s)}{(4u\omega)(2\Delta+s\omega)}\right] \tag{4.3.14}$$

$$F_{u2,2}^{(2)} = -\left[\frac{C(N-u)C(N)\xi^*(N-u)\xi(N)}{(4u\omega)(2\Delta+u\omega)}\right]$$

$$-\sum_{s\neq 0}\left[\frac{C(N-u-s)C(N-s)\xi^*(N-u-s)\xi(N-s)}{(4u\omega)(2\Delta+s\omega)}\right] \tag{4.3.15}$$

where $C(N+m)$ and $\xi(N+m)$ are given by Eqs. (4.2.21) and (4.2.22) respectively. The coefficients $F_{j\gamma,p}^{(m)}$ that are zero (see Eqs. (4.3.9), (4.3.12) and (4.3.13)) all involve matrix elements of $V_{\gamma\gamma}^{(n-k)}$ which, from Eq. (4.3.4), are zero. Here, and in what follows, $\sum_{x\neq 0}$ implies a sum over x ranging from $-\infty$ to $+\infty$ excluding the $x = 0$ term. Using Eq. (4.3.12) in Eq. (4.3.7) yields

$$(Z_{\gamma;\pm}^{(0)})^{(2)} = d_{0\gamma,\pm}F_{0\gamma,\gamma}^{(2)} \tag{4.3.16}$$

and using Eqs. (4.3.9) and (4.3.13) in Eq. (4.3.8) yields

$$(Z_{1,\pm}^{(u)})^{(1)} = d_{02,\pm}F_{u1,2}^{(1)} \tag{4.3.17}$$

$$(Z_{2,\pm}^{(u)})^{(1)} = d_{01,\pm}F_{u2,1}^{(1)}$$

and

$$(Z_{\gamma,\pm}^{(u)})^{(2)} = d_{0\gamma,\pm}F_{u\gamma,\gamma}^{(2)} \tag{4.3.18}$$

Comparing Eqs. (4.3.10) and (4.3.11) one can show that

$$F_{u1,2}^{(1)} = -(F_{-u2,1}^{(1)})^* \tag{4.3.19}$$

and similarly, from Eqs. (4.3.14) and (4.3.15), one obtains

$$F_{u1,1}^{(2)} = (F_{-u2,2}^{(2)})^* \tag{4.3.20}$$

The coefficients $d_{0\gamma,\pm}$ which occur in these results, and which are taken to be of zeroth order, can be obtained from Eqs. (B.10)-(B.12) and will be discussed later.

The eigenvectors given by Eqs. (4.3.5) and (4.3.6) are more easily identified in the transition probability if Eq. (4.2.36) is rewritten as follows:

$$\bar{P}_2^N = \sum_{s=-}^{+} [|Z_{2,\beta}^{(0)}|^2|Z_{1,\beta}^{(0)}|^2 + \sum_{p\neq 0}\sum_{s\neq 0}|Z_{2,\beta}^{(s)}|^2|Z_{1,\beta}^{(p)}|^2$$

$$+ \sum_{p\neq 0}(|Z_{2,\beta}^{(0)}|^2|Z_{1,\beta}^{(p)}|^2 + |Z_{2,\beta}^{(p)}|^2|Z_{1,\beta}^{(0)}|^2)] \tag{4.3.21}$$

where $\gamma = 1$ and 2 in Eq. (4.2.36) have been replaced by $\beta = -$ and $+$. Substituting Eqs. (4.3.5) and (4.3.6) into Eq. (4.3.21) and keeping terms through second order yields

$$\bar{P}_2^N = \sum_{\beta=-}^{+} [\,|(Z_{2,\beta}^{(0)})^{(0)}|^2 |(Z_{1,\beta}^{(0)})^{(0)}|^2$$

$$+ |(Z_{2,\beta}^{(0)})^{(0)}|^2 \{((Z_{1,\beta}^{(0)})^{(0)})((Z_{1,\beta}^{(0)})^{(2)})^* + \text{c.c.}\}$$

$$+ |(Z_{1,\beta}^{(0)})^{(0)}|^2 \{((Z_{2,\beta}^{(0)})^{(0)})((Z_{2,\beta}^{(0)})^{(2)})^* + \text{c.c.}\}$$

$$+ \sum_{p\neq 0} \{|(Z_{2,\beta}^{(0)})^{(0)}|^2 |(Z_{1,\beta}^{(p)})^{(1)}|^2$$

$$+ |(Z_{1,\beta}^{(0)})^{(0)}|^2 |(Z_{2,\beta}^{(p)})^{(1)}|^2\} + O(3)\,] \qquad (4.3.22)$$

Using Eqs. (4.3.7), (4.3.9), (4.3.12), (4.3.16)-(4.3.18) and, from Eqs. (B.10)-(B.12), the relationship

$$d_{01,-} = d_{02,+} \; ; \; d_{02,-} = -d_{01,+}^{*} \; , \qquad (4.3.23)$$

in Eq. (4.3.22) then gives

$$\bar{P}_2^N = |d_{01,+}|^2|d_{02,+}|^2[2|F_{01}^{(0)}|^2|F_{02}^{(0)}|^2$$

$$+ 2\{|F_{02}^{(0)}|^2F_{01}^{(0)}(F_{01,1}^{(2)})^* + c.c\}$$

$$+ 2\{|F_{01}^{(0)}|^2F_{02}^{(0)}(F_{02,2}^{(2)})^* + c.c.) + O(3)]$$

$$+ [|d_{01,+}|^4 + |d_{02,+}|^4] \sum_{p\neq 0} [|F_{02}^{(0)}|^2|F_{p1,2}^{(1)}|^2,$$

$$+ |F_{01}^{(0)}|^2|F_{p2,1}^{(1)}|^2 + O(3)]$$

(4.3.24)

It is easily seen from Eq. (4.3.12) that $F_{0\gamma,\gamma}^{(2)}$ is real and it can be shown, from Eq. (4.3.10) that

$$\sum_{p\neq 0} |F_{p1,2}^{(1)}|^2 = \sum_{p\neq 0}\left[\frac{C(N+p)}{2(2\Delta-p\omega)}\right]^2 = -2F_{0\gamma,\gamma}^{(2)} = -2F_{01,1}^{(2)}$$

(4.3.25)

and from Eq. (4.3.11)

$$\sum_{p\neq 0} |F_{p2,1}^{(1)}|^2 = \sum_{p\neq 0}\left[\frac{C(N-p)}{2(2\Delta+p\omega)}\right]^2 = -2F_{01,1}^{(2)} \qquad (4.3.26)$$

since $-\infty \leq p \leq +\infty$. Using Eqs. (4.3.9), (4.3.12), (4.3.25) and (4.3.26) in Eq. (4.3.24) yields

$$\bar{P}_2^N = 2|d_{01,+}|^2|d_{02,+}|^2[1 + 4F_{01,1}^{(2)} + O(3)]$$

$$+ [|d_{01,+}|^4 + |d_{02,+}|^4][-4F_{01,1}^{(2)} + O(3)] \qquad (4.3.27)$$

Eqs. (B.8), (B.10) and (B.11) give

$$|d_{01,+}|^2|d_{02,+}|^2 = (4\rho^2)^{-1}|E_{01,02}|^2 \qquad (4.3.28)$$

and

$$|d_{01,+}|^4 + |d_{02,+}|^4 = 1 - (2\rho^2)^{-1}|E_{01,02}|^2 \qquad (4.3.29)$$

and by substituting these results in Eq. (4.3.27), one obtains the following expression for the transition probability:

$$\bar{P}_2^N = (2\rho^2)^{-1}|E_{01,02}|^2[1 + 8F_{01,1}^{(2)} + O(3)]$$

$$- 4F_{01,1}^{(2)} + O(3) \qquad (4.3.30)$$

where ρ is given by Eq. (B.8).

Perturbative expansions for the energies, E, occurring in Eq. (4.3.30) are given by Eq. (B.15). Results explicit through third order can be obtained by substituting Eqs. (4.3.3) and (4.3.4) into the appropriately modified versions of Eqs. (B.19), (B.42),

(B.63) and (B.64). By omitting perturbation energies that are zero one obtains,

$$E_{01,02} = E_{01,02}^{(1)} + E_{01,02}^{(3)} + O(4) \qquad (4.3.31)$$

and

$$E_{01,01} = -E_{02,02} = E_{01}^{(0)} + E_{01,01}^{(2)} + O(4) \qquad (4.3.32)$$

where

$$E_{01}^{(0)} = -E_{02}^{(0)} = -\Delta = -\tfrac{1}{2}(\Delta E - N\omega) \qquad (4.3.33)$$

$$E_{01,02}^{(1)} = (E_{02,01}^{(1)})^* = -\tfrac{1}{2}C(N)\xi(N) \qquad (4.3.34)$$

$$E_{01,01}^{(2)} = -E_{02,02}^{(2)} = -\sum_{s\neq 0}\left[\frac{C^2(N+s)}{4(2\Delta - s\omega)}\right] \qquad (4.3.35)$$

$$E_{01,02}^{(3)} = (E_{02,01}^{(3)})^* = \sum_{s\neq 0}\left[\frac{C^2(N+s)C(N)\xi(N)}{8(2\Delta - s\omega)^2}\right]$$

$$+ \sum_{s\neq 0}\sum_{\ell\neq 0}\left[\frac{C(N-s)C(N-s+\ell)C(N+\ell)\xi(N-s)\xi^*(N-s+\ell)\xi(N+\ell)}{8(2\Delta - \ell\omega)(2\Delta + s\omega)}\right] \qquad (4.3.36)$$

The fourth order energy, $E_{01,01}^{(4)}$, is also required for

some of the analysis that follows and can be obtained from Eq. (B.67);

$$E_{01,01}^{(4)} = \frac{1}{16}\sum_{p\neq 0}\sum_{r\neq 0}\sum_{s\neq 0}\left[\frac{C(N-p+r)C(N+r-s)C(N-s)C(N-p)}{(2\Delta+p\omega)(r\omega)(2\Delta+s\omega)}\right]$$

$$\frac{1}{16}\sum_{p\neq 0}\sum_{r\neq 0}\left[\frac{2C(N-p+r)C(N+r)C(N-p)C(N)}{(2\Delta+p\omega)(2\Delta-r\omega)(r\omega)} \quad \frac{C^2(N-p)C^2(N+r)}{(2\Delta+p\omega)^2(2\Delta-r\omega)}\right]$$

$$+\frac{1}{16}\sum_{r\neq 0}\left[\frac{C^2(N-r)C^2(N)}{(r\omega)(2\Delta+r\omega)^2}\right] \qquad (4.3.37).$$

The expressions for $|E_{01,02}|^2$ and ρ^2 are

$$|E_{01,02}|^2 = |E_{01,02}^{(1)}|^2 + 2E_{01,02}^{(1)}(E_{01,02}^{(3)})^* + O(6) + O(5) \qquad (4.3.38)$$

where $E_{01,02}^{(1)}(E_{01,02}^{(3)})^* = (E_{01,02}^{(1)})^* E_{01,02}^{(3)}$ has been used and

$$\rho^2 = |E_{01}^{(0)}|^2 + 2E_{01}^{(0)}E_{01,01}^{(2)} + |E_{01,01}^{(2)}|^2 + O(4)$$

$$+ |E_{01,02}^{(1)}|^2 + 2E_{01,02}^{(1)}(E_{01,02}^{(3)})^* + O(6) + O(5) \qquad (4.3.39)$$

In obtaining this result use has been made of the fact that $E_{01}^{(0)} = -\frac{1}{2}(\Delta E - N\omega)$ is small and

$$\delta(4) = 2F_{01}^{(0)}E_{01,01}^{(4)} \; ; \; \delta(6) = |E_{01,02}^{(3)}|^2 \qquad (4.3.40)$$

Finally, the transition probability given by Eq. (4.3.30) becomes

$$\bar{P}_2^N = [2\rho^2]^{-1}[|E_{01,02}^{(1)}|^2\{1 + 8F_{01,1}^{(2)}\} + 2E_{01,02}^{(1)}(E_{01,02}^{(3)})^* + \delta(6) + O(5)] - 4F_{01,1}^{(2)} + O(3) \qquad (4.3.41)$$

In much of the work that follows, $\delta(4)$ is considered to be of higher order and therefore not retained in numerical computations involving Eq. (4.3.41); for frequencies around ω_{res}^N, which are of most significance here, $\Delta E - N\omega$ is of second order in the coupling $(\mu_{12}\cdot\mathcal{E})$ and therefore $E_{01}^{(0)}$ is actually of the same order as $|E_{01,02}^{(1)}|^2$. The sixth order term, $\delta(6)$, has been included in Eq. (4.3.41) for the purpose of comparison with the literature; this result is, in general, accurate only through fourth order in perturbation theory.

The relevant eigenvalues of the Floquet secular equation are (see Appendix B, Eq. (B.7))

$$q_{\pm} = \tfrac{1}{2}(E_{01,01} + E_{02,02}) \pm \rho = \pm\rho \qquad (4.3.42)$$

and are the characteristic exponents or dressed atom energies of the system [9,10,23,27-30,59,66] referred to in Sec. 2.4. By using the result for ρ given by Eq. (4.3.39) one can show that the transition probability given by Eq. (4.3.41) can be written as

$$\bar{P}_2^N = \tfrac{1}{2}[1-4(\partial\rho/\partial(\Delta E))^2] \qquad (4.3.43)$$

To obtain this result only terms through fourth order of $(\partial\rho/\partial(\Delta E))$ have been retained. Eq. (4.3.43) has been derived in general for the $\underline{d} = 0$ problem by Shirley [23,31].

Perturbation corrections for the full width at half maximum for the N-photon resonance profiles can also be obtained from the perturbation analysis of this section. Given Eq. (4.3.41), the derivation is analogous to that discussed in Sec. (3.3.2) for the RWA resonance profile and involves the assumption that the perturbed energies of order greater than zero and $F_{01,1}^{(2)}$ occurring in $\bar{P}_2^N$, do not vary appreciably with frequency over the width of the main N-photon resonance. The result for the $(FWHM)^N$ is given by

$$(FWHM)^N \approx \frac{2}{N}\left|\frac{C(N)}{(1+16F_{01,1}^{(2)})}\left[1+16F_{01,1}^{(2)} - \frac{4\xi(N)(E_{01,02}^{(3)})^*}{C(N)}\right.\right.$$

$$\left.\left. + \frac{O(5)}{|C(N)|^2}\right]^{\frac{1}{2}}\right|_{\omega-\omega_{res}^N} \qquad (4.3.44)$$

and using Taylor series expansions yields

$$(FWHM)^N \approx \frac{2}{N}\left|C(N) - 8C(N)F_{01,1}^{(2)}\right.$$

$$\left. - 2\xi(N)(E_{01,02}^{(3)})^*\right|_{\omega-\omega_{res}^N} + O(4) \qquad (4.3.45)$$

The first term in this expression is the RWA result for the FWHM of the N-photon transition discussed in Sec. 3.3.2.

The Rotating Wave Approximation

The RWA expression for the N-photon absorption spectra with $d \neq 0$, discussed in Sec. 3.3.2, corresponds to the perturbation solution through zeroth order in the $Z_{\gamma,\pm}(p)$ and through first order in the energies, $E_{n\alpha,k\gamma}$. Retaining only zeroth order terms in Eq. (4.3.24) yields

$$P_2^N \propto 2|d_{01,+1}|^2|d_{02,0}|^2|F_{01}^{(0)}|^2|F_{02}^{(0)}|^2 \qquad (4.3.46)$$

Using Eqs. (4.3.9) and (4.3.28) then gives

$$\bar{P}_2^N = (2\rho^2)^{-1}|E_{01,02}|^2 \tag{4.3.47}$$

where

$$\rho^2 = \tfrac{1}{4}(E_{02,02} - E_{01,01})^2 + |E_{01,02}|^2 \tag{4.3.48}$$

and through first order in the energies

$$\begin{aligned} E_{02,02} - E_{01,01} &= -2E_{01}^{(0)} + O(2) \\ E_{01,02} &= E_{01,02}^{(1)} + O(2) \end{aligned} \tag{4.3.49}$$

Then

$$\rho^2 = (E_{01}^{(0)})^2 + |E_{01,02}^{(1)}|^2 \tag{4.3.50}$$

and

$$\bar{P}_2^N = \frac{|E_{01,02}^{(1)}|^2}{2[(E_{01}^{(0)})^2 + |E_{01,02}^{(1)}|^2]} \tag{4.3.51}$$

which, when using the expressions for $E_{01}^{(0)}$ and $E_{01,02}^{(1)}$ given by Eqs. (4.3.33) and (4.3.34), agrees with the RWA absorption spectrum given by Eq. (3.3.5). Eq. (4.3.51) predicts the overall qualitative features of the absorption spectra of two-level molecules such as peak heights, the

full width at half maxima ($(FWHM)^N$), and oscillatory fringes (see the discussion in Sec. 3.3.2). However, the RWA fails to predict either the shifts of the main resonances to the high or low frequency side of $\omega = \Delta E/N$, or the background observed in spectra obtained from exact calculations.

Using Eqs. (4.2.4), (4.3.33), (4.3.34) and (4.3.50), it is easy to show that

$$\frac{\partial \rho}{\partial(\Delta E)} = \frac{1}{2\rho}[-\varepsilon_{01}^{(0)}] \qquad (4.3.52)$$

and substituting this into Eq. (4.3.43) yields the RWA result for $\bar{P}_2^N$. Setting Eq. (4.3.43) equal to 0.5 indicates that the resonance maxima occur when

$$\frac{\partial \rho}{\partial(\Delta E)} = \frac{1}{2\rho}\frac{\partial \rho^2}{\partial(\Delta E)} = 0 \qquad (4.3.53)$$

Using Eq. (4.3.52) in Eq. (4.3.53) then yields $\varepsilon_{01}^{(0)} = 0$ and the RWA result for the resonance frequency ($d \neq 0$)

$$\omega_{res} = \frac{\Delta E}{N} \qquad (4.3.54)$$

as expected. The $(FWHM)^N$ corresponding to the RWA, which is the first term in the perturbation expansion of Eq. (4.3.45), has been discussed in some detail in Sec. 3.3.2. The limit of the RWA molecular results for the resonance profile and FWHM as $d \to 0$ has also been discussed in this

section and in particular in Sec. 3.3.1. For $\underline{d} = 0$ the RWA supports only the one-photon resonance.

Perturbative Corrections to the RWA

Perturbative corrections to the RWA, through second order in the $Z_{\gamma,\pm}(P)$ and through third order in the energies $\varepsilon_{n\alpha,k\gamma}$ lead to the transition probability given by Eq. (4.3.41). It is interesting to note that there is no solution through first order in the $Z_{\gamma,\pm}(P)$, see Eq. (4.3.22). The perturbation corrections contain contributions to both the shifts of the main resonances from $\omega = \Delta E/N$ as well as the background seen in the exact spectra. Limitations of the perturbation solutions will be discussed later with the use of model calculations.

An expression for the resonance frequency can be obtained from Eq. (4.3.53). Making use of the expression for ρ, given by Eq. (4.3.39), yields

$$0 = \frac{\partial\rho}{\partial(\Delta E)} = \frac{1}{2\rho}\Big[-\varepsilon_{01}^{(0)} - \varepsilon_{01,01}^{(2)} - \varepsilon_{01,01}^{(4)} - 4\varepsilon_{01}^{(0)}F_{01,1}^{(2)}$$

$$- 4\varepsilon_{01,01}^{(2)}F_{01,1}^{(2)} + 2\varepsilon_{01,02}^{(1)}\frac{\partial(\varepsilon_{01,02}^{(3)})^*}{\partial(\Delta E)} + O(5)\Big] \qquad (4.3.55)$$

where use has been made of

$$\frac{\partial E_{0_1}^{(0)}}{\partial(\Delta E)} = -\frac{1}{2}\,;\quad \frac{\partial E_{0_1,0_2}^{(1)}}{\partial(\Delta E)} = 0\,;\quad \frac{\partial E_{0_1,0_1}^{(2)}}{\partial(\Delta E)} = -2P_{0_1,1}^{(2)} \tag{4.3.56}$$

and

$$\frac{\partial(E_{0_1,0_2}^{(3)})^*}{\partial(\Delta E)} = -\sum_{s\neq 0}\left[\frac{C^2(N+s)C(N)\xi^*(N)}{4(\Delta E - [N+s]\omega)^3}\right]$$

$$-\sum_{s\neq 0}\sum_{\ell\neq 0}\left[\left[\frac{C(N-s)C(N-s+\ell)C(N+\ell)\xi^*(N-s)\xi(N-s+\ell)\xi^*(N+\ell)}{8(\Delta E - [N+\ell]\omega)(\Delta E - [N-s]\omega)}\right]\right.$$

$$\left.\times\left[(\Delta E - [N+\ell]\omega)^{-1} + (\Delta E - [N-s]\omega)^{-1}\right]\right] \tag{4.3.57}$$

Noting $E_{0_1}^{(0)} = -\frac{1}{2}(\Delta E - N\omega)$, and rearranging some of the terms in Eq. (4.3.55), gives the following implicit expression for the resonance frequency,

$$\omega = \frac{\Delta E}{N} - \frac{2}{N}E_{0_1,0_1}^{(2)} - \frac{2}{N}E_{0_1,0_1}^{(4)} + \frac{4}{N}(\Delta E - N\omega)P_{0_1,1}^{(2)}$$

$$-\frac{8}{N}E_{0_1,0_1}^{(2)}P_{0_1,1}^{(2)} + \frac{4}{N}E_{0_1,0_2}^{(1)}\frac{\partial(E_{0_1,0_2}^{(3)})^*}{\partial(\Delta E)} + O(5) \tag{4.3.58}$$

Since most of the terms on the right-hand side of this result are functions of $C(N+m)$ and ω (see Eqs. (4.3.12), (4.3.35), (4.3.37) and (4.3.57) respectively), an iterative

technique must be used to obtain the final solution for the resonance frequency correct through a given order in perturbation theory.

While it is possible to solve Eq. (4.3.58) for ω_{res}^{N} iteratively in a numerical manner, it is more instructive from a qualitative point of view to carry out this procedure analytically and obtain an expression for ω_{res}^{N}, and hence obtain the shift of the resonance frequency from the RWA limit of $\Delta E/N$, in powers of the couplings $\underline{\mu}_{12}\cdot\hat{e}\varepsilon$ and $\underline{d}\cdot\hat{e}\varepsilon$. The result for ω_{res}^{N} will be obtained through fourth order in the product of the two couplings; that is to terms of order $(\underline{\mu}_{12}\cdot\hat{e}\varepsilon)^{n}(\underline{d}\cdot\hat{e}\varepsilon)^{m}$ where $n + m \leq 4$.

To begin, the right-hand side of Eq. (4.3.58) is expanded in powers of the couplings assuming initially that $\Delta E - N\omega$ is of unknown order in the couplings and that ω is fixed. This is accomplished by making use of the expansion [78] for the Bessel functions in the molecule-EMF coupling parameter $C(N+m)$, see Eq. (4.2.21), which occurs in the spectral results for the various quantities in Eq. (4.3.58):

$$J_n(Y) = Y^n \sum_{\ell=0}^{\infty}\left[\frac{(-1)^{\ell}\, Y^{2\ell}}{2^{2\ell+n}\, \ell!\, (n+\ell)!}\right], \quad Y = \frac{\underline{d}\cdot\hat{e}\varepsilon}{\omega} \tag{4.3.59}$$

The result through terms of fourth order overall is

$$\omega = \frac{\Delta E}{N} + \frac{(\underline{\mu}_{12}\cdot\hat{e}\varepsilon)^2}{2N}\left[\left[1 - \left[\frac{\underline{d}\cdot\hat{e}\varepsilon}{\omega}\right]^2\right]\left[\frac{1}{(\Delta E-\omega)}\Big|_{N\neq 1} + \frac{1}{(\Delta E+\omega)}\right]\right.$$

$$+\left[\frac{\underline{d}\cdot\delta\underline{\varepsilon}}{2\omega}\right]^2\left[\frac{1}{(\Delta E-2\omega)}\Big|_{N\neq 2}+\frac{1}{(\Delta E+2\omega)}\right]\Bigg]$$

$$-\frac{(\underline{\mu}_{12}\cdot\delta\underline{\varepsilon})^4}{8N}\left[\frac{1}{(2\omega)(\Delta E-\omega)^2}-\frac{1}{(2\omega)(\Delta E+\omega)^2}+\frac{1}{(\Delta E-\omega)^3}\right.$$

$$\left.+\frac{1}{(\Delta E-\omega)^2(\Delta E+\omega)}+\frac{1}{(\Delta E+\omega)^2(\Delta E-\omega)}\right]\Big|_{N\neq 1}$$

$$-\frac{(\underline{\mu}_{12}\cdot\delta\underline{\varepsilon})^4}{8N(\Delta E+\omega)^3}-\frac{(\underline{\mu}_{12}\cdot\delta\underline{\varepsilon})^2}{2N}(\Delta E-N\omega)\left[\left[1-\left[\frac{\underline{d}\cdot\delta\underline{\varepsilon}}{2\omega}\right]^2\right]\left[\frac{1}{(\Delta E-\omega)^2}\Big|_{N\neq 1}\right.\right.$$

$$\left.+\frac{1}{(\Delta E+\omega)^2}\right]+\left[\frac{\underline{d}\cdot\delta\underline{\varepsilon}}{2\omega}\right]^2\left[\frac{1}{(\Delta E-2\omega)^2}\Big|_{N\neq 2}+\frac{1}{(\Delta E+2\omega)^2}\right]\Bigg]$$

$$+\frac{(\underline{\mu}_{12}\cdot\delta\underline{\varepsilon})^4}{(2N)(\Delta E+\omega)^3}\Big|_{N-1}-\frac{(\underline{\mu}_{12}\cdot\delta\underline{\varepsilon})^4}{4N}\left[\frac{1}{(\Delta E-\omega)}\Big|_{N\neq 1}+\frac{1}{(\Delta E+\omega)}\right]$$

$$\times\left[\frac{1}{(\Delta E-\omega)^2}\Big|_{N\neq 1}+\frac{1}{(\Delta E+\omega)^2}\right]+O((\mu d)^5)$$

(4.3.60)

where $(\mu d)^5$ indicates terms of fifth or higher order overall in the coupling parameters $\underline{\mu}_{12}\cdot\delta\underline{\varepsilon}$ and $\underline{d}\cdot\delta\underline{\varepsilon}$. Eq. (4.3.60) can be used for all $N \geq 1$ but it simplifies for higher N values. For example

$$\frac{4}{N}E_{01,02}^{(1)}\frac{\partial(E_{01,02}^{(3)})^*}{\partial(\Delta E)}-\frac{(\underline{\mu}_{12}\cdot\delta\underline{\varepsilon})^4}{(2N)(\Delta E+\omega)^3}\Big|_{N-1}=0 \qquad (4.3.61)$$

if $N > 1$ through fourth order.

To proceed, $\omega = \Delta E/N$ is used as a first approximation on the right-hand side of Eq. (4.3.60). In the second approximation, ω_{res}^{N}, obtained from the first iteration accurate through second order overall in the couplings, is used for ω on the right-hand side of Eq. (4.3.60). The iteration involves Taylor series expansions of terms of the form $(\Delta E+c\omega)^{-1}$, where c is a constant, in powers of the coupling parameters. This procedure can be repeated until a result for ω_{res}^{N}, through any required overall order, is obtained; two iterations are sufficient for our purposes. It was found to be more convenient to treat N = 1, N = 2 and N > 3 separately. The resulting expressions for the resonance frequencies are

$$\omega_{res}^{1} = \Delta E + \frac{(\mu_{12}\cdot\hat{e}\varepsilon)^2}{4(\Delta E)} - \frac{7(\mu_{12}\cdot\hat{e}\varepsilon)^2(\underline{d}\cdot\hat{e}\varepsilon)^2}{48(\Delta E)^3} + \frac{(\mu_{12}\cdot\hat{e}\varepsilon)^4}{64(\Delta E)^3}$$

$$+ O((\mu d)^5) \; ; \; N = 1 \qquad (4.3.62)$$

$$\omega_{res}^{2} = \frac{\Delta E}{2} + \frac{2(\mu_{12}\cdot\hat{e}\varepsilon)^2}{3(\Delta E)} - \frac{13(\mu_{12}\cdot\hat{e}\varepsilon)^2(\underline{d}\cdot\hat{e}\varepsilon)^2}{24(\Delta E)^3}$$

$$- \frac{10(\mu_{12}\cdot\hat{e}\varepsilon)^4}{27(\Delta E)^3} + O((\mu d)^5) \; ; \; N = 2 \qquad (4.3.63)$$

and for N > 3

$$\omega_{res}^{N} = \frac{\Delta E}{N} + \frac{(\mu_{12}\cdot\hat{e}\varepsilon)^2}{(\Delta E)}T1 + \frac{(\mu_{12}\cdot\hat{e}\varepsilon)^2(\underline{d}\cdot\hat{e}\varepsilon)^2}{(\Delta E)^3}T2$$

$$+ \frac{(\mu_{12}\cdot\hat{e}\varepsilon)^4}{(\Delta E)^3}T3 + O((\mu d)^5) \qquad (4.3.64)$$

where

$$T1 = \frac{N}{N^2-1} \quad ; \quad T2 = \frac{3N^3}{4(N^2-1)(N^2-4)} \qquad (4.3.65)$$

$$T3 = \frac{N^3(7-3N^2)}{4(N^2-1)^3} \qquad (4.3.66)$$

These results agree with those in the literature for certain special cases, mostly those involving $\underline{d} = 0$. For $N = 1$, $\underline{d} = 0$, Eq. (4.3.62) agrees with the original work of Bloch and Siegert [22], Shirley [23] and others [53-56]. For $N > 3$ and odd, and $\underline{d} = 0$, Eq. (4.3.64) agrees with our inversion of the results of Hoie [101], who has expressions for ΔE as a function of ω through $O(\mu^8)$, and with other literature results [31,42,68] of lower order in the coupling $\mu_{12}\cdot\hat{e}\varepsilon$. When $\underline{d} = 0$ there are no even photon transitions for two-level systems, see Secs. 3.3.1 and 3.3.2 and the discussion of the $\underline{d} = 0$ limit of Eq. (4.3.41) that follows. Finally, for $\underline{d} \neq 0$ our expressions agree with what are apparently the only analogous literature results [34] which are available for $N = 1$ through $O((\mu d)^4)$ and for $N > 2$ through only $O(\mu^2)$. For all N, when $\underline{d} \neq 0$, it is clear from Eqs. (4.3,62)-(4.3.66) that the shift in

ω_{res}^{N} from the weak field or RWA resonance frequency of $\Delta E/N$ can be either to high or low frequency, depending on the magnitude of the coupling $\underline{d}\cdot\hat{e}\varepsilon$ relative to $\underline{\mu}_{12}\cdot\hat{e}\varepsilon$; for $\underline{d} = 0$ the shift is always to high frequency. Thus these results give analytical and qualitative support to the negative shifts from $\omega_{res}^{N} = \frac{\Delta E}{N}$ observed in the multi-photon molecular spectra discussed earlier in this thesis (see Sec. 3.3.2). It is important to note that the results for the shift from the zero field resonance frequency given here are valid only for small couplings $\underline{\mu}_{12}\cdot\hat{e}\varepsilon$ and $\underline{d}\cdot\hat{e}\varepsilon$; for large couplings the higher order terms, $\mu^n d^m$, in these power series results can become larger than the lower order terms leading to divergent results for the shifts. This divergence is not unexpected, see for example Eq. (4.3.59).

It is also interesting to compare the perturbative results for the resonance profile given by Eq. (4.3.41) with the results in the literature which are available for $\underline{d} = 0$. The limits of $E_{01,02}^{(1)}$, $F_{01,1}^{(2)}$, $E_{01,01}^{(2)}$ and $E_{01,02}^{(3)}$ as $\underline{d} \to 0$ are required to take this limit. A useful result is given by

$$\lim_{x\to 0} \frac{p}{x} J_p(x) = \tfrac{1}{2}\delta_{p,1} \quad , \quad p > 0$$

$$= \tfrac{1}{2}\delta_{p,-1} \quad , \quad p < 0 \qquad (4.3.67)$$

which can be obtained from Eq. (3.2.13) and the result [78] $J_k(0) = \delta_{k,0}$.

Using Eqs. (4.2.21), (4.2.22), (4.3.34) and (4.3.67), yields

$$\lim_{\underline{d}\to 0} E_{01,02}^{(1)} = -\tfrac{1}{2}\underline{\mu}_{12}\cdot\theta\varepsilon\delta_{N,1}\exp(iN\theta) \qquad (4.3.68)$$

Making use of Eqs. (4.2.4), (4.2.21) and (4.3.12) gives

$$F_{01,1}^{(2)} = -\frac{1}{8}\sum_{s\neq 0}\left[\frac{2\underline{\mu}_{12}\cdot\theta\varepsilon(s+N)Y^{-1}J_{s+N}(Y)}{(\Delta E - [s+N]\omega)}\right]^2 \qquad (4.3.69)$$

which upon using Eq. (4.3.67) yields

$$\lim_{\underline{d}\to 0} F_{01,1}^{(2)} = -\frac{1}{8}\left[\frac{\underline{\mu}_{12}\cdot\theta\varepsilon}{(\Delta E+\omega)}\right]^2, \quad N = 1$$

$$= -\frac{1}{8}\left[\left[\frac{\underline{\mu}_{12}\cdot\theta\varepsilon}{(\Delta E-\omega)}\right]^2 + \left[\frac{\underline{\mu}_{12}\cdot\theta\varepsilon}{(\Delta E+\omega)}\right]^2\right], \quad N > 1 \qquad (4.3.70)$$

Only one term occurs in the N = 1 limit since s + N = 1 implies s = 0 for N = 1. Similarly, it can be shown that

$$\lim_{\underline{d}\to 0} E_{01,01}^{(2)} = -\frac{1}{4}\left[\frac{(\underline{\mu}_{12}\cdot\theta\varepsilon)^2}{\Delta E+\omega}\right], \quad N = 1$$

$$= -\frac{1}{4}\left[\frac{(\underline{\mu}_{12}\cdot\hat{\boldsymbol{\epsilon}})^2}{(\Delta E-\omega)} + \frac{(\underline{\mu}_{12}\cdot\hat{\boldsymbol{\epsilon}})^2}{(\Delta E+\omega)}\right] \quad , \quad N > 1$$

(4.3.71)

and

$$\lim_{\underline{d}\to 0} E_{\sigma_1,\sigma_2}^{(3)} = \frac{1}{8}\left[\frac{(\underline{\mu}_{12}\cdot\hat{\boldsymbol{\epsilon}})^3\exp(i\delta)}{(\Delta E+\omega)^2}\right] \quad , \quad N = 1$$

$$= \frac{1}{8}\left[\frac{(\underline{\mu}_{12}\cdot\hat{\boldsymbol{\epsilon}})^3\exp(3i\delta)}{(\Delta E-\omega)^2}\right] \quad , \quad N = 3$$

$$= 0 \quad , \quad N = 2,\ N > 3$$

(4.3.72)

Using Eqs. (4.8.68) and (4.3.70)-(4.3.72) with N = 1 in Eq. (4.3.41) yields

$$\bar{P}_2^1 = [2\rho^2]^{-1}\left[\tfrac{1}{4}(\underline{\mu}_{12}\cdot\hat{\boldsymbol{\epsilon}})^2\left[1 - \frac{(\underline{\mu}_{12}\cdot\hat{\boldsymbol{\epsilon}})^2}{(\Delta E+\omega)^2}\right] - \frac{(\underline{\mu}_{12}\cdot\hat{\boldsymbol{\epsilon}})^4}{8(\Delta E+\omega)^2} + O(5)\right]$$

$$+ \frac{(\underline{\mu}_{12}\cdot\hat{\boldsymbol{\epsilon}})^2}{2(\Delta E+\omega)^2} + O(3) \qquad (4.3.73)$$

where from Eq. (4.3.39)

$$\rho^2 = \left[\tfrac{1}{2}(\Delta E-\omega) + \frac{(\underline{\mu}_{12}\cdot\hat{\boldsymbol{\epsilon}})^2}{4(\Delta E+\omega)}\right]^2 + \tfrac{1}{4}(\underline{\mu}_{12}:\hat{\boldsymbol{\epsilon}})^2 - \frac{(\underline{\mu}_{12}\cdot\hat{\boldsymbol{\epsilon}})^4}{8(\Delta E+\omega)^2} + O(5)$$

(4.3.74)

The terms $\delta(4)$ and $\delta(6)$, see Eq. (4.3.40), are not included in these results since they are of "sixth" order and the expression derived for $\bar{P}_2^N$ is reliable only through fourth order in the main resonance term. If $\Delta E \approx \omega$ is used in the denominator of the terms in Eqs. (4.3.73) and (4.3.74), one obtains

$$\bar{P}_2^1 = \frac{\tfrac{1}{4}(\underline{\mu}_{12}\cdot\hat{e}\varepsilon)^2\left[1-\frac{(\underline{\mu}_{12}\cdot\hat{e}\varepsilon)^2}{4\omega^2}\right] - \frac{(\underline{\mu}_{12}\cdot\hat{e}\varepsilon)^4}{32\omega^2} + O(5)}{2\left[\left[\tfrac{1}{2}(\Delta E-\omega)+\frac{(\underline{\mu}_{12}\cdot\hat{e}\varepsilon)^2}{8\omega}\right]^2+\tfrac{1}{4}(\underline{\mu}_{12}\cdot\hat{e}\varepsilon)^2 - \frac{(\underline{\mu}_{12}\cdot\hat{e}\varepsilon)^4}{32\omega^2}+O(5)\right]}$$

$$+ \frac{(\underline{\mu}_{12}\cdot\hat{e}\varepsilon)^2}{8\omega^2} + O(3) \qquad (4.3.75)$$

Due to differences in the type of perturbation theory used, and in the ordering of terms, this result is slightly different than that obtained by Shirley [23,31] which is given below:

$$P_{1\to 2}(t) = \frac{(\underline{\mu}_{12}\cdot\hat{e}\varepsilon)^2}{8\omega^2}$$

$$+ \frac{\tfrac{1}{4}(\underline{\mu}_{12}\cdot\hat{e}\varepsilon)^2\left[1-\frac{(\underline{\mu}_{12}\cdot\hat{e}\varepsilon)^2}{4\omega^2}\right]}{2\left[\left[\tfrac{1}{2}(\Delta E-\omega)+\frac{(\underline{\mu}_{12}\cdot\hat{e}\varepsilon)^2}{8\omega}\right]^2\left[1-\frac{(\underline{\mu}_{12}\cdot\hat{e}\varepsilon)^2}{16\omega^2}\right]^2+\tfrac{1}{4}(\underline{\mu}_{12}\cdot\hat{e}\varepsilon)^2\right]} \qquad (4.3.76)$$

Eq. (4.3.76) has been obtained by applying Brillouin-Wigner perturbation theory [31] to the Floquet secular equation with $\underline{d} = 0$, and agrees with Eq. (4.3.75) through $O(\mu^2)$, in

the numerator and through $O(\mu^4)$ in the denominator of the main resonance term. This approach was initially used with $\underline{d} \neq 0$ and difficulties were encountered in ordering the terms. Thus, Brillouin-Wigner perturbation theory was not used when $\underline{d} \neq 0$. In addition, if one follows the work of Shirley [28,31], but with $\underline{d} \neq 0$, a very different Floquet secular equation is obtained. Appendix C contains the derivation of this secular equation and clearly illustrates the problems associated with the $\underline{d} \neq 0$ case.

For N even one obtains

$$\bar{P}_2^N = \tfrac{1}{4}(\underline{\mu}_{12}\cdot\hat{e}\varepsilon)^2[(\Delta E-\omega)^{-2} + (\Delta E+\omega)^{-2}] + O(3) \tag{4.3.77}$$

Thus the transition probability consists of a dynamic background only, with no resonances, when $\underline{d} = 0$ as expected (see also Sec. 3.3.2). When $N \geq 3$ is odd,

$$\bar{P}_2^N = [2\rho^2]^{-1}[\delta(6)] + \tfrac{1}{4}(\underline{\mu}_{12}\cdot\hat{e}\varepsilon)^2[(\Delta E-\omega)^{-2} + (\Delta E+\omega)^{-2}] + O(3) \tag{4.3.78}$$

where ρ^2 is obtained from Eq. (4.3.39) with the $\underline{d} = 0$ limits given by Eqs. (4.3.68), (4.3.71) and (4.3.72). Also, from Eqs. (4.3.40) and (4.3.72) one obtains

$$\delta(6) = \frac{1}{64}(\underline{\mu}_{12}\cdot\hat{e}\varepsilon)^6(\Delta E-\omega)^{-4}\delta_{N,3} \tag{4.3.79}$$

Thus to this order of approximation, the transition probability for $N > 3$, N odd, will consist only of a background term since $\delta(6) = 0$ unless $N = 3$. Higher order perturbation corrections are necessary to obtain the results for odd photon resonances when $\underline{d} = 0$ and $N > 3$. Finally, it should be noted that the $\delta(6)$ term can be included rigorously in the numerator of the first term of Eq. (4.3.78) when $N = 3$ since the only other possible sixth order term, $(E_{01,02}^{(1)})^* E_{01,02}^{(5)}$, is zero when $\underline{d} = 0$. Thus when $\underline{d} = 0$, the transition probability for the three-photon resonance is given by Eq. (4.3.78). If one sets $\Delta E = 3\omega$ in the denominators of terms of the form $(\Delta E + c\omega)$, where c is a constant, in Eq. (4.3.78) and neglects both the small background term and $\delta(4)$ in ρ^2, the result obtained agrees precisely with that of Shirley [23].

Expansions in powers of the couplings $(\underline{\mu}_{12} \cdot \theta\varepsilon)$ and $(\underline{d} \cdot \theta\varepsilon)$, analogous to the results for ω_{res}^N given by Eqs. (4.3.58) and (4.3.62)-(4.3.66), can also be obtained for the $(FWHM)^N$. Since the major effects of $\underline{d} \neq 0$ on the FWHM is contained within the RWA, see Sec. 3.3.2, and expansions of this type are of limited validity, only a limited set of results are presented here. Using Eq. (4.3.45), and techniques similar to those used to derive the power series expansions of ω_{res}^N, it can be shown that

$$(\text{FWHM})^N = \left|2\underline{\mu}_{12}\cdot\hat{e}\varepsilon - \frac{1}{4(\Delta E)^2}(\underline{\mu}_{12}\cdot\hat{e}\varepsilon)(\underline{d}\cdot\hat{e}\varepsilon)^2 + O(\mu^3)\right|, \quad N = 1$$

$$= \left|\frac{1}{\Delta E}(\underline{\mu}_{12}\cdot\hat{e}\varepsilon)(\underline{d}\cdot\hat{e}\varepsilon) + O((\mu d)^4)\right|, \quad N = 2$$

$$= \left|\frac{3}{8(\Delta E)^2}(\underline{\mu}_{12}\cdot\hat{e}\varepsilon)^3 - \frac{3}{4(\Delta E)^2}(\underline{\mu}_{12}\cdot\hat{e}\varepsilon)(\underline{d}\cdot\hat{e}\varepsilon)^2 + O((\mu d)^5)\right|, \quad N = 3$$

$$= \left|\frac{2}{3(\Delta E)^3}(\underline{\mu}_{12}\cdot\hat{e}\varepsilon)(\underline{d}\cdot\hat{e}\varepsilon)^3 - \frac{8}{9(\Delta E)^3}(\underline{\mu}_{12}\cdot\hat{e}\varepsilon)^3(\underline{d}\cdot\hat{e}\varepsilon) + O((\mu d)^5)\right|, \quad N = 4$$

(4.3.80)

In general, when deriving expressions of this type the power series expansions for ω_{res}^N derived previously and expansions of terms like $(\Delta E+c\omega)^{-1}$ in powers of the couplings are required. Eqs. (4.3.80) are sufficient to analytically demonstrate that two of the effects of $\underline{d} \neq 0$ are to reduce the widths of the resonances and to induce even, as well as odd, photon transitions relative to atoms ($\underline{d} = 0$) as discussed previously (Secs. 3.3.1 and 3.3.2). The expressions for the $(\text{FWHM})^N$, for N = 2,3 and 4, agree with those in the literature [34] only for N = 2; those results for N = 3 and N = 4 differ by multiplicative factors that depend on N. For N = 1 and N = 3, Eq. (4.3.80) agrees

precisely with well known literature results [23] when $\underline{d} = 0$.

4.4 Numerical Examples of Perturbative Corrections to the RWA and a Discussion of Giant Dipole Molecular Spectra

As discussed previously, there are difficulties associated with the ordering of the perturbative corrections to the RWA expressions for the resonance profiles, and their full widths at half maxima, and with the convergence of the perturbation expansions for these quantities and the (μ,d) expansions arising from them. In this subsection these problems are discussed in more detail through the use of model calculations, some of which are related to the spectra of molecules with "giant" differences between the permanent dipoles of the states involved in the transition.

4.4.1 Numerical Examples of Perturbative Corrections to the RWA

Here the models associated with the exact two-level multi-photon spectra discussed in Sec. 3.3.2, for $\underline{d} \neq 0$ and $\varepsilon_g = 0$. are used to help discuss some of the perturbative corrections to the RWA. Extensive calculations have been carried out for these corrections for the model systems involved in the multi-photon spectra of Figures 3.3-3.5. Detailed discussions of these figures, with respect to the

effect of permanent dipoles in the spectra, can be found in Sec. 3.3.2 which also includes comparisons between the exact and RWA single- and multi-photon spectra. The purpose of what follows is to extend the earlier discussions to include the effects of the perturbative corrections to the RWA.

The quantities used in the perturbation expansion of the steady state transition probability given by Eq. (4.3.41), and in the analogous expressions for the $(FWHM)^N$, involve single or double infinite sums over molecule-EMF couplings involving Bessel functions of argument $\frac{d\cdot\theta\varepsilon}{\omega}$, see for example Eqs. (4.3.12), (4.3.35) and (4.3.36). The various terms in these sums can be either negative or positive depending on the values of the parameters involved in the problem, including the frequency ω. In the evaluation of the sums the positive and negative contributions were summed separately to check for roundoff errors and the convergence of the sums was investigated by systematically increasing the number of terms included in the sums. For the two-level models studied here it was found that truncations of the summation indicies to $-m \leq \ell \leq +m$, with $m \sim 90$, were sufficient to guarantee much more than graphical accuracy for the resulting spectra. The Bessel functions were computed using the subroutine MMBSJN from the IMSL [102] package.

The calculated absorption spectra obtained from the perturbative expansion given by Eq. (4.3.41) are not well

behaved in general. For the cases studied here, the third order energy $E_{01,02}^{(3)}$ as a function of ω often becomes large compared to the first and second order energies and as a result the values of the spectra can become much too large (>>0.5) and/or negative. For the strong molecule-EMF coupled example of Figure 3.5, even the second order energy misbehaves relative to the lower order energies and so the perturbative corrections to the RWA are not discussed for this case in any detail in what follows; only the RWA itself, discussed in Sec. 3.3.2, is meaningful for this example. Thus the absorption spectra are calculated using the following expression, obtained from Eq. (4.3.41) by setting $E_{01,02}^{(3)}$ equal to zero,

$$\bar{P}_2^N = [2\rho^2]^{-1}[|E_{01,02}^{(1)}|^2\{1 + 8F_{01,1}^{(2)}\}] - 4F_{01,1}^{(2)} \tag{4.4.1}$$

where

$$\rho^2 = |E_{01}^{(0)}|^2 + 2E_{01}^{(0)}E_{01,01}^{(2)} + |E_{01,01}^{(2)}|^2 + |E_{01,02}^{(1)}|^2 \tag{4.4.2}$$

Similarly, the $(FWHM)^N$ is also adversely affected by the third order energy in general and, from Eq. (4.3.45), is now taken to be

$$(\text{FWHM})^N = \frac{2}{N} \left| C(N) - 8C(N) F_{01,1}^{(2)} \right|_{\omega=\omega_{res}^N} \qquad (4.4.3)$$

In what follows, the absorption spectra will be discussed with the aid of the parameters b, $\eta = \eta(1)$ and $\beta(N)$, defined by Eqs. (3.3.4), (3.3.14) and (3.3.15) respectively. The physical significance of these coupling strength parameters has been discussed in Chapter 3. In evaluating $\beta(N)$, and $(\text{FWHM})^N$ through Eq. (4.4.3), ω_{res}^N is taken to be that which corresponds to the spectra generated from the second order perturbation result for $\bar{P}_2^N$ given by Eq. (4.4.1). In Figures 4.2 and 4.3, the N = 1,2 and 3 photon absorption spectra or resonance profiles, obtained from the second order perturbation expression (Eq. (4.4.1)), are compared to the RWA spectra for the two-level models associated with Figures 3.3 and 3.4 of Chapter 3. The relevant molecular and field parameters are summarized in the captions to Figures 4.2 and 4.3.

In Figure 4.2, the two-level model system is characterized by b = 0.5 and $\eta = 10.0$, and by $\beta(N) = 3.07 \times 10^{-3}$, 1.51×10^{-2} and 1.37×10^{-2} for the one-, two- and three-photon resonances in the second order perturbation spectra. Since the $\beta(N)$ are small, the peaks are narrow and from Eq. (4.4.3), $(\text{FWHM})^N = 0.0062$, 0.016 and 0.0092, for N = 1,2 and 3, in good agreement with those obtained from the RWA and exact spectra, see Figure 3.3, and from

Figure 4.2. Comparison of the RWA and the second order perturbation results for the absorption spectra, $\bar{P}_2^N$ as a function of $\omega/\Delta E$, for the two-level model characterized by $\mu_{12} = 1.0$, $d = 20.0$, $\Delta E = 1.0$ and $\varepsilon = 0.5$. The second order perturbation resonance profiles for $N = 1,2$ and 3 are illustrated in a, b and c and are calculated from Eqs. (4.4.1), (4.4.2), (4.3.12) and (4.3.33)-(4.3.35). d, e and f contain the corresponding RWA resonance profiles for $N = 1,2$ and 3 and are calculated from Eqs. (3.3.5)-(3.3.7). In this example $b = 0.5$ and $\eta = 10.0$. The corresponding exact spectrum is given in Figure 3.3.

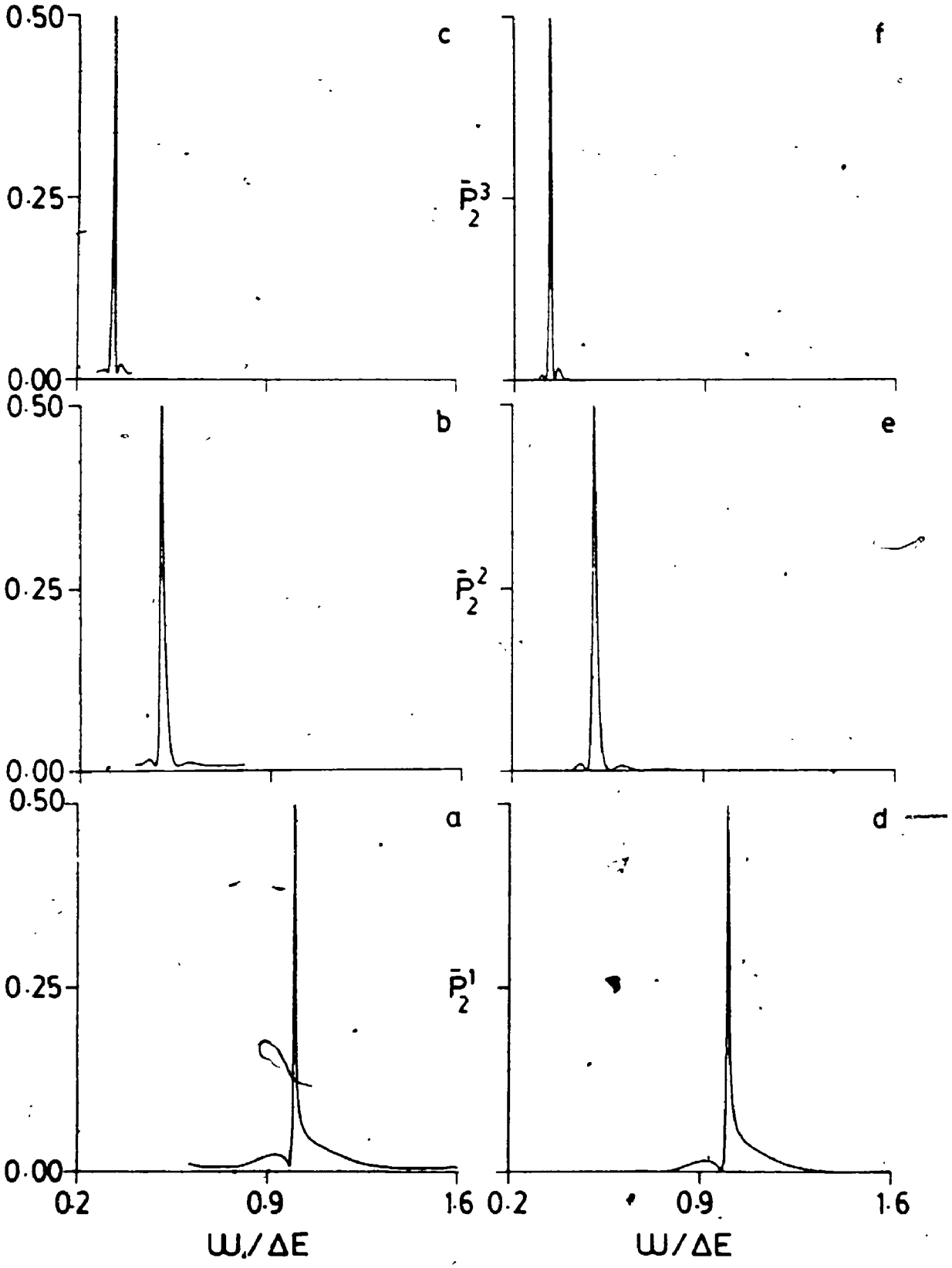
0·50
0·25
0·00
c
f
$\bar{P}_2^3$
b
e
$\bar{P}_2^2$
a
d
$\bar{P}_2^1$
0·2
0·9
1·6
$W_i/\Delta E$
$W/\Delta E$

Figures 4.2a,b,c, namely 0.007, 0.02 and 0.01 respectively.

The resonances in the second order perturbation spectra occur at $\omega/\Delta E = 0.995$, 0.4976 and 0.3317 for $N = 1,2$ and 3 respectively and are shifted slightly to the low frequency side of the RWA resonances which occur at $\omega/\Delta E = 1/N = 1.0$, 0.5 and 0.333 for $N = 1,2$ and 3. In addition, a very low background is present in the perturbation spectra that is not present in the RWA.

The effect of including second order correction terms, $E_{01,01}^{(2)}$ and $F_{01,1}^{(2)}$ (the latter term requires both the first and the second order wave functions, see Eqs. (4.3.25) and (4.3.26)), has been to provide both the small "negative Bloch-Siegert" shift and the slight background present in the exact spectra of Figure 3.3.

Figure 4.3 is an example of a more strongly coupled two-level system with $b = 6.84$ and $\eta = 26.98$. Here, for the perturbation spectra, $\beta(N) = 6.31 \times 10^{-2}$, 5.71×10^{-3} and 3.40×10^{-2} for $N = 1,2$ and 3 respectively and the $(FWHM)^N$, from Eq. (4.4.3), are 2.40×10^{-6}, 1.85×10^{-7} and 1.07×10^{-6} for the one-, two- and three-photon resonances whereas those measured from Figure 4.3 are 2.63×10^{-6}, 6.31×10^{-7} and 3.15×10^{-7}. The RWA predicts $(FWHM)^N = 4.26 \times 10^{-6}$, 2.01×10^{-6} and 1.09×10^{-6} for $N = 1,2$ and 3 (see Eq. (3.3.13)) while those measured from the exact spectrum in Figure 3.4 are 2.22×10^{-6} and 6.30×10^{-7} for $N = 1$ and 2. It was not possible to obtain the width of the three-photon resonance because of the occurrence of an

Figure 4.3. Comparison of the RWA and the second order perturbation results for the absorption spectra, $\bar{P}_2^N$ as a function of $\omega/\Delta E$, for the two-level model characterized by μ_{12} = -0.5072, d = 2.0, $\Delta E = 3.706 \times 10^{-5}$ and $\varepsilon = 5.0 \times 10^{-4}$. The second order perturbation resonance profiles for N = 1,2 and 3 are illustrated in a, b and c and are calculated from Eqs. (4.4.1), (4.4.2), (4.3.12) and (4.3.33)-(4.3.35). d, e and f contain the corresponding RWA resonance profiles for N = 1,2 and 3 and are calculated from Eqs. (3.3.5)-(3.3.7). Here b = 6.84 and η = 26.98. The corresponding exact spectrum is given in Figure 3.4. The perturbation correction terms occurring in Eq. (4.4.1) contain terms of the form $(\Delta E - c\omega)^{-I}$, where c and I are positive integers. When $\omega = \Delta E/c$ these terms tend to infinity. This occurs when ω is small in the examples presented here and in Figure 4.2. Thus the frequency sweep is not extended to smaller frequencies in these cases.

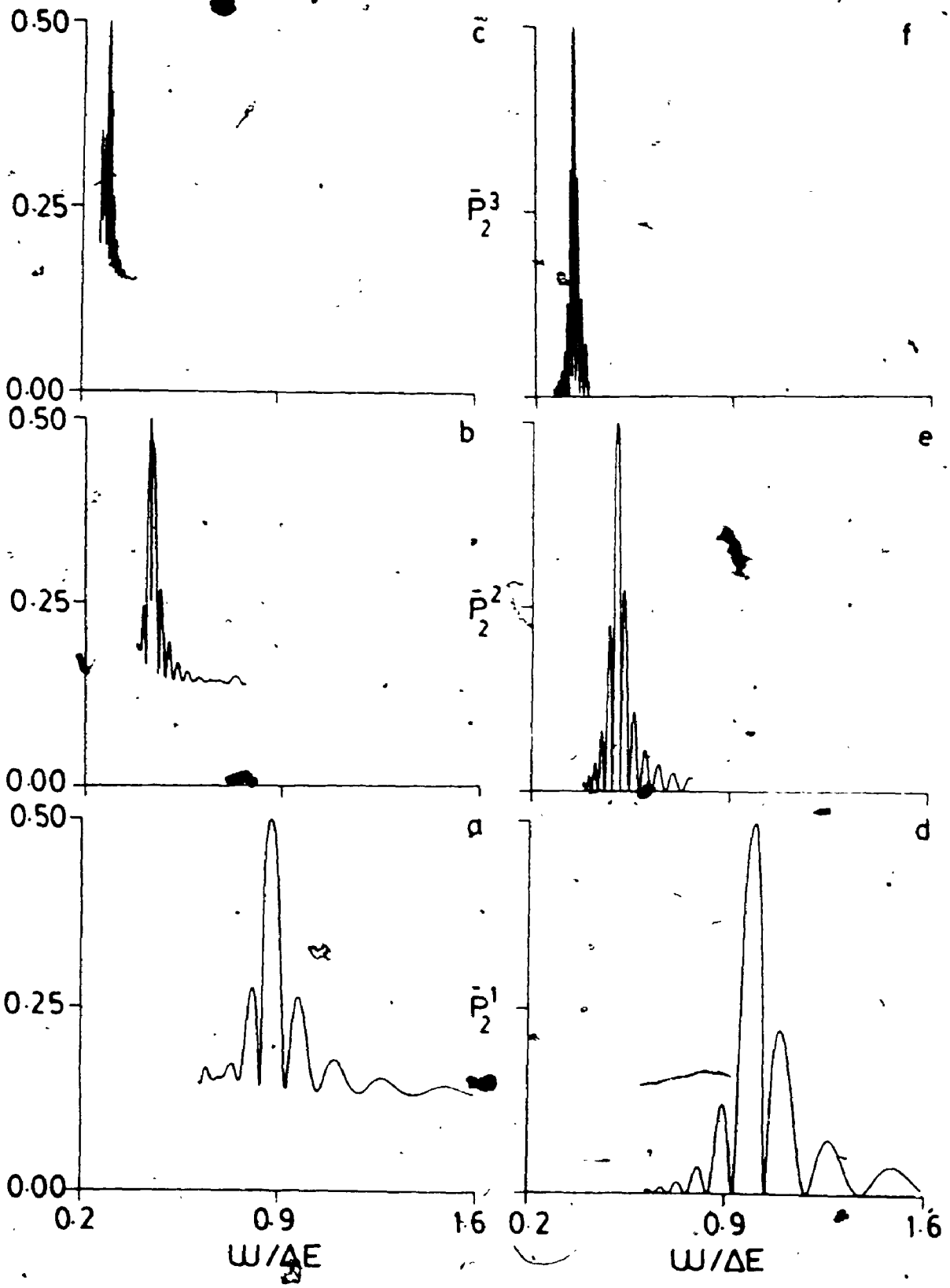
0.50
0.25
0.00
c
f
$\bar{P}_2^3$
e
b
e
$\bar{P}_2^2$
a
d
$\bar{P}_2^1$
0.2
0.9
1.6
W/ΔE

oscillatory fringe close to the main resonance, see Figure 3.4d. In general, the second order perturbation expression for the FWHM appears to be an improvement over the RWA expression given by Eq. (3.3.13). However, it does not successfully predict the widths of the exact spectra since, in this example, the resonances are relatively broad and the frequency varies significantly over them.

A background of approximately 0.15 is present in all the second order perturbation spectra of Figure 4.3. As well, the resonances in the perturbation spectra are shifted significantly to the low frequency side of the RWA resonances; they occur at $\omega/\Delta E$ = 0.88, 0.43 and 0.29 as opposed to $\omega/\Delta E = 1/N$ = 1.0, 0.5 and 0.33 for N = 1,2 and 3.

In this example, the effect of including the second order correction terms has been to introduce, relative to the RWA, a substantial background in the spectra and large negative shifts in the resonance frequencies in agreement with the exact spectra of Figure 3.4. The second order perturbation resonance frequencies are in good agreement with those of the exact spectra, namely $\omega_{res}^{N}/\Delta E$ = 0.87, 0.44 and 0.31 respectively for N = 1,2 and 3.

In the examples considered here the results for the resonance frequencies obtained from the (μ,d) expansions of Eqs. (4.3.62)-(4.3.66) are essentially meaningless; the couplings $\underline{\mu}_{12}\cdot\hat{e}\varepsilon$ and $\underline{d}\cdot\hat{e}\varepsilon$ and the coupling strength parameters b and η are large and the perturbation expansion in $\underline{\mu}$ and $\underline{d}$ does not converge. Similar comments apply for the

$\underline{\mu}$ and $\underline{d}$ expansions for the $(\text{FWHM})^N$ given by Eqs. (4.3.80). The implicit perturbation results for ω_{res}^N given by Eq. (4.3.58), without making a (μ,d) expansion, can be used iteratively to obtain meaningful results for ω_{res}^N. This method has been tested using Eq. (4.3.58) with terms of third and higher order set equal to zero. For example, one obtains values of ω_{res}^N = 0.88, 0.44 and 0.30, N = 1,2 and 3 respectively, for the spectra of Figure 4.3 in this way.

In summary, the second order perturbation expression for $\bar{P}_2^N$, generated by applying the near degenerate perturbation theory of Appendix B to the Floquet secular equation, appears to not be particularly useful for calculational purposes. In some problems, where the molecule-EMF couplings are relatively weak, the result through second order given by Eq. (4.4.1) agrees quite well with the exact calculations for two-level spectra; even for these cases the perturbation corrections can become unreliable for some frequencies (see the caption of Figure 4.3). In others, where the coupling between the molecule and the EMF becomes larger, the perturbation corrections to the RWA are not reliable. An example of this unreliability is furnished by the two-level model problem associated with Figure 3.5 where the multi-photon resonances are overlapping and are becoming quite saturated.

The perturbation treatment of these problems is not easily done. Not only are the zeroth order energies near degenerate but they can also be of the same magnitude as

the second order energy since $E_{01}^{(0)} = -E_{02}^{(0)} = -\Delta = -\frac{1}{2}(\Delta E - N\omega)$. For frequencies around ω_{res}^{N}, $\Delta E - N\omega$ is related to the shift of the resonance frequency from the RWA result of $\Delta E/N$ and is a small quantity (see Eqs. (4.3.62)-(4.3.66)). As pointed out in Sec. 4.3 this makes the ordering of the terms in order of smallness difficult in the perturbation expansion of $\bar{P}_2^N$. This difficulty is compounded by the fact that the perturbation, and the perturbed energies and wave functions, are functions of the frequency as well as the couplings $\underline{\mu}_{12}\cdot\hat{e}\mathcal{E}$ and $\underline{d}\cdot\hat{e}\mathcal{E}$. As pointed out earlier, the perturbation theory can appear to converge for certain frequencies in a given problem and then misbehave as ω is altered.

In general, the usefulness of the perturbation corrections to the RWA appears to be in the more qualitative and conceptual understanding of the differences between the RWA and the exact results for multi-photon spectra. The best example of this is given by the expansion of the resonance frequency shift from the RWA result of $\Delta E/N$, in powers of the couplings $\underline{\mu}_{12}\cdot\hat{e}\mathcal{E}$ and $\underline{d}\cdot\hat{e}\mathcal{E}$. This result, Eqs. (4.3.62)-(4.3.66), is obtained by making an iterative expansion of the result for ω_{res} obtained through perturbation theory. It gives analytical proof of the existence of negative shifts from $\omega_{res}^{N} = \Delta E/N$, observed in the numerical exact spectra of Sec. 3.3.2, which are in contradistinction to the usual positive Bloch-Siegert shifts for the atomic problem. These (μ,d)

expansions, and the analogous expansions for the $(FWHM)^N$ given by Eq. (4.3.80), are not useful computationally if the couplings, and coupling strengths, become at all large.

With considerable numerical investigation it may be possible to develop perturbation expansions for the resonance profiles, based on Eq. (4.3.41) and extensions of it, that are computationally viable for well defined classes of two-level problems. Such development would require investigations of the terms involving the fourth order energy, $E_{0i,0i}^{(4)}$, and other higher order effects not examined in detail in this thesis. If these higher order terms were required to obtain reasonable results, the expressions for the resonance profiles would clearly become very complicated and the viability of perturbation theory for this purpose becomes questionable. The use of the perturbation theory analysis of the Floquet secular problem is not analytically tractable for more than three levels.

The difficulties with perturbation theory can be avoided by using the exact methods for the solution of the two- (or many-) level problem discussed in Sec. 2.4.2. This is the approach used to complete the discussion of the effects of $\underline{d} \neq 0$ in multi-photon spectra in the next sub-section.

4.4.2 A Discussion of the Multi-Photon Spectra of Giant Dipole Molecules

This section further discusses, relative to Chapter 3, aspects of the spectra of molecules with large permanent dipoles that are, in part, related to recent papers [34,35] on "giant dipole molecules". These papers appeared after much of the work discussed in Chapter 3 was published and are concerned, more precisely, with the spectra of molecules possessing large or "giant" differences between the permanent dipole moments of the states involved in the transition. In addition to the parameters $b, \eta = \eta(1)$ and $\beta(N)$ used to help discuss the examples considered in Sec. 4.4.1, the parameter α is also used in the present discussion;

$$\alpha = \frac{|d|}{2|\mu_{12}|} \tag{4.4.4}$$

This parameter is related to the difference in the permanent dipole moments involved in the transition, normalized to the transition dipole, and was used by Hattori and Kobayashi [34] in their discussion of the spectra of giant dipole molecules. The physical rational for the trends in the two-level spectra to be discussed in what follows, as a function of $b, \eta, \beta(N)$ and α, are analogous to those discussed, and applied, in Secs. 3.3 and 4.4.1.

The two-level model chosen is based on the ground and lowest excited singlet states of the

1-[p-(N,N-dimethylamino)phenyl]-4-(p-nitrophenyl)-1,3-butadiene molecule and is characterized by $\Delta E = 8.56 \times 10^{-2}$ and d = 11.80 [35] with μ_{12} taken to be 3.93 [93] and $\underline{d} \| \underline{\mu}_{12} \| \underline{\epsilon}$. Various multi-photon spectra, as a function of b, η and α can be generated by varying the field strength ϵ and the value of d. In Figure 4.4 the exact two-level absorption spectra labelled with a, b and c correspond to α = 0, 1.1 and 1.5 respectively. In addition, each spectra labelled with 1, 2, 3 and 4 correspond to b = 0.2, 0.6, 1.0 and 1.8. The values of $\omega_{res}^{N}/\Delta E$, N = 1,2,...,6, for each spectrum are summarized in Table 4.1.

To begin, consider the spectra corresponding to a fixed value of α. When α = 0, η = 0.0 for the spectra in Figure 4.4a-1 to a-4. As b increases on going from a-1 to a-4 the spectra become more saturated as is expected and as is evident from the increasing background; the resonances shift significantly to higher values of $\omega/\Delta E$ (see Table 4.1). Only the odd photon resonances occur as usual since $\underline{d}$ = 0.

When α = 1.1, η = 0.44, 1.32, 2.20 and 3.96, and b = 0.2, 0.6, 1.0 and 1.8 for Figure 4.4b-1, b-2, b-3 and b-4 respectively. Initially as η increases, some of the resonances approach each other and eventually overlap very strongly. This effect is evident when η = 1.32 and b = 0.6 (Figure 4.4b-2). Here, the one- and two-photon resonances are very close and appear as one large, broad resonance with two maxima separated by a very slight minimum. The

Figure 4.4 Comparison of the absorption spectra, $\bar{P}_2$ as a function of $\omega/\Delta E$, obtained from exact calculations for the two-level systems specified by $\mu_{12} = 3.93$, $\Delta E = 8.56 \times 10^{-2}$ and $d = 0$ (a-1 to a-4), $d = 8.65$ (b-1 to b-4) and $d = 11.80$ (c-1 to c-4). In a-1, b-1 and c-1, $\varepsilon = 4.36 \times 10^{-3}$ and $b = 0.2$ while $\varepsilon = 1.31 \times 10^{-2}$ and $b = 0.60$ for a-2, b-2 and c-2, $\varepsilon = 2.18 \times 10^{-2}$ and $b = 1.00$ for a-3, b-3 and c-3 and $\varepsilon = 3.92 \times 10^{-2}$ and $b = 1.80$ for a-4, b-4 and c-4. Also, $\alpha = 0$ and $\eta = 0$ for a-1 to a-4, $\alpha = 1.1$ and $\eta = 0.44$, 1.32, 2.20 and 3.96 for b-1 to b-4 respectively and $\alpha = 1.5$ and $\eta = 0.60$, 1.80, 3.00 and 5.40 for c-1 to c-4.

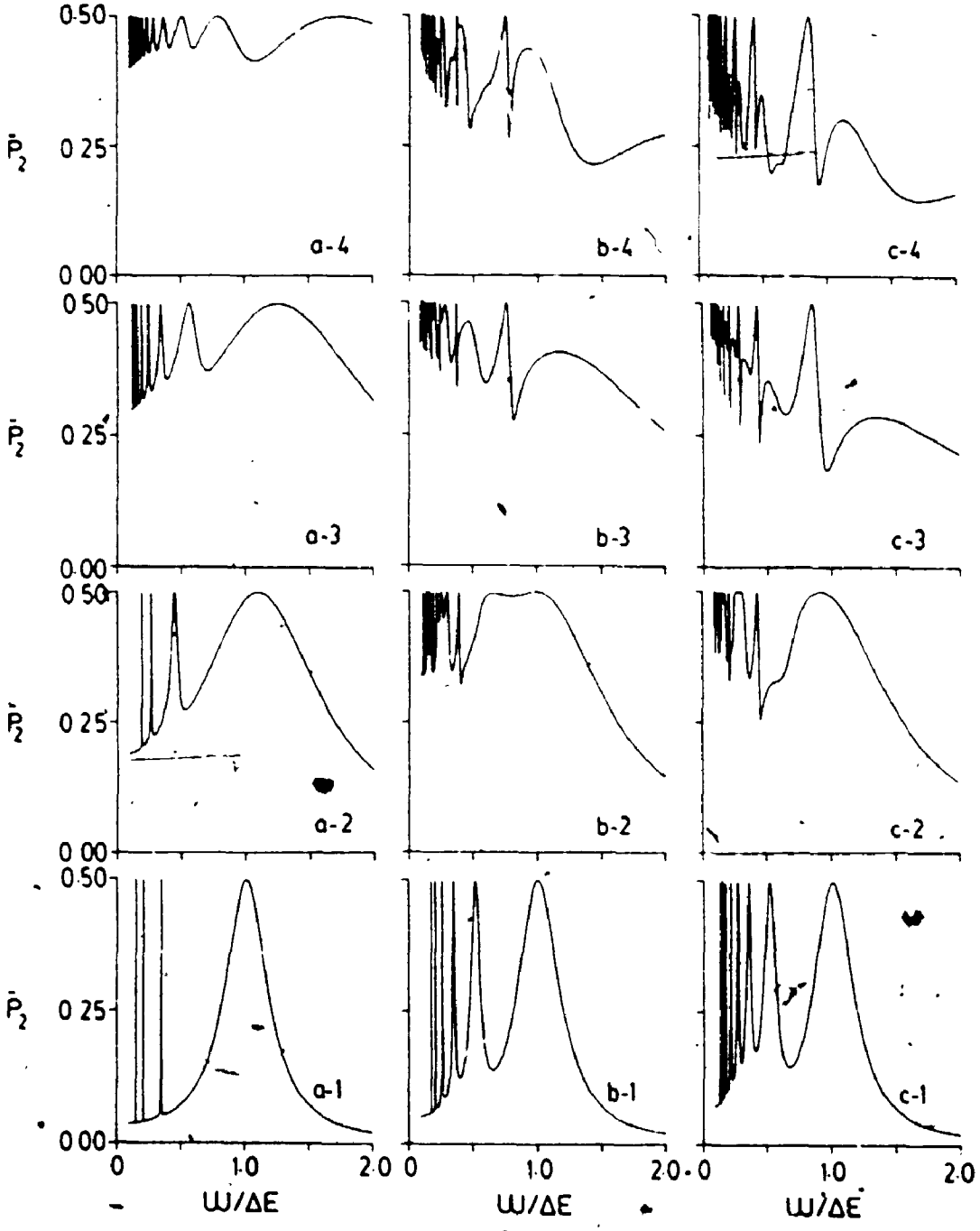
0·50
0 25
0 00
$\bar{P}_2$
a-4
b-4
c-4
a-3
b-3
c-3
a-2
b-2
c-2
a-1
b-1
c-1
0
1·0
2·0
ω/ΔE

Table 4.1. Summary of the values of $\omega_{res}^{N}/\Delta E$ for the exact spectra given in Figure 4.4. These spectra correspond to the two-level systems specified by $\mu_{12} = 3.93$, $\Delta E = 8.56 \times 10^{-2}$ and d = 0 (Figure 4.4a-1 to a-4), d = 8.65 (Figure 4.4b-1 to b-4) and d = 11.80 (Figure 4.4c-1 to c-4). b, $\eta = \eta(1)$ and α are defined in Eqs. (3.3.4), (3.3.14) and (4.4.4).

α	b	η	$\omega_{res}^{1}/\Delta E$	$\omega_{res}^{2}/\Delta E$	$\omega_{res}^{3}/\Delta E$	$\omega_{res}^{4}/\Delta E$	$\omega_{res}^{5}/\Delta E$	$\omega_{res}^{6}/\Delta E$
0.0								
	0.20	0.00	1.01	-	0.35	-	0.21	-
	0.60	0.00	1.09	-	0.44	-	0.26	-
	1.00	0.00	1.25	-	0.56	-	0.34	-
	1.80	0.00	1.73	-	0.79	-	0.51	-
1.1								
	0.20	0.44	1.01	0.52	0.35	0.26	0.21	0.17
	0.60	1.32	0.99	0.65	0.38	0.29	0.25	0.22
	1.00	2.20	0.76	0.37	0.28	0.24	0.21	0.20
	1.80	3.96	0.75	0.37	0.26	0.24	0.19	0.18
1.5								
	0.20	0.60	1.01	0.52	0.35	0.26	0.21	0.18
	0.60	1.80	0.92	0.43	0.30	0.27	0.26	0.21
	1.00	3.00	0.85	0.42	0.28	0.21	0.17	0.15
	1.80	5.40	0.85	0.42	0.28	0.21	0.17	0.14

one-photon resonance has shifted slightly to a lower value of $\omega/\Delta E$ while the two-photon resonance has shifted significantly to a higher value of $\omega/\Delta E$ relative to $\underline{d} = 0$ (see Table 4.1). The three-, four-, five- and six-photon resonances shift slightly to higher values of $\omega/\Delta E$ as well. When $\eta = 2.20$, the large, broad resonance of the $\eta = 1.32$ case, has been replaced by a one-photon resonance with a large oscillatory fringe on the high $\omega/\Delta E$ side. The one-, two- and three-photon resonance positions have undergone large negative shifts from those associated with the $\eta = 1.32$ calculation and an oscillatory fringe associated with the two-photon resonance is also clearly present. An increase in η, Figure 4.4b-4, further complicates the spectra for low frequency. There is an interesting interplay between increasing b and increasing η in proceeding from b-1 to b-4 in Figure 4.4. Increases in b tend to broaden and saturate, while increases in η tend to narrow and sharpen the absorption spectra as discussed in Sec. 3.3. For $\underline{d} \neq 0$ the appearance of even, as well as odd, photon resonances is clear and this can add to the crowding of the resonances, relative to the $\underline{d} = 0$ spectra of part a of Figure 4.4, as a function of ω and η.

Figure 4.4c-1 and c-4 correspond to the absorption spectra of 1-[p-(N,N-dimethylamino)phenyl]-4-(p-nitrophenyl)-1,3-butadiene [35], as a function of ε, where $\alpha = 1.5$. Here $\eta = 0.60$, 1.80, 3.00 and 5.40, and b = 0.2, 0.6, 1.0 and 1.8 for Figure 4.4c-1, c-2, c-3 and c-4 respec-

tively. In this example, no merging of the lower photon resonances is observed; for each b value, the value of η is larger in this example than in Figure 4.4b. The four-, five- and six-photon resonances shift to slightly higher values of $\omega/\Delta E$ when b = 0.6 and η = 1.80. In general though, all resonances shift to lower values of $\omega/\Delta E$ as b and η increase, illustrating again the negative Bloch-Siegert shifts due to the presence of $\underline{d}$.

Now consider the spectra for fixed values of b. When b = 0.2, Figure 4.4a-1, b-1 and c-1 correspond to η = 0, 0.44 and 0.60 respectively. The resonances occur at the same positions in each spectra for N = 1, 3 and 5 (see Table 4.1) and, when $\underline{d} \neq 0$, for N = 2 and 4, as well. The coupling strengths are quite similar for each resonance. For example, when N = 1, $\beta(1)$ = 0.20, 0.195 and 0.191 for a-1, b-1 and c-1 respectively and $\beta(1) \approx b$. The effect of $\underline{d} \neq 0$ is minimized for the small values of η occurring in this example (see Sec. 3.3).

The spectra characterized by b = 0.6 correspond to Figure 4.4a-2 where η = 0, $\beta(1)$ = 0.60, Figure 4.4b-2 where η = 1.32, $\beta(1) \approx 0.48$ and Figure 4.4c-2 where η = 1.80, $\beta(1)$ = 0.36. As η increases the one-photon resonance shifts to lower values of $\omega/\Delta E$. As discussed previously, the N > 1 resonances shift to high frequency when η = 1.32. However as η increases further to η = 1.8 the overall effect of increasing $\underline{d}$ from zero becomes clear in that it tends to induce shifts in the resonance frequency

to the low frequency side of the zero field or RWA limit of $\Delta E/N$.

Finally, Figures 4.4a-3, b-3 and c-3 correspond to b = 1.0 and to the parameters $\eta = 0$ and $\beta(1) = 1.00$, $\eta = 2.20$ and $\beta(1) = 0.26$ and $\eta = 3.00$ and $\beta(1) = 0.071$ while Figures 4.4a-4, b-4 and c-4 correspond to b = 1.8 and are characterized by $\eta = 0$ and $\beta(1) = 1.80$, $\eta = 3.96$ and $\beta(1) = 0.24$ and $\eta = 5.40$ and $\beta(1) = 0.11$. Both these examples illustrate the effect of $\underline{d} \neq 0$ on the absorption spectra of molecules. When $\underline{d} = 0$, the spectra are highly saturated and the resonances are quite broad; when $\underline{d} \neq 0$, the background is greatly reduced, and the resonances are narrowed appreciably, and oscillatory fringes occur in the spectra as explained and discussed in Sec. 3.3. For fixed b, as η increases, the "real" molecule-EMF coupling $\beta(1)$ differs more appreciably from b.

The spectra given in Figure 4.4 can also be used as models to help analyze the validity of the various perturbation expressions derived in Sec. 4.3. For example the (μ,d) expansions for ω_{res}^{N} given by Eqs.(4.3.62)-(4.3.66) yield results in agreement with Table 4.1, only for $N \leq 3$ and b = 0.2, and $\eta = 0.44$ and 0.60.

Hattori and Kobayashi [34] carried out frequency sweep absorption spectra for a system characterized by α = 0.3 and b = 0.2, 0.6, 1.0 and 1.8. Solving for the corresponding η values, one obtains $\eta = 0.12$, 0.36, 0.60, 1.08. Hence these calculations showed only some of the

effects discussed in this thesis, for example oscillatory fringes associated with main resonances were not observed. Also, the analysis given of the effects of $\underline{d} \neq 0$ on the absorption spectra was carried out using a Floquet secular equation, see Appendix C, which is not derived from the interaction representation used in Sec. 3.2. The use of this representation led to a discussion of the molecule-EMF interaction in terms of the important molecule-EMF coupling given by C(N) defined in Eq. (3.2.14). The form of the Floquet secular equation used in [34] is the $\underline{d} \neq 0$ analogue of Shirley's result [23] and leads to results like those of Eqs. (4.3.62)-(4.3.66) and Eq. (4.3.80) which, as discussed previously, cannot be used to analyze spectra like those of Figure 4.4 reliably. For $\underline{d} \neq 0$, these (μ,d) expressions correspond to making a power series expansion of the Bessel function occurring in C(N), see Eq. (4.3.59), and therefore cannot account, for example, for the oscillatory fringes in the absorption spectra discussed in this work. Further, the RWA arising from the Floquet secular equation of Appendix C corresponds to the usual atomic result of Eq. (3.3.2), and not the C(N) result of Eq. (3.3.5). The effects of $\underline{d} \neq 0$ in this approach arise from higher order perturbation terms in the treatment of the secular equation.

CHAPTER 5

SUMMARY AND CONCLUSIONS

One of the most important aspects of this work is the derivation, and application, of analytic expressions for the phase- and long time-averaged transition probabilities (absorption spectra) for the two-level model molecular system that includes the effects of permanent dipole moments and/or of static electric fields. The spectra are assumed to be induced by a plane-polarized sinusoidal electromagnetic field (EMF)..

The generalized (molecular) rotating wave approximation (RWA) result for the single- and multi-photon absorption spectra, derived in Sec. 3.2, is a closed form analytic expression that is very useful in helping to understand, interpret and predict the effects of permanent dipole moments and/or of static electric fields on the spectra. The RWA result for the coupling between the electromagnetic field and the molecule, Eq. (3.2.14), plays a central role in these interpretations and predictions. The usefulness, reliability and range of validity of the generalized RWA expressions as a function of the parameters specifying the two-level molecule and the applied fields are discussed in Sec. 3.3, with the help of several sets of model calculations where RWA results are compared with exact two-level calculations of the absorption spectra.

When the applied static electric field is zero the RWA expressions for the absorption spectra and the molecule-

EMF coupling are particularly simple functions of the transition dipole, $\underline{\mu}_{12}$, the difference between the permanent dipoles of the states involved in the transition, $\underline{d} = \underline{\mu}_{22} - \underline{\mu}_{11}$, and the magnitude, ε, and direction of polarization, $\hat{e}$, of the EMF (Sec. 3.3.2). The effects of permanent dipoles are relatively easy to understand using the RWA. In general, compared with the $\underline{d} = 0$ atomic problem, the presence of permanent dipoles (where $\underline{d} \neq 0$) reduces the coupling between the molecule and the applied EMF and causes oscillations to occur, as a function of frequency, in the molecule-EMF coupling. These effects are evident in the often drastic reduction of both resonance widths and dynamic backgrounds, which are seen when the $\underline{d} \neq 0$ spectra are contrasted with the analogous $\underline{d} = 0$ spectra. The effects of $\underline{d} \neq 0$ are further evident in the oscillatory fringes surrounding the resonance positions; these fringes are absent in the atomic case. Since the presence of permanent dipoles reduces the molecule-EMF coupling relative to the atomic problem, the molecular RWA expressions for the resonance profiles have a wider range of validity as a function of the parameters of the problem, than do the corresponding atomic results. This molecular RWA can be expected to play an analogous role in the spectroscopy for species with permanent dipoles to that played by the usual RWA in the spectroscopy of atoms. Finally it is interesting to note that as the coupling strength parameter $\underline{d} \cdot \hat{e}\varepsilon/\omega$ increases, the RWA predicts the

molecule-EMF coupling will eventually decrease with increasing field strength; this prediction is in agreement with the results obtained from the exact two-level calculations discussed in Sec. 3.3.2. The possible experimental implications of this are relevant: in some cases applied EMF's with large magnitudes actually interact weakly with molecules! In practical applications of this prediction, the effects of neighbouring states on the two-level transition under investigation will have to be taken into account, especially for intense applied fields. The generalized RWA results for the two-level absorption spectra, and for the molecule-EMF coupling, have recently been used by Jensen and Susskind [103] to help explain some of the effects associated with the ionization of highly excited state hydrogen atoms by intense microwave electromagnetic radiation.

As in any RWA-type solution to the time-dependent Schrodinger equation, the generalized (molecular) RWA becomes more reliable as the coupling between the transition dipole and the applied oscillatory electric field becomes small. In these cases the RWA accurately predicts the structure, resonance widths and the overall behaviour of the absorption spectra as a function of frequency. Although the RWA is a "resonance" approximation, it does very well off resonance when the coupling strengths are not too large. For stronger molecule-EMF coupling strengths the RWA can provide reasonable qualitative, but not

quantitative, predictions for two-level transitions as some of the examples in Chapter 3 illustrate.

The generalized RWA is not acceptable when the static electric field is zero and the difference between the permanent dipoles involved in the transition becomes very small. In this limit the generalized RWA supports only the one-photon transition, as do the well known atomic results, whereas physically all odd photon transitions can occur. Further, the exact calculations indicate that the resonance positions in the single- and multi-photon absorption spectra are generally shifted from the RWA predictions of $\omega_{res}^{N} = \Delta E/N$ and that for $\underline{d} \neq 0$, this shift can be to low frequency relative to the well known Bloch-Siegert shift to high frequency that always occurs in atoms for larger atom-EMF coupling strengths. Also the generalized RWA cannot satisfactorily treat the dynamic backgrounds in the absorption spectra and the overlapping of the single- and multi-photon resonances which are characteristic of very strong molecule-EMF coupling strengths. The development of perturbative corrections to the RWA can help in the understanding and in the analysis of these deficiencies in this model (Chapter 4); the exact calculations in Chapters 3 and 4 contain these corrections through all orders to the RWA.

The RWA expressions for the absorption spectra and molecule-EMF coupling are more complicated when static electric fields are taken into account (Sec. 3.3.3). The

interpretation of the results is analogous to that for zero static field if it is carried out in the representation that diagonalizes the static part of the Hamiltonian for the problem and if additional features due to the static background and the possibility of the mixing of states of different parity are taken into account. Thus, for example, both even and odd photon transitions can occur for two-level systems with energy states of definite parity (atoms for example) if there is a static electric field present; this effect arises for a two-level molecule with permanent dipoles in the absence of a static field, since a non-zero permanent dipole implies a state of mixed parity.

Perhaps the most interesting example involving static electric fields considered in this thesis is that of Sec. 3.3.3B which examines the interaction of a two-level dipolar molecule with static and sinusoidal electric fields. In this example, the Boltzmann orientationally averaged absorption spectra for a two-level model based on the pentadienal molecule is evaluated as a function of temperature. For finite temperatures the molecule is hindered in its rotations relative to the directions of the applied fields, by the interaction of the permanent dipole of the initial state with the static electric field. As the temperature increases each molecule-field configuration becomes equally probable and the problem corresponds to a gas phase molecule freely rotating in the presence of the applied fields. Of particular interest is the effect of

the permanent dipoles which cause a minimum in the Boltzmann orientationally averaged spectra for high temperatures (free rotation) which is removed as the temperature is reduced. The minimum occurs at the frequency $\omega = \Delta E$ where ΔE is the energy level separation in the isolated molecule. As the temperature is decreased the absorption maxima on the high frequency side of $\omega = \Delta E$ is reduced, and the maxima on the low frequency side of $\omega = \Delta E$ is increased, until finally for sufficiently low temperature the spectra corresponds to the fixed molecule-static field configuration spectrum where $\underline{d}$ is aligned with the applied static field. The analysis and prediction of such spectra can be carried out by using the RWA results for the fixed molecule-field configurations required for the orientationally averaged spectra and by using ideas associated with the two-level transitions occurring in the static diagonalized representation. As pointed out in Sec. 3.3.3B, the spectra can depend on the relative orientation of the transition and permanent dipole moments and they also depend on the relative orientations of the applied static and sinusoidal electric fields [104]. These sort of spectra, as a function of temperature, frequency and relative applied field directions, give information about the magnitude and relative orientations of the permanent and transition moments involved in the transition [104].

Perturbative corrections to the generalized RWA are obtained in Chapter 4, assuming $\epsilon_s = 0$, and used to help

investigate and explain some of the effects observed in the exact two-level spectra but missing in those obtained from the RWA. Correction terms to the RWA result for the absorption spectra are obtained through "third order" in perturbation theory in Sec. 4.3. The perturbation treatment for the problem considered here is difficult since the zeroth order energies are nearly degenerate and, for example, they are of the same magnitude as the second order energy, particularly around the resonance frequency which, in principle, is where the theory should behave best. It was also found numerically that for model calculations (Sec. 4.4.1), the third order energy, which also occurs in the perturbative result for the resonance profiles, was not well behaved and it was removed from the result in order to obtain a viable perturbative expression for the resonance profile. The resulting "second order" expression for the N-photon resonance profile is capable of introducing both low and high frequency shifts of the resonance frequencies (relative to $\Delta E/N$) and the dynamic spectral backgrounds absent in the RWA results for the spectra. This expression is relatively useful numerically as long as the molecule-EMF couplings are not too large and the frequencies of interest are not too far from resonance. For strong couplings, where the various resonances begin to overlap significantly, the perturbative results for the spectra, aside from qualitative results obtained from the RWA, are not meaningful.

It seems, in general, that the usefulness of the perturbative corrections to the RWA lies in the qualitative and conceptual understanding of the differences between the RWA and exact single- and multi-photon spectra. An example of this application is the expansion of the shift of the resonance frequencies, from the RWA result of $\Delta E/N$, in powers of the couplings between both the transition and the permanent moments and the electromagnetic field, $\underline{\mu}_{12}\cdot\hat{e}\varepsilon$ and $\underline{d}\cdot\hat{e}\varepsilon$ respectively, obtained in Sec. 4.3. This result is obtained by iteration from an implicit result for the N-photon resonance frequency obtained by the perturbation theory treatment of the problem and gives an analytical proof, see also Hattori and Kobayashi [34], of the possibility, if $\underline{d} \neq 0$, of low frequency shifts in the resonance frequencies relative to $\omega_{res}^{N} = \Delta E/N$. These "negative Bloch-Siegert" shifts are in contradistinction to the usual shifts to high frequency seen in atomic spectra. The $(\underline{\mu}_{12}\cdot\hat{e}\varepsilon, \underline{d}\cdot\hat{e}\varepsilon)$ expansions of ω_{res}^{N}, and the analogous expansions for the full width at half maximum (FWHM) for the N-photon resonance profile, are not useful computationally if the coupling strengths $(\underline{\mu}_{12}\cdot\hat{e}\varepsilon/\Delta E)$ and $(\underline{d}\cdot\hat{e}\varepsilon/\Delta E)$ are at all large.

It is very likely that the use of the perturbation theory analysis of the Floquet secular equation for the $\underline{d} \neq 0$ problem will not yield computationally useful results in general. If the effects of the fourth order energies $E_{pp}^{(4)}$, and other higher order effects, not examined in

detail in this thesis are required to obtain reasonable results, the use of perturbation theory for this purpose is doubtful. Indeed it would probably be easier to perform exact computations of the spectra which avoid the difficulties associated with perturbation theory and which are relatively inexpensive computationally for few-level systems.

Most of the conclusions summarized in the last two paragraphs are supported by the calculations involving giant dipole molecules discussed in Sec. 4.4.2, as well as those in Sec. 4.4.1. The discussion of the single- and multi-photon spectra of giant dipole molecules links the recent literature [34,35] with that of Sec. 3.3.2 and with the use of the generalized RWA to interpret such spectra. The analysis by Hattori and Kobayashi [34] of the effects of $\underline{d} \neq 0$ on the absorption spectra was carried out using a Floquet secular equation not derived from the interaction representation developed in Sec. 3.2 which leads to the Floquet equations (Sec. 4.2) used in this work. Their procedure, which is a direct $\underline{d} \neq 0$ extension of the $\underline{d} = 0$ approach used by Shirley [23], leads to the $\underline{\mu}_{12} \cdot \underline{\varepsilon}$ and $\underline{d} \cdot \underline{\varepsilon}$ expansions of the resonance frequency shifts and the $(\text{FWHM})^N$ discussed earlier, and cannot be used to analyze spectra like those discussed in Chapter 4 and Sec. 3.3.2. The molecule-EMF coupling C(N), given by Eq. (3.2.14), is essential in interpreting such spectra and it arises naturally in the treatment of the problem discussed in this thesis.

The two-level system in the dipole approximation studied here has long provided a basis for the study of a wide variety of linear and non-linear interactions between electromagnetic radiation and atoms and molecules [9,17,19,105,106]. While two-level calculations are certainly relevant and important in understanding the interaction of radiation and matter, they should be regarded as model calculations unless verified otherwise in explicit applications. The limitations of the two-level system as an approximation for "real" atoms and molecules have been discussed previously, see for example [19,30,45,86,107]. The validity of a two-level transition in a many-level system can often be estimated by comparing the two-level RWA full widths at half maxima for the various possible transitions arising from the initial state to the final state of interest, and to all nearby neighbouring states of the final state, with the energy separations between the final and its neighbouring states. This idea, and the RWA results of Chapter 3, have recently been used to help interpret the spectra of two- and many-level molecules which are adsorbed on a surface [98,108] or interacting with applied static and electric fields [104].

Finally, most of the results in this thesis are applicable, within the limitations discussed above, for both strong and weak electromagnetic field strengths. In some cases, however, intense fields and even pulsed rather

than continuous wave lasers may be appropriate. For example, to investigate some of the effects of $\underline{d} \neq 0$, namely those needing rather large values of the argument $(\underline{d}\cdot\hat{\epsilon}\mathcal{E}/\omega)$ of the Bessel functions occurring in the molecule-EMF coupling given by Eq. (3.2.14), large field amplitudes may well be useful [34]. The availability of lasers of high power has recently been reviewed by New [109], see also [110,111].

APPENDIX A

EXTRA TERMS IN THE EXPRESSION FOR THE TWO-LEVEL ABSORPTION SPECTRA WHEN p/ω = INTEGER

If p/ω is an integer then the following terms, see Eq. (3.2.39), should be considered in the derivation of the phase- and long time-averaged transition probability $\bar{P}_2^N$:

$$\begin{aligned}
\Delta = & \exp(iY\sin\delta) \\
& \times \lim_{T\to\infty}\{iA_+^*B_- \sum_{\substack{k=-\infty \\ k\neq N-p/\omega}}^{\infty} J_k(Y)\exp(-ik\delta)\left[\frac{1}{[k-N+p/\omega]\omega T}\right] \\
& \qquad \times (\exp(-i[k-N+p/\omega]\omega T)-1) \\
& + iA_-B_+^* \sum_{\substack{k=-\infty \\ k\neq N+p/\omega}}^{\infty} J_k(Y)\exp(-ik\delta)\left[\frac{1}{[k-N-p/\omega]\omega T}\right] \\
& \qquad \times (\exp(-i[k-N-p/\omega]\omega T)-1) \\
& + A_+^*B_-J_{N-p/\omega}(Y)\exp(-i[N-p/\omega]\delta) \\
& + A_-B_+^*J_{N+p/\omega}(Y)\exp(-i[N+p/\omega]\delta)\} \\
= & \exp(iY\sin\delta)[A_+^*B_-J_{N-p/\omega}(Y)\exp(-i[N-p/\omega]\delta) \\
& + A_-B_+^*J_{N+p/\omega}(Y)\exp(-i[N+p/\omega]\delta)]
\end{aligned} \tag{A.1}$$

By making use of Eqs. (3.2.35) and (3.2.28)-(3.2.31), Eq. (A.1) can be written explicitly as

$$\Delta = \frac{1}{8p^2}\{J_{N-p/\omega}(Y)\exp(i\frac{p}{\omega}\delta)[2C(N)(p-(\gamma-N\omega))\cos 2\theta$$

$$- ((p-(\gamma-N\omega))^2\xi^* - C^2(N)\xi)\sin 2\theta]$$

$$-J_{N+p/\omega}(Y)(-i\frac{p}{\omega}\delta)[2C(N)(p+\gamma-N\omega)\cos 2\theta$$

$$+ ((p+\gamma-N\omega)^2\xi^* - C^2(N)\xi)\sin 2\theta]\} \qquad (A.2)$$

The terms in Eq. (A.2) dependent on phase involve $\exp(-i\frac{p}{\omega}\delta)$, $\xi\exp(-i\frac{p}{\omega}\delta)$, $\xi^*\exp(-i\frac{p}{\omega}\delta)$ and their complex conjugates. Using the expansion for ξ given by Eq. (3.2.44), the relevant phase integrals are ($p \neq 0$):

$$I_1 = \frac{1}{2\pi}\int_0^{2\pi} \exp(-i\frac{p}{\omega}\delta)d\delta = 0 \qquad (A.3)$$

$$I_2 = \frac{1}{2\pi}\int_0^{2\pi} \xi\exp(-i\frac{p}{\omega}\delta)d\delta$$

$$= \frac{1}{2\pi}\sum_{\substack{k=-\infty \\ k\neq N-p/\omega}}^{\infty} J_k(Y)\left[\frac{i}{k-N+p/\omega}\right][\exp(-i[k-N+p/\omega]2\pi)-1] + J_{N-p/\omega}(Y)$$

$$= J_{N-p/\omega}(Y) \qquad (A.4)$$

and

$$I_3 = \frac{1}{2\pi}\int_0^{2\pi} \xi^*\exp(-i\frac{p}{\omega}\delta)d\delta = J_{N+p/\omega}(Y) \qquad (A.5)$$

Using Eqs. (A.3)-(A.5), the phase-average of Δ is given by

$$\bar{\Delta} = \frac{1}{2\pi}\int_0^{2\pi} \Delta \, d\delta$$

$$= \frac{-1}{8p^2}[(p+\gamma-N\omega)J_{N+p/\omega}(Y) - (p-(\gamma-N\omega))J_{N-p/\omega}(Y)]^2\sin 2\theta \qquad (A.6)$$

Thus, see Eq. (3.1.32), the contribution of the integer p/ω terms to the phase- and long time-averaged transition probability $\bar{P}_2^N$ is

$$\Delta\bar{P}_2^N = \tfrac{1}{4}\sin 2\theta[\bar{\Delta} + \bar{\Delta}^*]$$

$$= \frac{-1}{8p^2}[(p+\gamma-N\omega)J_{N+p/\omega}(Y)-(p-(\gamma-N\omega))J_{N-p/\omega}(Y)]^2\sin^2 2\theta \qquad (A.7)$$

$\Delta\bar{P}_2^N$ was calculated for the examples discussed in Sec. 3.3.3. The results corresponding to Figure 3.7 are summarized in Table A.1 and it can be seen, for this example, that $\Delta\bar{P}_2^N$ is insignificant relative to $\bar{P}_2^N$ except for frequencies far off resonance where it can be as large as 11% of $\bar{P}_2^N$. However, at these frequencies the RWA expressions for the N photon resonance profile are no longer reliable. Thus the contributions of $\Delta\bar{P}_2^N$ are not included in the calculations of $\bar{P}_2^N$ in the main text of this thesis. For the other examples considered in Chapter 3

$\Delta\bar{P}_2^N$ is insignificant for all relevant values of ω.

Table A.1. Values of $\bar{P}_2^N$ and $\Delta\bar{P}_2^N$, given by Eqs. (3.2.47) and (A.7) respectively, for values of $\omega/\Delta E$ corresponding to integer p/ω and relevant to the spectra of Figure 3.7. The RWA resonance values for $\omega/\Delta E$, for N = 1, 2 and 3, are 1.557, 0.735 and 0.481, respectively (see Figure 3.7).

N	p/ω	$\omega/\Delta E$	$\bar{P}_2^N$	$\Delta\bar{P}_2^N$
1	1	0.763	0.1827	-0.003944
	2	0.485	0.1851	-0.004619
	3	0.356	0.2262	-0.002873
2	1	0.517	0.2671	-0.0001764
	1	1.403	0.2571	-0.02764
	2	0.375	0.1962	-0.002161
3	1	0.382	0.3109	-0.000002919
	1	0.702	0.2601	-0.01118
	2	1.413	0.2498	-0.02750

APPENDIX B

ALMOST DEGENERATE PERTURBATION THEORY

The almost degenerate perturbation theory used to derive perturbation solutions to the Floquet secular equation in Sec. 4.3 is that of [32,33] and is summarized here in a form suitable for this application. It is designed for use when a set of states of a quantum mechanical system interact strongly as the result of near degeneracies or of complete degeneracies. This treatment redutes to the usual Rayleigh-Schrodinger perturbation equations [13,14,112] in the limit of complete degeneracy [113]. The following discussion pertains to two almost degenerate energy states which is the problem of interest in Sec. 4.3. The energies are obtained through fourth order and the wave functions through second order from the perturbation theory. The results for all orders of perturbation theory can be obtained by applying general results and procedures in the literature [32].

To begin, consider the following Schrodinger wave equation

$$(H - E_\ell)\Psi_\ell = 0 \qquad \ell = 1,2 \qquad (B.1)$$

where H is the Hamiltonian, and E_ℓ and Ψ_ℓ are the energies and orthonormalized wave functions, respectively, of the two almost degenerate energy states ℓ. The Ψ_ℓ can be

written as a linear combination of another set of two orthonormal basis functions Φ_p such that

$$\Psi_\ell = \sum_{p=1}^{2} d_{p\ell}\Phi_p \qquad (B.2)$$

Using Eq. (B.2) in Eq. (B.1) and then multiplying by Φ_b^* and integrating over all coordinate space yields the following

$$\sum_{p=1}^{2} [\langle\Phi_b|H|\Phi_p\rangle - E_\ell\delta_{pb}]d_{p\ell} = 0 \quad , \quad b = 1,2 \qquad (B.3)$$

The Φ_p can be written as linear combinations of the Ψ_ℓ,

$$\Phi_p = \sum_{\ell=1}^{2} \Psi_\ell c_{\ell p} \quad , \quad p = 1,2 \qquad (B.4)$$

where the square matrix $\underline{\underline{d}}$ is the inverse matrix of $\underline{\underline{c}}$. The Φ_p satisfy

$$H\Phi_p = \sum_{r=1}^{2} \Phi_r E_{rp} \qquad (B.5)$$

Substitution of Eq. (B.5) into (B.3) yields

$$\sum_{p=1}^{2} [E_{bp} - E_\ell\delta_{pb}]d_{p\ell} = 0 \qquad (B.6)$$

The eigenvalues, E_ℓ, and the eigenfunctions, Ψ_ℓ, are obtained using standard techniques [4,82,114]. The eigenvalues are

$$E_\pm = \tfrac{1}{2}(E_{11}+E_{22}) \pm \rho \tag{B.7}$$

where

$$\rho = [\tfrac{1}{4}(E_{22}-E_{11})^2 + |E_{12}|^2]^{\frac{1}{2}} \tag{B.8}$$

The eigenfunctions are given by

$$\Psi_\pm = d_{1,\pm}\Phi_1 + d_{2,\pm}\Phi_2 \tag{B.9}$$

where

$$d_{1,-} = d_{2,+} = \left[\frac{\rho + \tfrac{1}{2}(E_{22}-E_{11})}{2\rho}\right]^{\frac{1}{2}} \tag{B.10}$$

$$d_{1,+} = \exp(i\delta_{1+})\left[\frac{\rho - \tfrac{1}{2}(E_{22}-E_{11})}{2\rho}\right]^{\frac{1}{2}};\ \exp(i\delta_{1+}) = \frac{|E_{12}|}{E_{12}^*} \tag{B.11}$$

and

$$d_{2,-} = \exp(i\delta_{2-})\left[\frac{\rho - \tfrac{1}{2}(E_{22}-E_{11})}{2\rho}\right]^{\frac{1}{2}};\ \exp(i\delta_{2-}) = \frac{-|E_{12}|}{E_{12}} \tag{B.12}$$

When ε_{12} is real the results given above are analogous to those used in Sec. 3.1.

In order to obtain the Φ_p and the E_{bp}, perturbation theory is applied to Eq. (B.5) by writing

$$H = H^{(0)} + \lambda V \quad , \tag{B.13}$$

where λ is a perturbation parameter, which can be set equal to one at the end of the derivation, and by expanding Φ_p and E_{bp} as follows

$$\Phi_p = \sum_{i=0}^{\infty} \lambda^i \Phi_p^{(i)} \tag{B.14}$$

and

$$E_{bp} = \sum_{s=0}^{\infty} \lambda^s E_{bp}^{(s)} \tag{B.15}$$

Here, and in what follows, the indices b and p are defined to take on the values 1 and 2 only. The unperturbed (self-adjoint) Hamiltonian has a complete set of known orthonormalized eigenfunctions which satisfy

$$H^{(0)}\Phi_q^{(0)} = E_q^{(0)}\Phi_q^{(0)}, \quad q = 1,2,\ldots,\infty \tag{B.16}$$

Substitution of Eqs. (B.13)-(B.15) into Eq. (B.5) yields

$$H^{(0)} \sum_{m=0}^{\infty} \lambda^m \Phi_p^{(m)} + V \sum_{m=0}^{\infty} \lambda^{m+1} \Phi_p^{(m)} = \sum_{b=1}^{2} \sum_{m=0}^{\infty} \sum_{i=0}^{m} \lambda^m \Phi_b^{(i)} E_{bp}^{(m-i)} \tag{B.17}$$

The perturbation equations for the various orders of wave functions and energies are obtained by equating the terms of order m on the right-hand side of Eq. (B.17) to those on the left-hand side.

Thus the zeroth order wave equation is

$$H^{(0)} \Phi_p^{(0)} = \sum_{j=1}^{2} E_{jp}^{(0)} \Phi_j^{(0)} \tag{B.18}$$

It follows from Eq. (B.16) that

$$E_{bp}^{(0)} = E_p^{(0)} \delta_{bp} \tag{B.19}$$

The first order wave equation is given by

$$H^{(0)} \Phi_p^{(1)} + V \Phi_p^{(0)} = \sum_{j=1}^{2} [\Phi_j^{(0)} E_{jp}^{(1)} + \Phi_j^{(1)} E_{jp}^{(0)}]$$

$$= \sum_{j=1}^{2} \Phi_j^{(0)} E_{jp}^{(1)} + E_p^{(0)} \Phi_p^{(1)} \tag{B.20}$$

Multiplying Eq. (B.20) by $\Phi_q^{(0)*}$, and integrating over all

space, yields

$$\langle\Phi_q^{(0)}|H^{(0)}|\Phi_p^{(1)}\rangle + \langle\Phi_q^{(0)}|V|\Phi_p^{(0)}\rangle = \sum_{j=1}^{2} \langle\Phi_q^{(0)}|\Phi_j^{(0)}\rangle E_{jp}^{(1)} + E_p^{(0)}\langle\Phi_q^{(0)}|\Phi_p^{(1)}\rangle \tag{B.21}$$

An expression for the first order energy is obtained by using

$$\langle\Phi_q^{(0)}|\Phi_j^{(0)}\rangle = \delta_{jq} \tag{B.22}$$

$$\langle\Phi_q^{(0)}|H^{(0)}|\Phi_p^{(1)}\rangle = \langle H^{(0)}\Phi_q^{(0)}|\Phi_p^{(1)}\rangle = E_q^{(0)}\langle\Phi_q^{(0)}|\Phi_p^{(1)}\rangle \tag{B.23}$$

and by defining

$$\langle\Phi_q^{(0)}|V|\Phi_p^{(0)}\rangle = V_{qp} \tag{B.24}$$

Using Eqs. (B.22)-(B.24) in Eq. (B.21) with q = 1 or 2 yields

$$E_{bp}^{(1)} = (E_b^{(0)} - E_p^{(0)})\langle\Phi_b^{(0)}|\Phi_p^{(1)}\rangle + V_{bp} \tag{B.25}$$

Similarly the second order wave equation is

$$H^{(0)}\Phi_p^{(2)} + V\Phi_p^{(1)} = \sum_{j=1}^{2} [\Phi_j^{(0)}E_{jp}^{(2)} + \Phi_j^{(1)}E_{jp}^{(1)}] + E_p^{(0)}\Phi_p^{(2)} \tag{B.26}$$

and manipulations analogous to those used to derive Eq. (B.25) yield the following expression for the second order energy

$$E_{bp}^{(2)} = (E_b^{(0)} - E_p^{(0)})\langle\Phi_b^{(0)}|\Phi_p^{(2)}\rangle + \langle\Phi_b^{(0)}|V|\Phi_p^{(1)}\rangle - \sum_{j=1}^{2} E_{jp}^{(1)}\langle\Phi_b^{(0)}|\Phi_j^{(1)}\rangle \tag{B.27}$$

Using the differential equation for the third order wave equation, it can be shown that the third order energy is

$$E_{bp}^{(3)} = (E_b^{(0)} - E_p^{(0)})\langle\Phi_b^{(0)}|\Phi_p^{(3)}\rangle + \langle\Phi_b^{(0)}|V|\Phi_p^{(2)}\rangle - \sum_{j=1}^{2} [E_{jp}^{(1)}\langle\Phi_b^{(0)}|\Phi_j^{(2)}\rangle + E_{jp}^{(2)}\langle\Phi_b^{(0)}|\Phi_j^{(1)}\rangle] \tag{B.28}$$

Eqs. (B.25), (B.27) and (B.28) can be further simplified by making use of full normalization [32,33] to complete the specification of the $\Phi_p^{(m)}$. This is done by requiring

$$\delta_{pb} = \langle\Phi_p|\Phi_b\rangle \tag{B.29}$$

One of the advantages of this type of normalization is that $\varepsilon_{pb} = \varepsilon_{bp}^{*}$ if H is hermitean [32]. Using Eq. (B.14) in Eq. (B.29) yields

$$\delta_{pb} = \sum_{m=0}^{\infty} \sum_{j=0}^{m} \lambda^{m} \langle \Phi_p^{(m-j)} | \Phi_b^{(j)} \rangle \qquad (B.30)$$

When m = 0,

$$\delta_{pb} = \langle \Phi_p^{(0)} | \Phi_b^{(0)} \rangle \qquad (B.31)$$

Therefore the coefficients of all the other powers of the perturbation parameter λ are equal to zero in Eq. (B.30) giving

$$\sum_{j=0}^{m} \langle \Phi_p^{(m-j)} | \Phi_b^{(j)} \rangle = 0 \qquad (B.32)$$

When m = 1, 2 and 3 respectively one obtains

$$0 = \langle \Phi_p^{(1)} | \Phi_b^{(0)} \rangle + \langle \Phi_p^{(0)} | \Phi_b^{(1)} \rangle \qquad (B.33)$$

$$0 = \langle \Phi_p^{(2)} | \Phi_b^{(0)} \rangle + \langle \Phi_p^{(1)} | \Phi_b^{(1)} \rangle + \langle \Phi_p^{(0)} | \Phi_b^{(2)} \rangle \qquad (B.34)$$

and

$$0 = \langle\Phi_p^{(3)}|\Phi_b^{(0)}\rangle + \langle\Phi_p^{(2)}|\Phi_b^{(1)}\rangle + \langle\Phi_p^{(1)}|\Phi_b^{(2)}\rangle + \langle\Phi_p^{(0)}|\Phi_b^{(3)}\rangle \tag{B.35}$$

The condition of Eq. (B.32) only determines the real part of $\langle\Phi_p^{(0)}|\Phi_b^{(m)}\rangle$ since

$$\langle\Phi_p^{(0)}|\Phi_b^{(m)}\rangle + \langle\Phi_p^{(m)}|\Phi_b^{(0)}\rangle = -\sum_{j=1}^{m-1}\langle\Phi_p^{(j)}|\Phi_b^{(m-j)}\rangle$$

$$= 2\mathrm{Re}(\langle\Phi_p^{(0)}|\Phi_b^{(m)}\rangle) \tag{B.36}$$

The imaginary part of $\langle\Phi_p^{(0)}|\Phi_b^{(m)}\rangle$ is fixed by the conditions [33]

$$\langle\Phi_p^{(0)}|\Phi_b^{(2m+1)}\rangle = -\sum_{j=1}^{m}\langle\Phi_p^{(j)}|\Phi_b^{(2m+1-j)}\rangle \tag{B.37}$$

and

$$\langle\Phi_p^{(0)}|\Phi_b^{(2m)}\rangle = -\tfrac{1}{2}\langle\Phi_p^{(m)}|\Phi_b^{(m)}\rangle - \sum_{j=1}^{m-1}\langle\Phi_p^{(j)}|\Phi_b^{(2m-j)}\rangle \tag{B.38}$$

which are consistent with Eq. (B.36). Using Eqs. (B.37) and (B.38) in Eqs. (B.33)-(B.35) yields the following

$$\langle\Phi_p^{(0)}|\Phi_b^{(1)}\rangle = 0 \tag{B.39}$$

$$\langle \Phi_p^{(0)} | \Phi_b^{(2)} \rangle = -\tfrac{1}{2} \langle \Phi_p^{(1)} | \Phi_b^{(1)} \rangle \qquad \text{(B.40)}$$

and

$$\langle \Phi_p^{(0)} | \Phi_b^{(3)} \rangle = -\langle \Phi_p^{(1)} | \Phi_b^{(2)} \rangle \qquad \text{(B.41)}$$

Eqs. (B.39)-(B.41) can be used to simplify Eqs. (B.25), (B.27) and (B.28) to obtain

$$E_{bp}^{(1)} = V_{bp} \qquad \text{(B.42)}$$

$$E_{bp}^{(2)} = -\tfrac{1}{2}(E_b^{(0)} - E_p^{(0)}) \langle \Phi_b^{(1)} | \Phi_p^{(1)} \rangle + \langle \Phi_b^{(0)} | V | \Phi_p^{(1)} \rangle \qquad \text{(B.43)}$$

and

$$E_{bp}^{(3)} = -(E_b^{(0)} - E_p^{(0)}) \langle \Phi_b^{(1)} | \Phi_p^{(2)} \rangle + \langle \Phi_b^{(0)} | V | \Phi_p^{(2)} \rangle + \tfrac{1}{2} \sum_{j=1}^{2} E_{jp}^{(1)} \langle \Phi_b^{(1)} | \Phi_j^{(1)} \rangle \qquad \text{(B.44)}$$

Explicit expressions for the first and second order wave functions are obtained by expanding in the complete set of zeroth order wave functions defined by Eq. (B.16)

$$\Phi_p^{(m)} = \sum_s c_{sp}^{(m)} \Phi_s^{(0)} \quad , \; m = 1,2,\ldots \qquad \text{(B.45)}$$

This result is the so-called spectral expansion of the m-th order wave functions and in what follows we will also derive spectral expansions for some of the perturbed energies, $E_{bp}^{(m)}$.

Using Eq. (B.45) with m = 1 in Eq. (B.20) gives

$$H^{(0)}\sum_s c_{sp}^{(1)}\Phi_s^{(0)} + V\Phi_p^{(0)} = \sum_{j=1}^{2} \Phi_j^{(0)}E_{jp}^{(1)} + E_p^{(0)}\sum_s c_{sp}^{(1)}\Phi_s^{(0)} \qquad (B.46)$$

Multiplying by $\Phi_q^{(0)*}$ and then integrating over all coordinate space gives

$$\sum_s c_{sp}^{(1)}\langle\Phi_q^{(0)}|H^{(0)}|\Phi_s^{(0)}\rangle + \langle\Phi_q^{(0)}|V|\Phi_p^{(0)}\rangle = \sum_{j=1}^{2} E_{jp}^{(1)}\langle\Phi_q^{(0)}|\Phi_j^{(0)}\rangle + E_p^{(0)}\sum_s c_{sp}^{(1)}\langle\Phi_q^{(0)}|\Phi_s^{(0)}\rangle \qquad (B.47)$$

Using manipulations similar to those used to obtain Eq. (B.25) yields

$$E_q^{(0)}c_{qp}^{(1)} + V_{qp} = \sum_{j=1}^{2} E_{jp}^{(1)}\delta_{jq} + E_p^{(0)}c_{qp}^{(1)} \qquad (B.48)$$

When q = p, Eq. (B.48) becomes

$$E_{pp}^{(1)} = V_{pp} \qquad (B.49)$$

which agrees with Eq. (B.42). When $q \neq p$ and $q < 2$, i.e. $q = b$,

$$c_{bp}^{(1)} = \frac{\varepsilon_{bp}^{(1)} - V_{bp}}{(E_b^{(0)} - E_p^{(0)})} = 0 \quad , \quad b \neq p \qquad (B.50)$$

which follows from Eq. (B.42). If $q \neq 1,2$ i.e. $q > 2$

$$c_{qp}^{(1)} = \frac{-V_{qp}}{(E_q^{(0)} - E_p^{(0)})} \qquad (B.51)$$

An expression for $c_{pp}^{(1)}$ is obtained by using Eq. (B.45), with $m = 1$, in the normalization condition given by Eq. (B.39) with $b = p$. Thus

$$\sum_s c_{sp}^{(1)} \langle \Phi_p^{(0)} | \Phi_s^{(0)} \rangle = 0 \qquad (B.52)$$

and since $\langle \Phi_p^{(0)} | \Phi_s^{(0)} \rangle = \delta_{sp}$

$$c_{pp}^{(1)} = 0 \qquad (B.53)$$

Using Eqs. (B.50), (B.51) and (B.53) in Eq. (B.45), with $m = 1$, yields

$$\Phi_p^{(1)} = -\sum_{s>2}^{\infty} \left[\frac{V_{sp}}{(E_s^{(0)} - E_p^{(0)})} \right] \Phi_s^{(0)} \qquad (B.54)$$

Similar manipulations of Eq. (B.45) in Eq. (B.26) for the second order wave function gives the following expression

$$-E_q^{(0)}c_{qp}^{(2)} + \langle\Phi_q^{(0)}|V|\Phi_p^{(1)}\rangle = \sum_{j=1}^{2}\left[E_{jp}^{(2)}\delta_{jq} + E_{jp}^{(1)}\langle\Phi_q^{(0)}|\Phi_j^{(1)}\rangle\right] + E_p^{(0)}c_{qp}^{(2)} \qquad (B.55)$$

When $q = p$, Eq. (B.55), with Eq. (B.39), yields

$$E_{pp}^{(2)} = \langle\Phi_p^{(0)}|V|\Phi_p^{(1)}\rangle \qquad (B.56)$$

which agrees with Eq. (B.43). When $q \neq p$ and $q < 2$ i.e. $q = b$,

$$(E_b^{(0)} - E_p^{(0)})c_{bp}^{(2)} = E_{bp}^{(2)} - \langle\Phi_b^{(0)}|V|\Phi_p^{(1)}\rangle \quad , \quad b \neq p \qquad (B.57)$$

Using the expression for $E_{bp}^{(2)}$ given by Eq. (B.43) yields

$$c_{bp}^{(2)} = -\tfrac{1}{2}\langle\Phi_b^{(1)}|\Phi_p^{(1)}\rangle$$

$$= -\tfrac{1}{2}\sum_{s>2}^{\infty}\left[\frac{V_{bs}V_{sp}}{(E_s^{(0)} - E_b^{(0)})(E_s^{(0)} - E_p^{(0)})}\right] \quad , \quad b \neq p \qquad (B.58)$$

When $q > 2$

$$c_{qp}^{(2)} = \frac{-\langle\Phi_q^{(0)}|V|\Phi_p^{(1)}\rangle}{(\varepsilon_q^{(0)} - \varepsilon_p^{(0)})} + \sum_{j=i}^{2} \left[\frac{\varepsilon_{jp}^{(1)}\langle\Phi_q^{(0)}|\Phi_j^{(1)}\rangle}{(\varepsilon_q^{(0)} - \varepsilon_p^{(0)})}\right]$$

$$= \sum_{s>2}^{\infty} \left[\frac{V_{qs}V_{sp}}{(E_q^{(0)} - E_p^{(0)})(E_s^{(0)} - E_p^{(0)})}\right]$$

$$- \sum_{j=1}^{2} \left[\frac{V_{qj}V_{jp}}{(\varepsilon_q^{(0)} - \varepsilon_j^{(0)})(\varepsilon_q^{(0)} - \varepsilon_p^{(0)})}\right] \quad (B.59)$$

Using Eq. (B.45) with m = 2 in Eq. (B.40) with b = p yields the following expression

$$\sum_s c_{sp}^{(2)}\langle\Phi_p^{(0)}|\Phi_s^{(0)}\rangle = -\tfrac{1}{2}\langle\Phi_p^{(1)}|\Phi_p^{(1)}\rangle \quad (B.60)$$

which gives

$$c_{pp}^{(2)} = -\tfrac{1}{2}\langle\Phi_p^{(1)}|\Phi_p^{(1)}\rangle \quad (B.61)$$

Using Eqs. (B.58)) (B.59) and (B.61) in Eq. (B.45), with m = 2, yields

$$\Phi_p^{(2)} = -\tfrac{1}{2}\sum_{r=1}^{2}\sum_{s>2}^{\infty}\left[\frac{V_{rs}V_{sp}}{(\varepsilon_s^{(0)} - \varepsilon_r^{(0)})(\varepsilon_s^{(0)} - \varepsilon_p^{(0)})}\right]\Phi_r^{(0)}$$

$$+ \sum_{r>2}^{\infty} \left[\sum_{s>2}^{\infty} \left[\frac{V_{rs}V_{sp}}{(E_r^{(0)} - E_p^{(0)})(E_s^{(0)} - E_p^{(0)})} \right] \right.$$

$$\left. - \sum_{j=1}^{2} \left[\frac{V_{rj}V_{jp}}{(E_r^{(0)} - E_j^{(0)})(E_r^{(0)} - E_p^{(0)})} \right] \right] \Phi_r^{(0)}$$

(B.62)

Substituting Eqs. (B.54) and (B.62) into Eqs. (B.43) and (B.44) gives the spectral expansions for the second and third order energies;

$$E_{bp}^{(2)} = -\tfrac{1}{2}(E_b^{(0)} - E_p^{(0)}) \sum_{s>2}^{\infty} \left[\frac{V_{bs}V_{sp}}{(E_s^{(0)} - E_b^{(0)})(E_s^{(0)} - E_p^{(0)})} \right]$$

$$- \sum_{s>2}^{\infty} \left[\frac{V_{bs}V_{sp}}{(E_s^{(0)} - E_p^{(0)})} \right] \qquad \text{(B.63)}$$

and

$$E_{bp}^{(3)} = (E_b^{(0)} - E_p^{(0)}) \sum_{\ell>2}^{\infty} \sum_{s>2}^{\infty} \left[\frac{V_{bs}V_{s\ell}V_{\ell p}}{(E_s^{(0)} - E_b^{(0)})(E_s^{(0)} - E_p^{(0)})(E_\ell^{(0)} - E_p^{(0)})} \right]$$

$$- (E_b^{(0)} - E_p^{(0)}) \sum_{s>2}^{\infty} \sum_{j=1}^{2} \left[\frac{V_{bs}V_{sj}V_{jp}}{(E_s^{(0)} - E_b^{(0)})(E_s^{(0)} - E_j^{(0)})(E_s^{(0)} - E_p^{(0)})} \right]$$

$$- \tfrac{1}{2} \sum_{r=1}^{2} \sum_{s>2}^{\infty} \left[\frac{V_{br}V_{rs}V_{sp}}{(E_s^{(0)} - E_r^{(0)})(E_s^{(0)} - E_p^{(0)})} \right]$$

$$+\tfrac{1}{2}\sum_{j=1}^{2}\sum_{s>2}^{\infty}\left[\frac{V_{bs}V_{sj}V_{jp}}{(E_s^{(0)}-E_b^{(0)})(E_s^{(0)}-E_j^{(0)})}\right]$$

$$+\sum_{r>2}^{\infty}\left[\sum_{s>2}^{\infty}\left[\frac{V_{br}V_{rs}V_{sp}}{(E_r^{(0)}-E_p^{(0)})(E_s^{(0)}-E_p^{(0)})}\right]\right.$$

$$\left.-\sum_{j=1}^{2}\left[\frac{V_{br}V_{rj}V_{jp}}{(E_r^{(0)}-E_j^{(0)})(E_r^{(0)}-E_p^{(0)})}\right]\right] \qquad \text{(B.64)}$$

Also required for part of the analysis of Sec. 4.3 of the main text, is the spectral expansion for the fourth order energy $E_{pp}^{(4)}$. This can be obtained in an analogous fashion to the derivation of Eqs. (B.63) and (B.64) following the work of Hirschfelder [32]. It can be shown that

$$E_{pp}^{(4)} = \langle\Phi_p^{(0)}|V|\Phi_p^{(3)}\rangle - \sum_{\ell=1}^{2} E_{\ell p}^{(3)}\langle\Phi_p^{(0)}|\Phi_\ell^{(1)}\rangle$$

$$-\sum_{\ell=1}^{2} E_{\ell p}^{(2)}\langle\Phi_p^{(0)}|\Phi_\ell^{(2)}\rangle + \sum_{\ell=1}^{2} E_{\ell p}^{(1)}\langle\Phi_p^{(1)}|\Phi_\ell^{(2)}\rangle \qquad \text{(B.65)}$$

where from [32]

$$\Phi_k^{(3)} = \sum_{p>2}^{\infty}\left[\frac{\langle\Phi_p^{(0)}|V|\Phi_k^{(2)}\rangle\Phi_p^{(0)}}{(E_k^{(0)}-E_p^{(0)})}\right] - \sum_{\ell=1}^{2}\langle\Phi_\ell^{(1)}|\Phi_k^{(2)}\rangle\Phi_\ell^{(0)},$$

$$- \sum_{p>2}^{\infty} \sum_{\ell=1}^{2} \left[\frac{E_{\ell k}^{(2)} \langle \Phi_p^{(0)} | \Phi_\ell^{(1)} \rangle \Phi_p^{(0)} + E_{\ell k}^{(1)} \langle \Phi_p^{(0)} | \Phi_\ell^{(2)} \rangle \Phi_p^{(0)}}{(E_k^{(0)} - E_p^{(0)})} \right] \tag{B.66}$$

Substitution of Eq. (B.66) into (B.65), followed by substitution of the spectral expansions for the perturbed wave functions into the resulting expression, yields

$$E_{pp}^{(4)} = -\frac{1}{2} \sum_{\ell>2}^{\infty} \sum_{s>2}^{\infty} \sum_{r=1}^{2} \left[\frac{V_{\ell r} V_{rs} V_{sp} V_{p\ell}}{(E_p^{(0)} - E_\ell^{(0)})(E_s^{(0)} - E_r^{(0)})(E_s^{(0)} - E_p^{(0)})} \right]$$

$$+ \sum_{\ell>2}^{\infty} \sum_{r>2}^{\infty} \sum_{s>2}^{\infty} \left[\frac{V_{\ell r} V_{rs} V_{sp} V_{p\ell}}{(E_p^{(0)} - E_\ell^{(0)})(E_r^{(0)} - E_p^{(0)})(E_s^{(0)} - E_p^{(0)})} \right]$$

$$- \sum_{\ell>2}^{\infty} \sum_{r>2}^{\infty} \sum_{s=1}^{2} \left[\frac{V_{\ell r} V_{rs} V_{sp} V_{p\ell}}{(E_p^{(0)} - E_\ell^{(0)})(E_r^{(0)} - E_s^{(0)})(E_r^{(0)} - E_p^{(0)})} \right]$$

$$+ \sum_{\ell>2}^{\infty} \sum_{s=1}^{2} \left[\frac{E_{sp}^{(2)} V_{\ell s} V_{p\ell}}{(E_p^{(0)} - E_\ell^{(0)})(E_\ell^{(0)} - E_s^{(0)})} \right]$$

$$- \sum_{\ell>2}^{\infty} \sum_{r>2}^{\infty} \sum_{s=1}^{2} \left[\frac{E_{sp}^{(1)} V_{\ell r} V_{rs} V_{p\ell}}{(E_p^{(0)} - E_\ell^{(0)})(E_\ell^{(0)} - E_s^{(0)})(E_r^{(0)} - E_s^{(0)})} \right]$$

$$+ \sum_{\ell>2}^{\infty} \sum_{r=1}^{2} \sum_{s=1}^{2} \left[\frac{E_{rp}^{(1)} V_{\ell s} V_{sr} V_{p\ell}}{(E_p^{(0)} - E_\ell^{(0)})(E_\ell^{(0)} - E_s^{(0)})(E_\ell^{(0)} - E_r^{(0)})} \right]$$

$$+ \sum_{\ell>2}^{\infty} \sum_{s>2}^{\infty} \sum_{r=1}^{2} \left[\frac{V_{r\ell} V_{\ell s} V_{sp} V_{pr}}{(E_\ell^{(0)} - E_r^{(0)})(E_\ell^{(0)} - E_p^{(0)})(E_s^{(0)} - E_p^{(0)})} \right]$$

$$- \sum_{\ell>2}^{\infty} \sum_{r=1}^{2} \sum_{s=1}^{2} \left[\frac{V_{r\ell} V_{\ell s} V_{sp} V_{pr}}{(E_\ell^{(0)} - E_r^{(0)})(E_\ell^{(0)} - E_s^{(0)})(E_\ell^{(0)} - E_p^{(0)})} \right]$$

$$+ \frac{1}{2} \sum_{s>2}^{\infty} \sum_{\ell=1}^{2} \left[\frac{E_{\ell p}^{(2)} V_{\ell s} V_{s\ell}}{(E_s^{(0)} - E_\ell^{(0)})(E_s^{(0)} - E_\ell^{(0)})} \right]$$

$$- \sum_{r>2}^{\infty} \sum_{s>2}^{\infty} \sum_{\ell=1}^{2} \left[\frac{E_{\ell p}^{(1)} V_{pr} V_{rs} V_{s\ell}}{(E_r^{(0)} - E_\ell^{(0)})(E_s^{(0)} - E_\ell^{(0)})(E_r^{(0)} - E_p^{(0)})} \right]$$

$$+ \sum_{r>2}^{\infty} \sum_{\ell=1}^{2} \left[\frac{E_{\ell p}^{(1)} V_{pr} V_{rp} V_{p\ell}}{(E_r^{(0)} - E_p^{(0)})(E_r^{(0)} - E_\ell^{(0)})(E_r^{(0)} - E_p^{(0)})} \right] \tag{B.67}$$

Perturbative expressions for $\Psi_\pm$ can be obtained from Eq. (B.9) by making use of the expansions for the Φ_p, given in Eq. (B.14), with $\lambda=1$. Keeping terms explicitly through second order yields

$$\Psi_\pm = \sum_{p=1}^{2} d_{p\pm} [\Phi_p^{(0)} + \Phi_p^{(1)} + \Phi_p^{(2)} + O(3)] \tag{B.68}$$

where $O(3)$ represents third or higher order terms in Φ_p. Eq. (B.68) can also be written in terms of the complete set of eigenfunctions of $H^{(0)}$ to obtain

$$\Psi_{\pm} = \sum_{\nu=1}^{\infty} C_{\nu,\pm} \Phi_{\nu}^{(0)} \qquad (B.69)$$

where

$$C_{\nu,\pm} = \sum_{m=0}^{\infty} C_{\nu,\pm}^{(m)} \qquad (B.70)$$

and $C_{q,\pm}^{(m)}$ is the m-th order contribution to $C_{q,\pm}$. Expressions for the $C_{q,\pm}^{(m)}$, through second order, are obtained by substituting the expressions for $\Phi_p^{(1)}$ and $\Phi_p^{(2)}$, given by Eqs. (B.54) and (B.62), into Eq. (B.68) and then comparing the result with Eq. (B.69):

$$C_{1,\pm}^{(0)} = d_{1,\pm} \; ; \; C_{2,\pm}^{(0)} = d_{2,\pm} \qquad (B.71)$$

$$C_{1,\pm}^{(1)} = 0 \quad ; \; C_{2,\pm}^{(1)} = 0 \qquad (B.72)$$

$$C_{r,\pm}^{(1)} = \sum_{p=1}^{2} d_{p,\pm} \left[\frac{-V_{rp}}{(E_r^{(0)} - E_p^{(0)})} \right] \; , \; r = 1,2 \qquad (B.73)$$

$$C_{1,\pm}^{(2)} = d_{1,\pm} \left[-\tfrac{1}{2} \sum_{s>2}^{\infty} \left[\frac{V_{1s}V_{s1}}{(E_s^{(0)} - E_1^{(0)})^2} \right] \right]$$

$$+ d_{2,\pm} \left[-\tfrac{1}{2} \sum_{s>2}^{\infty} \left[\frac{V_{1s}V_{s2}}{(E_s^{(0)} - E_1^{(0)})(E_s^{(0)} - E_2^{(0)})} \right] \right] \qquad (B.74)$$

$$c_{2,\pm}^{(2)} = d_{1,\pm}\left[-\tfrac{1}{2}\sum_{s>2}^{\infty}\left[\frac{V_{2s}V_{s1}}{(E_s^{(0)}-E_2^{(0)})(E_s^{(0)}-E_1^{(0)})}\right]\right] + d_{2,\pm}\left[-\tfrac{1}{2}\sum_{s>2}^{\infty}\left[\frac{V_{2s}V_{s2}}{(E_s^{(0)}-E_2^{(0)})^2}\right]\right] \tag{B.75}$$

$$c_{r,\pm}^{(2)} = \sum_{p=1}^{2} d_{p,\pm}\left[\sum_{s>2}^{\infty}\left[\frac{V_{rs}V_{sp}}{(E_r^{(0)}-E_p^{(0)})(E_s^{(0)}-E_p^{(0)})}\right] - \sum_{j=1}^{2}\left[\frac{V_{rj}V_{jp}}{(E_r^{(0)}-E_j^{(0)})(E_r^{(0)}-E_p^{(0)})}\right]\right], \quad r=1,2 \tag{B.76}$$

The coefficients $d_{p,\pm}$ are given by Eqs. (B.10)-(B.12) and the required energies E_{bp} are given by the perturbation expansion of Eq. (B.15) where explicit results for the energies through third order are given by Eqs. (B.42), (B.63) and (B.64). In obtaining Eqs. (B.71)-(B.76), the $d_{p,\pm}$ are taken to be of "zeroth-order" overall.

The perturbative solutions given above are used in Sec. 4.3 to help solve the Floquet secular equation perturbatively. The relationship between the Floquet secular equation, which is a special case of the general secular equation with near degenerate energy roots, and the perturbation treatment of two almost degenerate states follows.

The Schrodinger wave equation is

$$H\Psi_L = E_L\Psi_L \quad , \quad L = 1,2,\ldots,\infty \tag{B.77}$$

where the Ψ_L are the eigenfunctions of H with energies E_L. The wave functions can be expanded using the complete set of eigenfunctions of $H^{(0)}$ such that

$$\Psi_L = \sum_{s=1}^{\infty} c_{sL}\Phi_s^{(0)} \tag{B.78}$$

Using Eq. (B.78) in Eq. (B.77) yields

$$\sum_{s=1}^{\infty} [H\Phi_s^{(0)} - E_L\Phi_s^{(0)}]c_{sL} = 0 \tag{B.79}$$

Multiplying by $\Phi_r^{(0)*}$ and integrating over all space gives the following system of equations

$$\sum_{s=1}^{\infty} [H_{rs} - E_L\delta_{sr}]c_{sL} = 0 \quad , \quad L = 1,2,\ldots,\infty \tag{B.80}$$

where

$$H_{rs} = \langle\Phi_r^{(0)}|H|\Phi_s^{(0)}\rangle \tag{B.81}$$

Perturbation expansions of Eq. (B.80) can be used to obtain the Ψ_L and E_L [31,112,115-117]. If two of the energy roots, E_1 and E_2 say, are almost degenerate when $V = H-H^{(0)}$ is small, the perturbation theory derived in this Appendix can be applied to obtain results for Ψ_1 and Ψ_2 and their eigenvalues. The corresponding 2 x 2 near degenerate portion of the secular equation arising from Eq. (B.80) is identifiable with the states (1,2) or (-,+) of this Appendix.

APPENDIX C

"μ–$\underline{d}$" FLOQUET SECULAR EQUATION

A very different type of Floquet secular equation is obtained if the transformations leading to the "Bessel function solution" (see Sec. 3.2) are not used. In what follows, the Floquet secular equation obtained by following Shirley [23], with $\underline{d}$'s included, will be derived in order to illustrate the drawbacks inherent in it for $\underline{d} \neq 0$ problems. This Floquet approach is that used by Hattori and Kobayashi [34], see the discussion of Sec. 4.4.2.

To begin, the Hamiltonian given by Eq. (3.1.8) with $\varepsilon_s = 0$ is

$$\underline{\underline{H}}(t) = \tfrac{1}{2}(\Delta E - \underline{d}\cdot\underline{E}(t))\begin{bmatrix} 1 & 0 \\ 0 & 1 \end{bmatrix} - \mu_{12}\cdot\underline{E}(t)\begin{bmatrix} 0 & 1 \\ 1 & 0 \end{bmatrix} \tag{C.1}$$

and the relevant differential equation is

$$i\frac{d}{dt}\underline{\underline{c}}(t) = \underline{\underline{H}}(t)\underline{\underline{c}}(t) \tag{C.2}$$

This differential equation is transformed into a phase factored form [31], see also Sec. 4.2, by using

$$c_{(1,2)}(t) = K_{(1,2)}(t)\exp(\pm\tfrac{1}{2}i\Omega t) \tag{C.3}$$

where N = 1,2,3,.... Substituting Eq. (C.3) into Eq. (C.2) yields

$$i\frac{d}{dt}\underline{\underline{K}}(t) = \underline{\underline{H}}(t)\underline{\underline{K}}(t) \tag{C.4}$$

where

$$H_{11}(t) = -H_{22}(t) = -\Delta+\tfrac{1}{2}\underline{d}\cdot\underline{E}(t) \tag{C.5}$$

where $\Delta = \frac{1}{2}(\Delta E-N\omega)$ and

$$H_{12}(t) = (H_{21}(t))^* = -\underline{\mu}_{12}\cdot\underline{E}(t)\exp(-iN\omega t) \tag{C.6}$$

$\underline{E}(t)$ is given by Eq. (2.2.1) and can be written as

$$\underline{E}(t) = \tfrac{1}{2}\hat{e}\varepsilon[\exp(i[\omega t+\delta]) + \exp(-i[\omega t+\delta])] \tag{C.7}$$

Substituting Eq. (C.7) into Eqs. (C.5) and (C.6) yields

$$H_{11}(t) = -H_{22}(t) = -\Delta + \tfrac{1}{2}\underline{d}\cdot\hat{e}\varepsilon[\exp(i\omega t)\exp(i\delta) + \exp(-i\omega t)\exp(-i\delta)] \tag{C.8}$$

and

$$H_{12}(t) = (H_{21}(t))^* = -\tfrac{1}{2}\mu_{12}\cdot\hat{e}\varepsilon[\exp(-i[N-1]\omega t)\exp(i\delta) + \exp(-i[N+1]\omega t)\exp(-i\delta)] \tag{C.9}$$

The Fourier coefficients, $H_{\alpha\gamma}^{(n-k)}$, occurring in Eq. (4.2.17) are easily identified by comparing Eqs. (C.8) and (C.9) with Eq. (4.2.12) and are given by

$$H_{11}^{(0)} = -H_{22}^{(0)} = -\Delta = -\tfrac{1}{2}(\Delta E - N\omega) \tag{C.10}$$

$$H_{11}^{(1)} = -H_{22}^{(1)} = \tfrac{1}{2}d\cdot\hat{e}\varepsilon\exp(i\delta) \tag{C.11}$$

$$H_{11}^{(-1)} = -H_{22}^{(-1)} = \tfrac{1}{2}d\cdot\hat{e}\varepsilon\exp(-i\delta) \tag{C.12}$$

$$H_{11}^{(m)} = -H_{22}^{(m)} = 0\ ,\ m = n-k \neq 0,\pm 1 \tag{C.13}$$

and

$$H_{12}^{-(N+1)} = (H_{21}^{(N+1)})^* = -\tfrac{1}{2}\mu_{12}\cdot\hat{e}\varepsilon\exp(i\delta) \tag{C.14}$$

$$H_{12}^{-(N-1)} = (H_{21}^{(N-1)})^* = -\tfrac{1}{2}\mu_{12}\cdot\hat{e}\varepsilon\exp(i\delta) \tag{C.15}$$

$$H_{12}^{(-m)} = (H_{21}^{(m)})^* = 0\ ,\ m \neq N\pm 1 \tag{C.16}$$

As an example consider the one-photon transition with N = 1. Using Eqs. (C.10)-(C.16) in Eq. (4.2.17) yields the secular equation for the one-photon resonance, see Figure C.1. When $\Delta E \approx \omega$, the states 0,1 and 0,2 are almost degenerate. An RWA solution can be obtained by solving the 2 × 2 secular equation defined by these states. Thus, one obtains

$$\bar{P}_2 = \frac{|\underline{\mu}_{12}\cdot\hat{\epsilon}|^2}{2[(\Delta E-\omega)^2 + |\underline{\mu}_{12}\cdot\hat{\epsilon}|^2]} \qquad (C.17)$$

which is the usual RWA, see Sec. 3.3.1, and does not contain the effect of the $\underline{d}$. When N > 1, the off-diagonal elements in the 2 × 2 secular equation are zero (see Eq. (C.13)) and hence the RWA solutions are zero. Since the effect of $\underline{d}$ can be obtained only by applying perturbation theory to Figure C.1 to determine higher order corrections to the RWA, Floquet secular equations in the form given by Figure C.1 were not used in the main text of this thesis.

Figure C.1. A portion of the Floquet secular equation, for N = 1 only, given by Eq. (4.2.17) with the $H_{\alpha\gamma}^{(n-k)}$ defined by Eqs. (C.10)-(C.16). Here $C = -\frac{1}{2}\mu_{12}\cdot\hat{\epsilon}\mathcal{E}\exp(i\delta)$ and $D = \frac{1}{2}\underline{d}\cdot\hat{\epsilon}\mathcal{E}\exp(i\delta)$, $\Delta = \frac{1}{2}(\Delta E - N\omega)$ and the q's are the eigenvalues obtained by solving the secular equation.

n,α \ k,γ	-2,2	-1,1	-1,2	0,1	0,2	1,1	1,2	2,1
-2,2	$\Delta-2\omega-q$	0	$-D^*$	0	0	0	0	0
-1,1	0	$-\Delta-\omega-q$	C	D^*	0	0	C^*	0
1,2	-D	C^*	$\Delta-\omega-q$	0	$-D^*$	0	0	0
0,1	0	D	0	$-\Delta-q$	C	D^*	0	0
0,2	0	0	-D	C^*	$\Delta-q$	0	$-D^*$	0
1,1	0	0	0	D	0	$-\Delta+\omega-q$	C	D^*
1,2	0	C	0	0	-D	C^*	$\Delta+\omega-q$	0
2,1	0	0	0	0	0	D	0	$-\Delta+2\omega-q$

$= 0$

REFERENCES

1. Pantell, R. H., and Puthoff, H. E., 1969, "Fundamentals of Quantum Electronics" (Wiley), Chapter 5.

2. Dick, B., and Hohlneicher, G., 1982, J. Chem. Phys., 76, 5755.

3. Meath, W. J., and Power, E. A., 1984, J. Phys. B, 17, 763.

4. Meath, W. J., and Power, E. A., 1984, Molec. Phys., 51, 585.

5. Thomas, G. F., and Meath, W. J., 1982, Molec. Phys., 46, 743.

6. Ho, T-S., and Chu, S-I., 1983, J. Chem. Phys., 79, 4708.

7. Leasure, S., Milfeld, K. F., and Wyatt, R. E., 1981, J. Chem. Phys., 74, 6197.

8. Chu, S-I., Tietz, J. V., and Datta, K. K., 1982, J. Chem. Phys., 77, 2968.

9. Dion, D. R., and Hirschfelder, J. O., 1976, Adv. Chem. Phys., 35, 265.

10. Chu, S-I., 1985, Adv. At. Molec. Phys., 21, 197.

11. Thomas, G. F., and Meath, W. J., 1983, J. Phys. B, 16, 951.

12. Dirac, P.A.M., 1927, Proc. Roy. Soc., A114, 243 and 710.

13. Langhoff, P. W., Epstein, S. T., and Karplus, M., 1972, Rev. Mod. Phys., 44, 602.

14. Schiff, L. I., 1955, "Quantum Mechanics" (McGraw Hill), Chapter 3.

15. Messiah, A., 1962, "Quantum Mechanics", Vol. 2 (North Holland), Chapter 17.

16. Dalgarno, A., 1966, "Perturbation Theory and Its Application in Quantum Mechanics" (Wiley), p.145.

17. Sargent III, M., Scully, M.O., and Lamb, Jr., W. E., 1974, "Laser Physics" (Addison-Wesley), Chapter 2.

18. Rabi, I. I., 1937, Phys. Rev., 51, 652.

19. Allen, L., and Eberly, J. H., 1975, "Optical Resonance and Two-Level Atoms" (Wiley), Chapter 2.

20. Macomber, J. D., 1976, "The Dynamics of Spectroscopic Transitions" (Wiley), Chapter 6.

21. Goppert-Mayer, M., 1949, Ann. Phys., 9, 273.

22. Bloch, F., and Siegert, A., 1940, Phys. Rev., 57, 522.

23. Shirley, J. H., 1965, Phys. Rev., 138, B979.

24. Dollard, J. D., and Friedman, C. N., 1977, J. Math. Phys., 18, 1598, and 1978, J. Funct. Anal., 28, 309.

25. Walker, R. B., and Preston, R. K., 1977, J. Chem. Phys., 67, 2017; Dougherty, Jr., E. P., Augustin, S. D., and Rabitz, H., 1981, J. Chem. Phys., 74, 1175.

26. Plaat, O., 1971, "Ordinary Differential Equations" (Holden-Day); Erugin, N. P., 1966, "Linear Systems of Ordinary Differential Equations" (Academic Press).

27. Moloney, J. V., and Meath, W. J., 1975, Molec. Phys., 30, 171.

28. Moloney, J. V., and Meath, W. J., 1976, Molec. Phys., 31, 1537.

29. Salzman, W. R., 1974, Phys. Rev. A, 10, 461 and 1977, Phys. Rev. A, 16, 1552.

30. Burrows, M. D., and Salzman, W. R., 1977, Phys. Rev. A, 15, 1636.

31. Shirley, J. H., 1963, Ph.D. Thesis, California Institute of Technology.

32. Hirschfelder, J. O., 1978, Chem. Phys. Lett., 54, 1.

33. Certain, P. R., and Hirschfelder, J. O., 1970, J. Chem. Phys., 52, 5977.

34. Hattori, T., and Kobayashi, T., 1987, Phys. Rev. A, 35, 2733.

35. Terauchi, M., and Kobayashi, T., 1987, Chem. Phys. Lett., 137, 319.

36. Bethe, H. A., and Salpeter, E. E., 1957, "Quantum Mechanics of One- and Two-Electron Atoms" (Academic Press), p.3.

37. Cohen, E. R., and Taylor, B. N., 1973, J. Phys. Chem. Ref. Data, 2, 663.

38. Cohen-Tannoudji, C., Diu, B., and Laloe, F., 1977, "Quantum Mechanics", Vol. 1 (Wiley), p.237.

39. Weisskopf, V., and Wigner, E., 1930, Z. Physik, 63, 54; an English translation of this article appears in Hindmarsh, W. R., 1967, "Atomic Spectra" (Pergamon Press), pp.304-327.

40. Quack, M., 1978, J. Chem. Phys., 69, 1282.

41. Shore, B. W., 1979, Am. J. Phys., 47, 262.

42. Stenholm, S., 1972, J. Phys. B, 5, 878.

43. Pauling, L., and Wilson, Jr., E. B., 1935, "Introduction to Quantum Mechanics With Applications to Chemistry" (McGraw-Hill); Hecht, E., and Zajac, A., 1979, "Optics" (Addison-Wesley).

44. Brooks, Jr., G. L., and Scarfone, L. M., 1969, Phys. Rev., 185, 82.

45. Wong, J., Garrison, J. C., and Einwohner, T. H., 1976, Phys. Rev. A, 13, 674.

46. Pantell, R. H., and Puthoff, H. E., 1969, "Fundamentals of Quantum Electronics" (Wiley), pp.135-143.

47. Gold, A., 1969, "Quantum Optics", edited by R. J. Glauber (Academic Press), p.397 ff.

48. Grynberg, G., Cagnac, B., and Biraben, F., 1980, "Topics in Current Physics: Coherent Nonlinear Optics", edited by M. S. Feld and V. S. Letokhov (Springer-Verlag); Schulz, P. A., Sudbø, S. Aa., Krajnovich, D. J., Kwok, H. S., Shen, Y. R., and Lee, Y. T., 1979, Ann. Rev. Phys. Chem., 30, 379.

49. Lin, S. H., Fujimura, Y., Neusser, H. J., and Schlag, E. W., 1984, "Multiphoton Spectroscopy of Molecules" (Academic Press).

50. Freed, K., 1965, J. Chem. Phys., 43, 1113.

51. Javan, A., 1957, Phys. Rev., 107, 1579.

52. Roberts, D. E., and Fortson, E. N., 1973, Phys. Rev. Lett., 31, 1539.

53. Cohen-Tannoudji, C., Dupont-Roc, J., and Fabre, C., 1973, J. Phys. B, 6, L214 and L218.

54. Stenholm, S., 1973, J. Phys. B, 6, L240.

55. Hannaford, P., Pegg, D. T., and Series, G. W., 1973, J. Phys. B, 6, L222.

56. Ahmad, F., and Bullough, R. K., 1974, J. Phys. B., 7, L147.

57. Thomas, G. F., 1983, J. Chem. Phys., 79, 4912.

58. Hirschfelder, J. O., and Pyzalski, R. W., 1985, Phys. Rev. Lett., 55, 1244.

59. Moloney, J. V., and Meath, W. J., 1978, Molec. Phys., 35, 1163.

60. Pilar, F. L., 1968, "Elementary Quantum Chemistry" (McGraw-Hill), Chapter 9.

61. Roman, P., 1965, "Advanced Quantum Theory" (Addison-Wesley); Weissbluth, M., 1978, "Atoms and Molecules" (Academic Press), Chapter 9.

62. Taylor, A. E., 1955, "Advanced Calculus" (Blaisdell), pp. 51-53; Thomas, Jr., G. B., and Finney, R. L., 1981, "Calculus and Analytic Geometry" (Addison-Wesley), pp. 155-159.

63. Volterra, V., and Hostinsky, B., 1938, "Operations Infinitesimales Lineaires" (Gauthier-Villars).

64. Margenau, H., and Murphy, G. M., 1956, "The Mathematics of Physics and Chemistry", second edition (Van Nostrand), Chapter 3.

65. Autler, S. H., and Townes, C. H., 1955, Phys. Rev., 100, 703.

66. Moloney, J. V., and Meath, W. J., 1978, Phys. Rev. A, 17, 1550.

67. Bennett, W. R., 1973, "Atomic Physics and Astrophysics", Vol. 2, edited by M. Chrétien and E. Lipworth (Gordon and Breach), p.120 ff.

68. Pegg, D. T., 1973, J. Phys. B, 6, 246.

69. Oliver, G., 1971, Nuovo. Cim. Lett., 2, 1075 and 1975, Phys. Rev. A, 15, 2424.

70. Loudon, R., 1983, "The Quantum Theory of Light", second edition (Clarendon Press), pp, 90-100.

71. Hornbeck, R. W., 1975, "Numerical Methods" (Prentice-Hall), Chapter 8.

72. The computational techniques used have been established over a number of years [11,28,59,73,74]. The quoted accuracy in the results of this thesis have been verified by increasing the number of subdivisions used in the Riemann product integral method and the number of quadrature points used in calculating the averages.

73. Thuraisingham, R. A., and Meath, W. J., 1985, Molec. Phys., 56, 193.

74. Kmetic, M.A., Thuraisingham, R. A., and Meath, W. J., 1986, Phys. Rev. A, 33, 1688.

75. "Eigenvalue System Package (EISPACK)", 1972, Edition 2 (Argonne National Laboratory).

76. Atkins, P. W., 1970, "Molecular Quantum Mechanics: An Introduction to Quantum Chemistry" (Clarendon Press).

77. Watson, G. N., 1958, "Theory of Bessel Functions", second edition (Cambridge University Press), p. 22.

78. Watson, G. N., 1958, "Theory of Bessel Functions", second edition (Cambridge University Press), Chapter 3.

79. Carrier, G. F., and Pearson, C. E., 1968, "Ordinary Differential Equations" (Blaisdell).

80. Bonch-Bruevich, A. M., and Khodovoi, V. A., 1967, Sov. Phys.-Usp., 10, 637.

81. Gush, R., and Gush, H. P., 1972, Phys. Rev. A, 6, 129.

82. Aravind, P. K., and Hirschfelder, J. O., 1984, J. Phys. Chem., 88, 4788.

83. Kmetic, M. A., and Meath, W. J., 1985, Phys. Lett., 108A, 340.

84. Thomas, G. F., 1986, Phys. Rev. A, 33, 1033.

85. Yamaoka, K., and Charney, E., 1972, J. Am. Chem. Soc., 94, 8693; Liptay, W., and Czekalla, J., 1961, Z. Elektrochem., 65, 721.

86. Moloney, J. V., and Meath, W. J., 1978, J. Phys. B, 11, 2641.

87. Liptay, W., 1974, "Excited States", Vol. 1, edited by E. C. Lim (Academic Press), p.198.

88. Gaponov, A. V., Demkov, Y. N., Protopopova, N. G., and Fain, V. M., 1965, Opt. Spectros., 19, 279.

89. Rahman, N. K., 1975, Phys. Lett. A, 54, 8.

90. Thomas, G. F., and Meath, W. J., 1979, Phys. Lett. A, 70, 396.

91. Pegg, D. J., and Series, G. W., 1970, J. Phys. B, 3, L33.

92. Moloney, J. V., 1976, Ph.D. Thesis, The University of Western Ontario.

93. Huber, K. P., and Herzberg, G., 1978, "Molecular Spectra and Molecular Structure IV. Constants of Diatomic Molecules" (Van Nostrand), p.196.

94. Power, E. A., and Thirunamachandran, T., 1974, J. Chem. Phys., 60, 3695.

95. Andrews, D. L., and Thirunamachandran, T., 1977, J. Chem. Phys., 67, 5026.

96. Hirschfelder, J. O., Curtiss, C. F., and Bird, R. B., 1954, "Molecular Theory of Gases and Liquids" (Wiley).

97. Margenau, H., and Kestner, N. R., 1969, "Theory of Intermolecular Forces" (Pergamon Press).

98. Meath, W. J.; Thuraisingham, R. A., and Kmetic, M. A., 1988, Adv. Chem. Phys., 73, 0000 (in press).

99. Kreyszig, E., 1983, "Advanced Engineering Mathematics", second edition (Wiley).

100. Levine, S. N., 1983, "Quantum Chemistry", third edition (Allyn and Bacon), pp.178-186.

101. Hioe, F. T., private communication.

102. IMSL Library, 1982, Edition 9 (IMSL Inc., Houston).

103. Jensen, R. V., and Susskind, S. M., 1987, "Photon and Continuum States of Atoms and Molecules", Springer Proceedings in Physics, Vol. 16, edited by N. K. Rahman, C. Guidotti and M. Allegrini (Springer-Verlag), p.13.

104. Thuraisingham, R. A., and Meath, W. J., Chem. Phys., in press.

105. Delone, N. B., and Krainov, V. P., 1985, "Atoms in Strong Light Fields", Springer Series in Chemical Physics, Vol. 28, edited by V. I. Goldanskii, R. Gomer, F. P. Schafer and J. P. Toennies (Springer-Verlag).

106. Adam, A. G., Gough, T. E., Isenor, N. R., and Scoles, G., 1985, Phys. Rev. A, 32, 1451.

107. Berman, P. R., 1974, Am. J. Phys., 42, 992.

108. Thuraisingham, R. A., and Meath, W. J., 1988, Surf. Sci., 199, 199.

109. New, G.H.C., 1983, Rep. Prog. Phys., 46, 877.

110. Siegman, A. E., 1986, "Lasers" (University Science Books).

111. Shapiro, S. L., editor, 1977, "Ultrashort Light Pulses", Topics in Applied Physics, 18.

112. Dalgarno, A., 1961, "Quantum Theory", Vol. 1, edited by D. R. Bates (Academic Press), Chapter 5; Hirschfelder, J. O., Byers Brown, W., and Epstein, S. T., 1964, Adv. Quant. Chem., 1, 255.

113. Certain, P. R., Dion, D. R., and Hirschfelder, J. O., 1970, J. Chem. Phys., 52, 5987.

114. Bell, W. W., 1975, "Matrices for Scientists and Engineers" (Van Nostrand), Chapter 4.

115. Wigner, E. P., 1935, Math. Naturwiss. Anz. Ungar. Akad. Wiss., 53, 475.

116. Brillouin, L., 1932, J. Phys. Radium, 7, 373.

117. Lennard-Jones, J. E., 1930, Proc. Roy. Soc., A129, 598.

EMF coupling are particularly simple functions of the transition dipole, $\underline{\mu}_{12}$, the difference between the permanent dipoles of the states involved in the transition, $\underline{d} = \underline{\mu}_{22} - \underline{\mu}_{11}$, and the magnitude, ε, and direction of polarization, $\hat{e}$, of the EMF (Sec. 3.3.2). The effects of permanent dipoles are relatively easy to understand using the RWA. In general, compared with the $\underline{d} = 0$ atomic problem, the presence of permanent dipoles (where $\underline{d} \neq 0$) reduces the coupling between the molecule and the applied EMF and causes oscillations to occur, as a function of frequency, in the molecule-EMF coupling. These effects are evident in the often drastic reduction of both resonance widths and dynamic backgrounds, which are seen when the $\underline{d} \neq 0$ spectra are contrasted with the analogous $\underline{d} = 0$ spectra. The effects of $\underline{d} \neq 0$ are further evident in the oscillatory fringes surrounding the resonance positions; these fringes are absent in the atomic case. Since the presence of permanent dipoles reduces the molecule-EMF coupling relative to the atomic problem, the molecular RWA expressions for the resonance profiles have a wider range of validity as a function of the parameters of the problem, than do the corresponding atomic results. This molecular RWA can be expected to play an analogous role in the spectroscopy for species with permanent dipoles to that played by the usual RWA in the spectroscopy of atoms. Finally it is interesting to note that as the coupling strength parameter $\underline{d} \cdot \hat{e}\varepsilon/\omega$ increases, the RWA predicts the